Title
Controlling Wine Oxidation: Redox Cycling of Iron and the Formation of Acetaldehyde

Author
Nguyen, Thi

Publication Date
2021

Peer reviewed|Thesis/dissertation

Controlling Wine Oxidation:
Redox Cycling of Iron and the Formation of Acetaldehyde

By

THI HOANG NGUYEN

DISSERTATION

Submitted in partial satisfaction of the requirements for the degree of

DOCTOR OF PHILOSOPHY

in

Agricultural and Environmental Chemistry

in the

OFFICE OF GRADUATE STUDIES

of the

UNIVERSITY OF CALIFORNIA

DAVIS

Approved:

Andrew L Waterhouse, Chair

Anita Oberholster

Michael D Toney

Committee in Charge

2021

Vitae Summa Brevis Spem Nos Vetat Incohare Longam

They are not long, the weeping and the laughter,
Love and desire and hate:
I think they have no portion in us after
We pass the gate.

They are not long, the days of wine and roses:
Out of a misty dream
Our path emerges for a while, then closes
Within a dream.

Ernest Dowson (1896)

Table of Contents

List of Tables

Chapter 2: A Production-Accessible Method: Spectrophotometric Iron Speciation in Wine using Ferrozine and Ethylenediaminetetraacetic Acid

Chapter 3: Redox Cycling of Iron: Effects of Chemical Composition on Reaction Rates with Phenols and Oxygen in Model Wine

Chapter 4: Controlling the Fate of Hydrogen Peroxide in Wine through Complexation of Iron by Wine Acids

Chapter 5: Yeast Induce Acetaldehyde in Wine Micro-oxygenation Treatments

List of Figures

Chapter 1: An Introductory Review of Wine Aging and Oxidation

Chapter 2: A Production-Accessible Method: Spectrophotometric Iron Speciation in Wine using Ferrozine and Ethylenediaminetetraacetic Acid

Chapter 3: Redox Cycling of Iron: Effects of Chemical Composition on Reaction Rates with Phenols and Oxygen in Model Wine

Chapter 4: Controlling the Fate of Hydrogen Peroxide in Wine through Complexation of Iron by Wine Acids

Chapter 5: Yeast Induce Acetaldehyde in Wine Micro-oxygenation Treatments

List of Reactions, Schemes, and Equations

Chapter 1: An Introductory Review of Wine Aging and Oxidation

Chapter 2: A Production-Accessible Method: Spectrophotometric Iron Speciation in Wine using Ferrozine and Ethylenediaminetetraacetic Acid

Chapter 3: Redox Cycling of Iron: Effects of Chemical Composition on Reaction Rates with Phenols and Oxygen in Model Wine

Chapter 4: Controlling the Fate of Hydrogen Peroxide in Wine through Complexation of Iron by Wine Acids

Abstract

Over time and with oxygen ingress, the chemical composition of wine evolves through a cascade of reactions comprising many pathways, one of which yields acetaldehyde, an oxidation product which not only directly impacts wine aroma but also facilitates further reactions altering other sensory properties such as color and mouthfeel. Key reactions in this pathway are catalyzed by the redox cycling of iron between two oxidation states, iron(II) and iron(III), thus the majority of the work presented herein focuses on control of iron's reactivity. A spectrophotometric method of iron speciation was developed as a means of monitoring the reciprocal processes of iron reduction and oxidation in wine. The method relies on the combined use of two opposing chelating agents, ferrozine and ethylenediaminetetraacetic acid (EDTA), iron(II)- and iron(III)-selective respectively, to halt redox reactions, thereby providing a stable measurement of iron(II):iron(III) ratios in wine. This method was used to investigate the redox cycling of iron in model wine as it occurs in the primary reactions of the oxidation pathway: the oxidation of iron(II) by oxygen and the reduction of iron(III) by phenols. The rates of both processes varied with changes to model wine composition, though the former was found to be consistently slower. This suggests that iron(II) oxidation is the rate-determining reaction for the wine oxidation pathway, and wine ages at a rate limited not necessarily by its chemical composition but by oxygen ingress. Despite this, different wines subject to the same oxidative conditions will often vary in their response to oxygen, thus the reactions of hydrogen peroxide, a key branchpoint further down the oxidation pathway, were investigated, specifically as influenced by complexation of iron by major wine acids (tartaric, malic, and citric). The rate of the iron(II)-catalyzed Fenton oxidation of ethanol into acetaldehyde was found to occur more quickly toward the upper limits of typical wine pH, an effect most apparent with citrate complexation of iron. This appeared to affect the efficacy of sulfur dioxide as an antioxidant in competing with iron(II) for hydrogen peroxide. In addition, acetaldehyde formation in wine was found also to depend on oft-overlooked biotic factors post-fermentation. In a series of experiments pertaining to micro-oxygenation, found critical to the process were residual sugar and populations of *Saccharomyces cerevisiae*, without which acetaldehyde production would not occur. The question of why acetaldehyde does not accumulate with oxygenation alone warrants further investigation.

Chapter 1

An Introductory Review of Wine Aging and Oxidation

“C’est l'oxygène qui fait le vin; c'est par son influence que le vin vieillit.”

In his 1866 *Etudes sur le vin*, Louis Pasteur first noted the role of oxygen in the development of wine color and aroma, stating, “It is oxygen that makes wine; it is by its influence that wine ages.”

The following century, Jean Ribéreau-Gayon began his investigations into the chemical mechanisms by which oxygen interacts with wine. In 1931, he reported the presence of iron in its ferrous state, iron(II), in wine that had been protected from oxygen. Following saturation with air, the concentration of dissolved oxygen in the wine after several hours was found to have decreased, which Ribéreau-Gayon surmised was due to the oxidation of iron(II) to its ferric form, iron(III). As oxygen levels declined, iron then returned to its reduced iron(II) form, providing what is likely the earliest evidence for the redox cycling of iron in wine.

This work and others early on have furnished much of our understanding of *what* takes places during wine aging, paving the way for research which continues to this day toward answering questions of *why*. Premature oxidation, first observed in Burgundy in the late 1900s, has caused wines around the world deemed ageworthy to inexplicably deteriorate. Micro-oxygenation, a fairly recent but widely used technology by which controlled amounts of oxygen are deliberately introduced into wine to simulate or even accelerate the aging process, has not consistently achieved its intended outcomes. Different wines age differently, but what is it about their chemical composition that causes such varied responses to oxygen?

Winemaking is now a global endeavor, and research conducted toward answering this question must necessarily also be global. This introductory chapter serves to contextualize the experiments presented in later chapters, which constitute but a small part of a much larger international research effort toward better understanding wine aging and the underlying chemistry of oxidation.

1.1 Oxygen in Winemaking

While generally detrimental to most foods and beverages, oxidation might be considered an integral part of the wine production process. Wine oxidation comprises a cascade of chemical reactions, triggered by oxygen, which alter wine's chemical composition and consequently its sensory properties, such as color, flavor, and mouthfeel. To what extent these changes improve or worsen the quality of wine is subjective (Waterhouse and Elias 2010), though it is commonly believed that wines attain at some point in their development a maximum level of complexity, after which quality is expected to decline (Jackson 2016). When exactly this peak occurs, or rather how much oxygen it takes to get there, is a question asked by many wine researchers, producers, and consumers alike, though chemical composition and storage conditions are expected play a fundamental role. A more complete understanding of wine oxidation chemistry would allow winemakers more control over the production process to achieve their desired style of wine, as well as give consumers some indication of cellaring time or shelf life.

Detrimental effects of oxygen include browning (Singleton and Kramling 1976) and possibly increased bitterness (Laurie and Clark 2010). Fruity aromas vital to the character of certain wine varieties may be overtaken by notes of *honey*, *boiled potato*, *farm feed*, and others (Blanchard et al. 2004, Escudero et al. 2000, Bueno et al. 2015). Through related mechanisms, oxidation can also remove undesirable sulfur-containing compounds (Waterhouse and Nikolantonaki 2015), and in red wines, actually deepen and stabilize color as well as soften astringency (Atanasova et al. 2002, Castellari et al. 1998, Oliveira et al. 2011).

It has been estimated that white wines can consume about ten air saturations (totaling approximately 80 mg/L oxygen) before developing overly "oxidized" character, while red wines can tolerate more than thirty saturations before such defects become apparent (Singleton 1987, Singleton et al. 1979). Relative to white wines, this greater resistance of red wines to oxidation may be attributed largely to their higher concentrations of phenolic compounds, major contributors to color and mouthfeel, and the primary substrates for oxidation (Waterhouse and Laurie 2006, Rossi and Singleton 1966).

1.1.1 Winery Operations. Exposure to oxygen occurs at virtually every step of the winemaking process, with estimates of total oxygen ingress, from fermentation to bottling, being as much as 70 mg/L (du Toit et

al. 2006). Large cellar operations performed in open air with vigorous agitation, including pressing, pumpovers, and délestage (rack-and-return), as well as operations involving refrigeration, such as cold stabilization, can result in saturation with oxygen (Castellari et al. 2004, Singleton 1987, Waterhouse and Laurie 2006). Other enological processes will typically increase the dissolved oxygen content of wines by no more than 2 mg/L: "high enrichment" (1-2 mg/L) treatments include racking, centrifugation, and bottle filling, while "low enrichment" (<1 mg/L) treatments include tank transfers and filtration (Castellari et al. 2004).

1.1.2 Barrel and Bottle Aging. Oxygen ingress also occurs long-term during aging in barrels and bottles, neither of which completely exclude oxygen. Historical estimates of the annual rate of oxygen transfer into oak barrels have been between 25 and 45 mg/L, though recent studies on changes to the physical properties of barrels over time (e.g. moisture content) have noted a general decline in oxygen transfer, shifting the annual rate closer to 10 mg/L (del Alamo-Sanza and Nevares 2014, 2019).

It has been noted that most oxygen in bottled wine initially comes from the cork closures themselves, which, given their porous nature, contain oxygen. Following this initial "injection" of oxygen into the wine at bottling, oxygen transfer rates (OTRs) will vary with closure type (Lopes et al. 2005). Despite their variability, natural and technical (agglomerated) cork closures will generally have low OTRs which decrease over time, while synthetic corks have relatively high OTRs (Lopes et al. 2007, Oliveira et al. 2013, 2015). In the first month after bottling, OTRs reported for natural, technical, and synthetic corks are 2.0-3.0 mg/L, 1.4-2.8 mg/L, and 3.6-4.3 mg/L respectively. For the remainder of the first year in bottle, OTRs decreased to 0.25-0.5 mg/L, 0.01-0.1 mg/L, and 0.85-1.5 mg/L per month respectively. While such closures allow the oxidative development of wine, metal roll-on tamper evident closures (i.e. screwcaps), are virtually impenetrable to oxygen, even leading to "reduced" character (Brajkovich et al. 2005, Skouroumounis et al. 2005). It is estimated that 85-90% of the oxygen present in bottles with screwcaps can be attributed to the bottling process, rather than oxygen transfer through the closures (Lopes et al. 2006). While likely to be a multifactorial issue, premature oxidation of wine in some instances has been attributed at least in part to poorly performing closures.

Ullage or headspace oxygen in bottles can also be a major determinant of wine's development (Dimkou et al. 2011, Morozova et al. 2014). Other storage conditions can additionally affect wine stability. Temperature will alter rates of oxygen ingress and subsequent oxidation reactions (Lopes et al. 2006, 2007, Skouroumounis et al. 2005), and light can produce degradative effects similar to those of oxygen (Bielski and Gibicki 1982, Clark et al. 2011).

1.1.3 Micro-oxygenation. Developed in 1900 in France as a means of softening wines produced from the famously astringent Tannat grape (Robinson and Harding 2015), micro-oxygenation (MOx) is now commonly used worldwide, perhaps in light of studies reporting the benefits of controlled oxygen exposure. MOx is thought to simulate or even accelerate the aging process, in order deliver to consumers a more palatable product in a shorter timeframe (Anli and Cavuldak 2012), and is sometimes viewed as an alternative to barrel aging (del Carmen Llaudy et al. 2006, Cano-López et al. 2010, Oberholster et al. 2015).

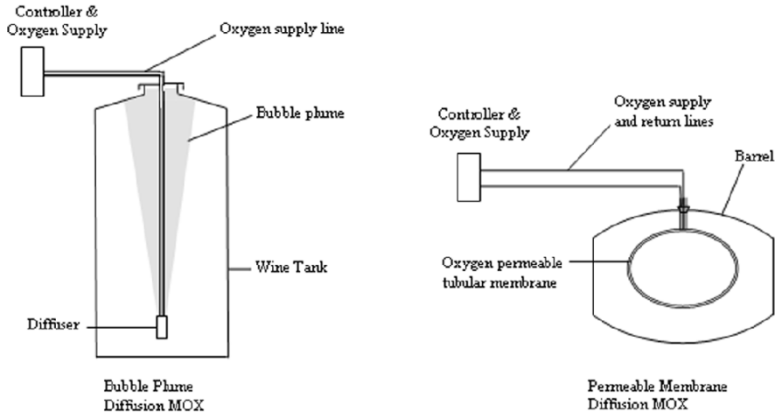

Figure 1.1 Schematics of bubble plume diffusion (left) and permeable membrane diffusion (right) for micro-oxygenation (from Schmidtke et al. 2011).

The practice of MOx constitutes the addition of small, controlled amounts of oxygen into wine during the extended period of time between fermentation and bottling. Oxygen is typically introduced through a diffuser or permeable membrane which bubbles the specified dosage of oxygen directly into the wine (Figure 1.1) (Schmidtke et al. 2011). MOx will vary greatly in commercial applications, with parameters including oxygen delivery rate and treatment duration chosen based on wine variety and initial chemical and sensory properties. Timing is also key, with MOx treatments often conducted in two phases: phase one prior to malolactic fermentation (MLF) providing up to 30 mg/L oxygen over one month, and phase two after

MLF at a rate of 1-5 mg/L/mo for several months (Gómez-Plaza and Cano-López 2011). This distinction between phases before and after MLF is made primarily to account for differences in microbial activity (section 1.3.2), which can result in the consumption of not only oxygen but certain oxidation products as well (Osborne et al. 2000, Li and Mira de Orduña 2011).

MOx can reduce vegetal character, with notes of *green pepper* and *asparagus* demonstrated to decrease with MOx treatments, though the chemical mechanism by which this occurs has yet to be determined (Cejudo-Bastante et al. 2011a, Durner et al. 2010a). Other undesirable "reductive" odors from sulfur-containing compounds have also been treated using MOx (Nguyen et al. 2010).

However, the main effects of MOx reported are decreased astringency and improved color (Anli and Cavuldak 2013, Gómez-Plaza and Cano-López 2011). These changes can be attributed to acetaldehyde, a key product and marker of oxidation, which subsequently reacts with phenolic compounds (section 1.3.1), thereby impacting these sensory properties. Applied properly, MOx supplies enough oxygen to create the acetaldehyde needed for these reactions, but not so much that browning and other oxidative defects develop (del Carmen Llaudy et al. 2006). Some studies have observed increased color stability and intensity following MOx treatment (Cano-López et al. 2008, Sanchez-Iglesias et al. 2009, Cejudo-Bastante et al. 2011a), though others have noted this effect disappeared after as little as two months (Cano-López et al. 2010, Geldenhuys et al. 2010); decreases in color have also been observed (del Carmen Llaudy et al. 2006). Effects of MOx on astringency have been similarly variable (Arfelli et al. 2011, Caillé et al. 2010, Oberholster et al. 2015, Parpinello et al. 2011).

Production of acetaldehyde via MOx has been inconsistent (Gonzalez-del Pozo et al. 2010, Cano-López et al. 2008, Durner et al. 2010a), or delays have been observed where acetaldehyde accumulates only toward the end of MOx treatment or afterward during storage (Carlton et al. 2007, Cejudo-Bastante et al. 2011b, Gambuti et al. 2015). It has been hypothesized that acetaldehyde levels increase only when the phenolic compounds it reacts with (e.g. anthocyanins and flavanols) have been depleted (Carlton et al. 2007). Consequently, the appearance of unreacted acetaldehyde may indicate a "tipping point" during oxidation (Kilmartin 2010).

1.2 The Wine Oxidation Cascade

The ultimate goal of oxygenation and aging is the improvement of wine quality, thus chemical and sensory analysis to monitor its development are of the utmost importance. While we have the means to control the level of oxygen provided, there is no way as of yet to predict wine's response. However, much research has been done to elucidate the chemical pathways and reaction mechanisms of wine oxidation, providing an increasingly clearer understanding of how compositional parameters control the course of aging.

1.2.1 Primary Reactions: Redox Cycling of Iron. Phenolic compounds are the primary substrates for oxidation, and the many chemical reactions comprising the oxidation cascade begin with the oxidation of phenols coupled to the reduction of oxygen (Danilewicz 2003, Waterhouse and Laurie 2006). While phenols are singlet compounds, molecular oxygen is a diradical existing in a paramagnetic triplet ground state, thus a direct reaction is spin-forbidden (Green and Hill 1984, Singleton 1987). This reaction cannot occur without the catalysis of transition metals, particularly iron, whose function is to circumvent the kinetic energy barrier associated with electron transfer (Miller et al. 1990). Concentrations of iron in wine have been reported in the range of 0.06-55 mg/L, though the global average has been estimated to be 5.5 mg/L (Danilewicz 2007). Sources of iron in wine include soil and grapes themselves, filtration and fining agents, various additives and winemaking equipment (Waterhouse et al. 2016).

Studies conducted in model wine have demonstrated that oxygen consumption by phenols does not occur without the inclusion of iron (Danilewicz 2007, 2011, Danilewicz and Wallbridge 2010). Furthermore, slowing of oxidation reactions in both model wine and real wine has been observed with the addition of potassium ferrocyanide and other iron chelating agents, providing additional evidence for the central role of iron in wine oxidation (Danilewicz and Wallbridge 2010, Kreitman et al. 2013a, Ribéreau-Gayon 1931). Copper and manganese have been found to facilitate wine oxidation, likely through mechanisms which enhance iron's reactivity with oxygen (Danilewicz 2007, 2011, 2016a, 2016b, Danilewicz and Wallbridge 2010).

With iron acting as an electron carrier between phenols and oxygen, the initial reactions of wine oxidation are characterized by the redox cycling of iron between two oxidation states: iron(II) and iron(III) (Scheme 1.1). Building on Ribéreau-Gayon's original observations (1931), much of the current evidence for

the redox cycling of iron stems primarily from studies in which oxygen consumption was monitored in air-saturated model wine. Rapid oxygen consumption was found to occur with iron(II), in proportion to the concentration of iron(II) used, but not with iron(III) (Danilewicz 2011). Following this initial phase of oxygen consumption attributable to iron(II) oxidation, uptake could continue only when iron(III) was reduced by phenols to regenerate the necessary iron(II) (Danilewicz 2011, Danilewicz et al. 2008, Danilewicz and Wallbridge 2010). In real wines, iron(III) has been found to accumulate following exposure to excess oxygen, though iron(II) comes to be the predominant species in storage (Danilewicz 2016b, 2018, Ferreira et al. 2007, Lopez-Lopez et al. 2015). These findings illustrate the indirect nature of the reaction between wine phenols and oxygen, and the central role of iron.

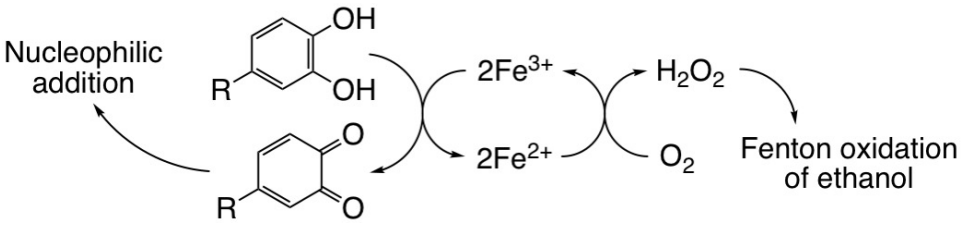

Scheme 1.1 Reduction of oxygen coupled to phenol oxidation via redox cycling of iron (from Nguyen and Waterhouse 2019).

It has been proposed that the iron(II):iron(III) ratio in wine indicates its "redox status," as this ratio depends on the relative reaction rates of iron(II) with oxygen and of iron(III) with phenols (Danilewicz 2016b, 2018). A high iron(II):iron(III) ratio in wine would suggest that it is able to effectively maintain a reductive environment, perhaps due to phenolic content and composition, while a low iron(II):iron(III) ratio would suggest oxygen ingress has outpaced the wine's capabilities. Measurements of this ratio could be used to assess oxygen exposure during cellar operations and storage, and anticipate further reactions.

The oxidation of phenols occurs through the sequential removal of two electrons: first to produce a semiquinone radical intermediate, then to a fully oxidized quinone. Constituting the vast majority of wine phenols, those susceptible to oxidation are phenols possessing vicinal hydroxyl groups (i.e. ortho-dihydroxy- and 1,2,3-trihydroxyphenols) due to stabilization of their semiquinone afforded by electron delocalization to their additional oxygen atom(s). Monophenols, meta-diphenols, and substituted phenols, relatively minor components in wine, are not readily oxidized as they do not produce stable semiquinone intermediates

(Danilewicz 2003, Waterhouse and Laurie 2006). The resultant quinones are highly electrophilic species which react with nucleophiles, namely thiols and other phenols in wine (Nikolantonaki and Waterhouse 2012, Waterhouse and Nikolantonaki 2015). Reactions with thiols, such as 3-mercaptohexanol, a key contributor to the fruity character of many wine varieties, can result in changes to aroma (Blanchard et al. 2004). Reactions with phenolic compounds can lead to polymerization and the formation of increasingly complex tannin and pigment molecules, consequently altering wine color and mouthfeel (Waterhouse and Laurie 2006).

Through the redox cycling of iron, phenol oxidation is coupled to the reduction of oxygen. The addition of two electrons to oxygen produces the peroxide anion (O_2^{2-}), though at wine pH, this is protonated to give hydrogen peroxide (H_2O_2) (Danilewicz 2003, Waterhouse and Laurie 2006). H_2O_2 subsequently triggers the Fenton oxidation of ethanol (section 1.2.3), a series of radical-mediated reactions which ultimately produce acetaldehyde (Danilewicz 2011, Elias et al. 2009, Elias and Waterhouse 2010).

1.2.2 Reduction Potentials and Complexation of Iron. The reduction potential (E) of a chemical species is its tendency to acquire electrons, measured relative to a reference redox couple (e.g. H^+/H_2 of a standard hydrogen electron). In acidic aqueous solutions, iron exists primarily as a hexa-aquo complex, and the formal reduction potential at pH 0 (E_0) of the Fe(III)/Fe(II) couple is 770 mV (Danilewicz 2003, Miller et al. 1990). However, the reduction potential of iron changes when the water molecules at the coordination sites of iron are replaced by other ligands, primarily the carboxylate groups of tartaric acid in wine (Danilewicz 2003). Tartrate forms a bidentate complex more strongly with iron(III) than with iron(II), thereby displacing the equilibrium toward oxidation and decreasing the reduction potential of iron. In an aqueous solution of excess tartaric acid, the reduction potential at pH 3.5 ($E_{3.5}$), typical of wine, for the Fe(III)/Fe(II) couple was measured to be 360 mV (Danilewicz 2003, Green and Parkins 1961). Higher pH increases the extent of deprotonation of tartaric acid, required for complexation, and prompts the formation of dimeric (2:2) and trimeric (3:3) iron-tartrate complexes (Timberlake 1964a, Yokoi et al. 1994), thereby decreasing the reduction potential of iron by -130 mV per pH unit increase (Green and Parkins 1961).

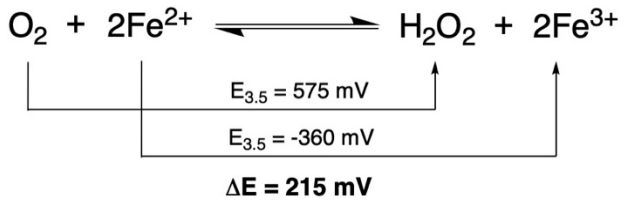

Reaction 1.1 Reduction of oxygen by iron(II).

The reduction of oxygen to hydrogen peroxide requires protonation, thus its reduction potential is also pH-dependent. E_0 for the O_2/H_2O_2 couple is 780 mV and decreases -59 mV per pH unit increase (Danilewicz 2003, 2012), thus $E_{3.5}$ is approximately 575 mV. The difference in potential for two half-reactions (ΔE) indicates the thermodynamic favorability of the overall reaction and the direction in which equilibrium lies. The positive value for ΔE indicates the reduction of oxygen by iron(II) (Reaction 1.1) is a thermodynamically favored reaction in wine, which would not be the case without tartrate complexation of iron (Danilewicz 2012, 2013, 2014). It should be noted that a negative value for reduction potential is used for the redox couple that is being oxidized, given the loss of electrons.

The reduction potentials of several ortho-dihydroxy phenolic compounds (catechols) in wine were found to vary between 577 and 604 mV when measured by cyclic voltammetry in model wine at pH 3.6 (Danilewicz 2012, Kilmartin et al. 2001). Given the same pH-dependence as the O_2/H_2O_2 couple (Danilewicz 2003, 2012), $E_{3.5}$ for a general quinone/catechol couple can be estimated to be 595 mV. The oxidation of catechols by iron(III) (Reaction 1.2) is therefore not feasible and cannot occur without coupling to a more thermodynamically favored reaction. Studies in model wine have demonstrated that a nucleophile must be present to react with quinones as they are produced, in order to displace this otherwise unfavorable equilibrium and "pull" catechol oxidation forward (Danilewicz 2011, Danilewicz et al. 2008, Danilewicz and Wallbridge 2010).

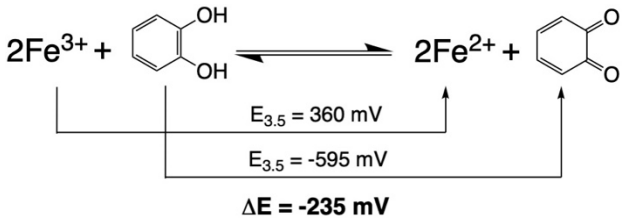

Reaction 1.2 Oxidation of catechol by iron(III).

While the change in free energy for a reaction should have no bearing on its rate, thermodynamics and kinetics appear to be closely related for pH-dependent redox reactions. For tartrate-complexed iron, the rate of oxidation by oxygen increases as the reduction potential of iron decreases, illustrating this two-fold effect of pH (Michaelis and Smythe 1931). With regards to thermodynamics, iron's reduction potential decreases due to deprotonation of tartaric acid into tartrate, which forms more stable complexes with

iron(III) than with iron(II) (Timberlake 1964a, Green and Parkins 1961, Danilewicz 2014). With regards to kinetics, iron oxidation occurs more rapidly with higher pH due to the increased abundance of the iron(II)-tartrate complex, its stability relative to iron(III)-tartrate notwithstanding. The oxidation of a free iron(II) cation would involve the extraction of a negative charge from an already positively charged species, an energetically demanding process in comparison to the oxidation of iron(II) within an electrically neutral complex with tartrate (Smythe 1931).

The reduction potential of phenolic compounds decreases with pH in the same manner as that of the O_2/H_2O_2 couple because quinone formation entails the loss of two protons (Danilewicz 2003, 2012). Early studies on wine oxygen consumption found it to be immeasurably slow, thus alkaline conditions were forced using potassium hydroxide in order to obtain what were believed to be rapid estimates of oxygen consumption capacity. It was proposed that the anionic phenolate forms of phenols, more prevalent at higher pH, are more susceptible to oxidation than their protonated conjugates (Rossi and Singleton 1966, Singleton 1987), a reasonable hypothesis in light of other studies elucidating the mechanisms of phenol oxidation. Electron transfer occurs with a transient iron(III)-phenolate complex, after which the oxidized semiquinone (or quinone) and reduced iron(II) are released (Scheme 1.2) (Avdeef et al. 1978, Hynes and O'Coinceanainn 2001, Mentasti and Pelizzetti 1973, Powell and Taylor 1982). It should be noted that such complexation would require the displacement of other ligands already present, such as tartrate.

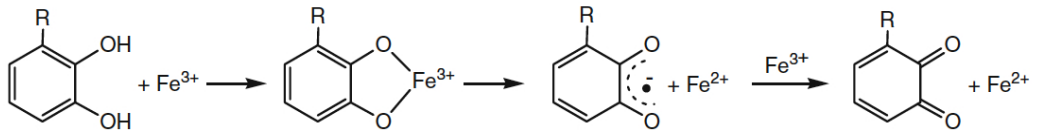

Scheme 1.2 Coordination of iron(III) by phenols (R = H, OH), subsequent iron(III) reduction to iron(II), and semiquinone and quinone formation (from Perron and Brumaghim 2009).

Although tartaric acid is considered the predominant acid in wine (2-6 g/L) (Waterhouse et al. 2016) and is often used in model wine to represent all of wine acidity, other acids found in wine are also expected to complex with iron and co-determine its reduction potential. The complexation of iron by malic acid, another dicarboxylic acid found in wine (at concentrations similar to tartaric acid), has been found to have a similar effect as tartrate on the thermodynamics of iron reactions: iron(II) oxidation readily occured in a model

wine buffered with malate while the reduction of iron(III) by 4-methylcatechol, a model for ortho-dihydroxy phenols, was not possible without the addition of a nucleophile. On the other hand, acetic acid (0.1-0.5 g/L in wine) was found incapable of decreasing the reduction potential of iron to below that of oxygen, likely due to the relative weakness of its monodentate complexation with iron(III). Iron(II) could not be oxidized by oxygen in an acetate model wine, while iron(III) was readily reduced by 4-methylcatechol without assistance from a nucleophile (Danilewicz 2014). The other major carboxylic acids found in wine, namely citric (0.1-0.7 g/L), succinic (0.5-1.0 g/L), and lactic acid (0-3 g/L), are known to form complexes with iron (Gorman and Clydesdale 1984, Timberlake 1964b), and therefore may contribute to control of iron's reactivity.

Exogenous iron chelators, often used to probe the oxidation reactions in wine, have been demonstrated to alter the reduction potential of iron. As an iron(III)-selective chelating agent like tartaric and malic acid, ethylenediaminetetraacetic acid (EDTA) lowers the reduction potential of iron and was found to facilitate iron(II) oxidation and the Fenton oxidation of ethanol (Kreitman et al. 2013a). On the other hand, ferrozine, an iron(II)-selective chelator, has been found to increase the reduction potential of iron, causing iron(III) to rapidly react with phenols where it would not have otherwise (Elias and Waterhouse 2010, Danilewicz 2016b).

1.2.3 Fenton Oxidation of Ethanol. The sequential addition of electrons to oxygen yields a series of reactive oxygen species (ROS) constituting the ladder of oxygen reduction, which ultimately results in water (Scheme 1.3). The transfer of one electron from iron(II) to oxygen is thought to produce superoxide ($O_2^{\bullet-}$), presumably protonated at wine pH to give the hydroperoxyl radical ($HO_2^{\bullet}$) (Behar et al. 1970, Waterhouse and Laurie 2006), though attempts to detect this radical via spin trapping and electron paramagnetic resonance spectroscopy have not been successful (Elias et al. 2009). It is possible that this species eludes detection by undergoing rapid disproportionation to form oxygen and hydrogen peroxide (Andersen and Skibsted 1998), though alternatively, a mechanism has been proposed by

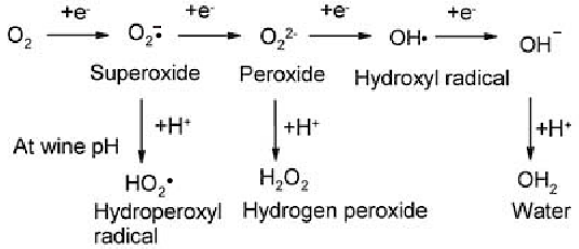

Scheme 1.3 Ladder of oxygen reduction (from Waterhouse and Laurie 2006).

which two equivalents of iron(II) reduce oxygen to H_2O_2 directly, forgoing the intermediate step of hydroperoxyl formation (Danilewicz 2013).

Regardless of how it is formed, H_2O_2 is the next species on the reduction ladder, and has been detected in both real wine and model systems (Clark et al. 2007, Coleman et al. 2020, Heritier et al. 2016). It decomposes to yield the hydroxyl radical ($HO^{\bullet}$) in an iron(II)-catalyzed reaction now commonly referred to as the Fenton reaction (Reaction 1.3), named after Henry John Horstman Fenton, the chemist who first described the use of iron(II) and H_2O_2 to oxidize tartaric acid (1894). This strongly oxidative combination of iron(II) and H_2O_2, together referred to as "Fenton's reagent," now has an immensely wide range of applications, from chemical and clinical analysis to wastewater treatment and environmental remediation, and plays an integral part in wine oxidation.

$$Fe^{2+} + H_2O_2 \xrightarrow{H^+} Fe^{3+} + HO^{\bullet} + H_2O$$

Reaction 1.3 The Fenton reaction in acidic conditions.

The hydroxyl radical is a highly unstable oxidant and will react non-selectively with most organic molecules at diffusion-controlled rates, in proportion to their concentration in solution (Buxton et al. 1988, Danilewicz 2003). With their precursors present at relatively high levels, among the expected products of Fenton oxidation in wine are glyceraldehyde from glycerol, pyruvate from malic acid, and a number of small aldehydes from tartaric acid (Laurie and Waterhouse 2006, Fenton 1894, Waterhouse and Laurie 2006). However, its sheer abundance in wine makes ethanol (CH_3CH_2OH) the primary target for oxidation by the hydroxyl radical, producing the 1-hydroxyethyl radical ($CH_3^{\bullet}CHOH$).

While the ladder of oxygen reduction ends with the reduction of the hydroxyl radical to water, the 1-hydroxyethyl radical continues to react through what appears to be an oxygen-dependent mechanism to produce acetaldehyde (CH_3CHO) (Scheme 1.4). In a study conducted in model wine containing iron(II), the addition of an excess of

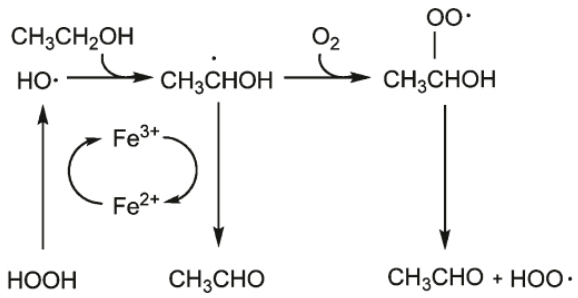

Scheme 1.4 Fenton oxidation of ethanol in wine under high and low oxygen conditions (from Elias and Waterhouse 2010).

H_2O_2 (six times the concentration of iron(II)) in the absence of oxygen resulted in the stoichiometric yield of acetaldehyde from H_2O_2, but in the presence of oxygen yield was instead limited by the initial iron(II) concentration (Elias and Waterhouse 2010). Findings from this study and others prior suggest the 1-hydroxyethyl radical, in low-oxygen conditions, can rapidly reduce iron(III) back to iron(II), forming acetaldehyde and thereby allowing the continuation of the Fenton reaction (Kolthoff and Medalia 1949a, 1949b). In the presence of oxygen, however, the radical has been proposed to react instead with oxygen to form the 1-hydroxyethylperoxyl radical ($CH_3CH[-OO^{\bullet}]OH$), and no recycling of iron occurs. This radical is thought to decompose slowly to yield acetaldehyde and a hydroperoxyl radical (Elias and Waterhouse 2010).

1.2.4 Sulfur Dioxide and Other Antioxidants. Sulfur dioxide (SO_2) is widely used in wine production as a preservative due to its antimicrobial and antioxidant properties (Boulton et al. 1996). It gives a weak diprotic acid in aqueous solutions and exists in a pH-dependent equilibrium (pK_{a1} = 1.81, pK_{a2} = 7.20 in water at 20°C). At wine pH (3-4), the vast majority of SO_2 (>95%) exists in the anionic bisulfite form (HSO_3^-), primarily responsible for antioxidant functions. The remainder is present as neutral "molecular" SO_2, considered the antimicrobial form, while the doubly deprotonated sulfite form (SO_3^{2-}) is virtually nonexistent at wine pH (Jenkins et al. 2020, Zoecklein et al. 1995).

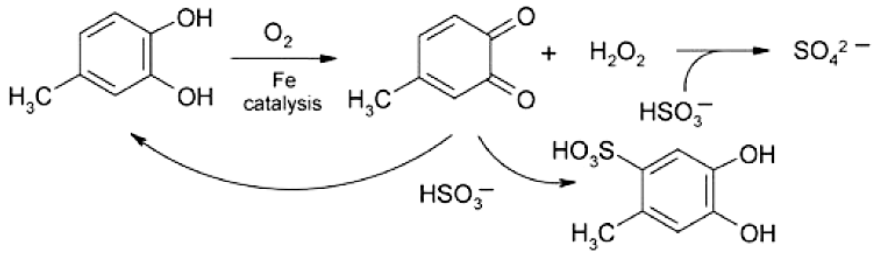

Scheme 1.5 Reactions of sulfur dioxide (as bisulfite) with quinones and hydrogen peroxide following phenol oxidation (from Danilewicz et al. 2008).

Originally thought to react directly with oxygen, SO_2 (as bisulfite) actually counteracts the effects of oxidation primarily by reacting with the quinones and hydrogen peroxide produced during the initial reactions (Scheme 1.5), thereby limiting the cascade otherwise ensued (Danilewicz and Standing 2018). Reactions with quinones can reduce them back to the phenolic forms, essentially reversing the effects of oxidation, or result in the formation of hydroxyalkylsulfonate adducts (Danilewicz et al. 2008, Danilewicz and Wallbridge

2010). The reaction with H_2O_2 produces sulfate (SO_4^{2-}) and prevents the Fenton reaction and subsequent oxidation of ethanol into acetaldehyde. It should be noted that this constitutes a key branchpoint in the oxidation pathway where the fate of H_2O_2 is governed by a competition between its reactions with iron(II) and with SO_2, the relative rates of which are likely influenced by wine composition (Elias and Waterhouse 2010). Under ideal model wine conditions, SO_2 reacts (indirectly) with oxygen at a molar ratio of 2:1, where one mole of SO_2 reacts with a quinone and the second with H_2O_2 (Danilewicz et al. 2008, Danilewicz and Wallbridge 2010). However, in real wines, lower ratios closer to 1:1 have been observed (Carrascon et al 2015, 2018, Danilewicz et al. 2008, Danilewicz 2016c, Ferreira et al. 2015), indicating variable matrix effects on the efficacy of SO_2 as an antioxidant.

Sulfur dioxide can also form adducts of varied stabilities with a number of other wine constituents, including anthocyanins and aldehydes (Beech et al. 1979, Burroughs and Sparks 1973). This binding establishes a chemical equilibrium between “free” and “bound” SO_2. While free SO_2 remains capable of performing its antioxidant functions, bound SO_2 has significantly reduced protective properties. Winemakers typically aim to maintain free SO_2 levels between 10 and 30 mg/L (Coehlo et al. 2015).

Other commonly used antioxidants include ascorbic acid and glutathione. Ascorbic acid may be added to wine to recycle quinones back to phenols in the same manner as SO_2. It is typically used in conjunction with SO_2 given its inability to react with H_2O_2. In certain conditions, used alone it can oxidize in the same manner as phenols, resulting in H_2O_2 production and increased browning (Barril et al. 2012, Bradshaw et al. 2001). Glutathione is a thiol endogenous to grapes, though it may be added during the winemaking process as an additional preservative, given its ability to form innocuous adducts with quinones. There is growing interest in its use as a “sacrificial” nucleophile to protect more sensorially desirable thiols (Nikolantonaki and Waterhouse 2012).

Additionally worth mentioning are hydroxycinnamic acids, endogenous phenolic compounds which have been shown to quench 1-hydroxyethyl radicals and prevent acetaldehyde formation (Gislason et al. 2013, Kreitman et al. 2013b) The “natural” antioxidant capacity of wines to quench radicals and deter oxidative reactions is a current topic of investigation (Nikolantonaki et al. 2019).

1.3 Acetaldehyde

A variety of aldehydes can arise in wine due to the oxidation of alcohols, typically imparting undesirable aromas with such descriptors as *cheese*, *cabbage*, and *varnish* (Waterhouse et al. 2016). Given its precursor is ethanol, acetaldehyde comes to be the most abundant in wine (Wildenradt and Singleton 1974).

Known systematically as ethanal, acetaldehyde is a simple carbonyl compound which contributes to the aroma of many foods and beverages. Sensory detection thresholds will vary with the matrix; in wine, acetaldehyde can be perceived at 100-125 mg/L (Berg et al. 1955). At low levels, it confers a pleasant, fruity aroma, but higher concentrations can be pungent and irritating, often described as *grassy*, *nutty*, or reminiscent of *bruised apples*. Typical levels of acetaldehyde in wine are below the limit of olfactory detection: about 30 mg/L in red wine and 80 mg/L in white wine (McCloskey and Mahaney 1981), though concentrations in the ranges of 4-212 mg/L and 11-493 mg/L have been reported for red and white wines respectively (Liu and Pilone 2000). Given the unique manner in which it is produced (section 1.3.2), sherry possesses relatively high, readily perceptible levels of acetaldehyde (90-500 mg/L), thus other wines with aldehydic character are often described as *sherry-like*.

1.3.1 Chemical Reactions. Beyond its impact on wine aroma, acetaldehyde can react with flavonoids, in particular anthocyanins and flavanols, to produce a wide array of condensation and polymerization products (Atanasova et al. 2002, Fulcrand et al. 2006, Timberlake and Bridle 1976), thereby altering other sensory properties such as color, taste, and mouthfeel. Among the desirable effects of acetaldehyde reactions are reduced bitterness and astringency, and increased color intensity and stability (Anli and Cavuldak 2012, Oliveira et al. 2011).

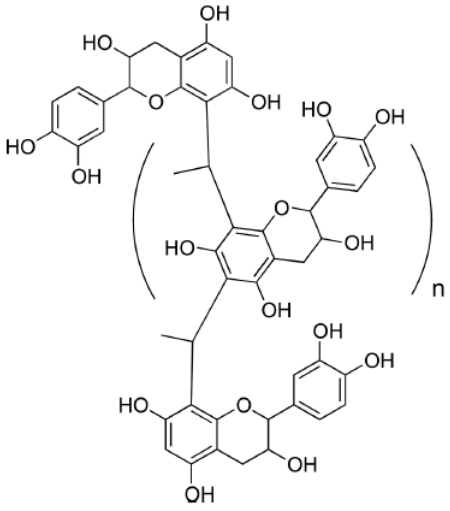

Figure 1.2 Ethylidene-bridged catechin oligomer (from Sheridan and Elias 2016).

Acetaldehyde can facilitate “indirect” condensation reactions between anthocyanin and/or flavanol molecules by linking them through an ethylidene-bridge (Figure 1.2) (Dueñas et al. 2006. Pissarra et al.

2003). Acetaldehyde-mediated ethylidene-bridging is thermodynamically favorable, with dimers often continuing to react to form ethyl-dimer adducts and even ethylidene-bridged trimers (Peterson and Waterhouse 2016, Sheridan and Elias 2016). Direct condensation products of acetaldehyde with flavanols and anthocyanins have also been observed, the latter belonging to a class of compounds termed pyranoanthocyanins (Bakker and Timberlake 1997, de Freitas and Mateus 2011, Saucier et al. 1997).

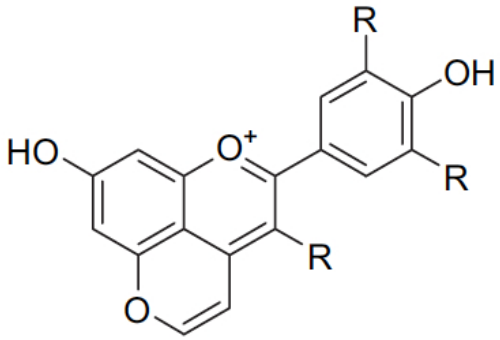

Figure 1.3 Vitisin-B type pyranoanthocyanin (from Rentzch et al. 2007).

While anthocyanins are primary contributors to red wine color, their cationic flavylium form is unstable. Hydration of anthocyanins with increased pH results in the colorless carbinol form. Similarly, the addition of sulfur dioxide (as bisulfite) yields a colorless flavene sulfonate. Pyranoanthocyanins, by virtue of their added pyran ring (Figure 1.3), are protected against such color loss reactions, thereby stabilizing red wine color over a wider pH range (Bakker and Timberlake 1997, Fulcrand et al. 2006, Schwarz et al. 2003). Furthermore, the extended conjugation conferred by this pyran ring generally results in a hypsochromic shift in color, from bright red/violet toward a deeper brick-red/orange hue.

These compounds are not end products, however, instead continuing to react in complex pathways yet to be completely elucidated. Included in this “wine polyphenol iceberg” (Vallverdú-Queralt et al. 2017) are ethyl- and vinyl-flavonoid adducts, as well as oligomeric and polymeric pigments, or modified tannin (Cruz et al. 2009, Fulcrand et al. 1996, Mateus et al. 2002, He et al. 2012). With age, the proportion of low molecular weight, monomeric phenols tends to decrease, while the higher molecular weight fraction, including ethylidene-bridged compounds, pyranoanthocyanins, pigments, and other derived compounds, will increase (Castellari et al. 2000, de Beer et al. 2008, Oliveira et al. 2011, Roginsky et al. 2006, Tao et al. 2007). It has been estimated such derivatives are responsible for 70-90% of red wine color, a contribution that rises toward the upper end of this range over time (Schwarz et al. 2003).

Acetaldehyde can also react with SO_2 to form a strongly bound 1-hydroxyethylsulfonate adduct (de Azevedo et al. 2007, Burroughs and Sparks 1973). The sensory impact of acetaldehyde is diminished significantly upon binding to SO_2, as this adduct is no longer odorous; it is also substantially less reactive. High levels of SO_2 have been found to slow the oxidation-driven development of phenolic compounds (Tao et al. 2007); binding of acetaldehyde by SO_2 may be a contributing factor. However, this adduct cannot be considered completely inert. As free SO_2 is gradually depleted in performing its various antioxidant and antimicrobial functions, cleavage of these adducts serves to replenish this pool of SO_2, consequently releasing acetaldehyde (Carrascon et al. 2015, Sheridan and Elias 2016).

Condensation of alcohols with aldehydes will form products belonging to a class of compounds called acetals. The high concentration of ethanol in wine all but guarantees its reaction with acetaldehyde and formation of the diethyl acetal (1,1-diethoxyethane), though reports of its detection have been limited, as acyclic acetals are thermodynamically unstable. In contrast, the heterocyclic acetal alcohols from glycerol and acetaldehyde are produced with no such decrease in entropy. An array of four isomers (*cis*- and *trans*-1,3-dioxolanes and dioxanes) resulting from this reaction have been found in aged Madeira and Port wines (Camara et al. 2003, 2006, da Silva Ferreira et al. 2002, Es-Safi et al. 2002). Given the relatively high concentration of glycerol in wines and its propensity to react with acetaldehyde, analysis of these acetals has been proposed as a means of monitoring oxidation (Peterson et al. 2015).

1.3.2 Microbiological Considerations. As wine is essentially a natural product of fermentation, biotic factors should not be overlooked when discussing wine aging. In addition to being a key component in the chemical pathways of wine oxidation, acetaldehyde is a similarly integral intermediate in microbial metabolism, thus aging is not necessarily a strictly chemical process.

In the fermentative glucose metabolism of *Saccharomyces cerevisiae* (Scheme 1.6), glycolysis produces pyruvate, generating the reduced form of nicotinamide adenine dinucleotide (NADH) from its oxidized form (NAD^+). The enzyme pyruvate decarboxylase (PDC) then converts pyruvate into acetaldehyde, which acts as the terminal electron acceptor and is converted to ethanol by the enzyme alcohol dehydrogenase (ADH) in the final step of the fermentation pathway. This restores NAD^+ from NADH, thereby maintaining balanced

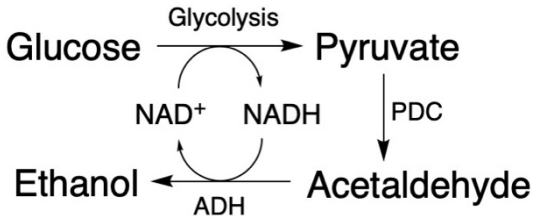

Scheme 1.6 Alcoholic fermentation of glucose in *Saccharomyces cerevisiae*.

redox conditions and allowing consumption of glucose to continue (Pronk et al. 1996, Swanson and Clifton 1948, van Dijken and Scheffers 1986).

While it can be retrieved and catabolized, acetaldehyde regularly leaks from yeast cells during alcoholic fermentation (Fornachon 1953, Liu and Pilone 2000). Acetaldehyde accumulation in wine can be strain-dependent (Li and Mira de Orduña 2011, Cheraiti et al. 2010), likely due to differential ADH gene expression (Romano et al. 1994). Moreover, strain variability has been found to affect the concentrations of pyranoanthocyanins (Morata et al. 2003) and other derived pigments (Hayasaka et al. 2007, Morata et al. 2016).

Saccharomyces cerevisiae is a facultatively fermentative yeast, meaning that in high-glucose environments it ferments even in the presence of oxygen, thus fermentation is not restricted to anaerobic conditions. Despite this, *S. cerevisiae* cannot flourish in the complete absence of oxygen as they are auxotrophic for certain growth factors under such conditions, including sterols and fatty acids crucial to maintaining cell membrane integrity in the presence of ethanol (Fornairon-Bonnefond et al. 2002, Weusthuis et al. 1994). Yeast growth is known to be stimulated by oxygen, even for non-respiratory metabolism, and studies have demonstrated the benefits of aeration to cell mass, cell viability, and rate of fermentation (Lin et al. 2011, Rosenfeld and Beauvoit 2003). Yeast populations are seldom monitored after fermentation, and few studies have addressed the possibility of oxidative stimulation/maintenance of yeast post-fermentation, as in applications of micro-oxygenation (Han et al. 2017), though the potential effect this may have on acetaldehyde accumulation is not without precedent.

The *flor* strains of *S. cerevisiae* used in sherry production are known to remain active after alcoholic fermentation (Pozo-Bayón and Moreno-Arribas 2011). In response to a largely inhospitable environment with a lack of glucose and an excess of highly toxic ethanol, these strains undergo a dramatic overhaul in gene expression constituting a diauxic shift: the full switch from fermentative to respiratory metabolism (Aranda et al. 2002, Ingram and Buttke 1984, Jones 1989). Yeast growth resumes with ethanol as the carbon source,

which by reverse action of ADH is reassimilated to produce acetaldehyde, consequently giving sherries their characteristic aroma (Pozo-Bayón and Moreno-Arribas, Aranda et at. 2002). Moreover, this "biological aging" of sherry can be accelerated through aerative practices such as stirring, pumpovers, and MOx (Munoz et al. 2005, Ough and Amerine 1972).

With regards to bacterial metabolism, lactic acid bacteria can utilize acetaldehyde as an alternative electron acceptor for the purposes of additional NAD^+ regeneration, leading to increased growth (Collins and Speckman 1974). Lactic acid bacteria in wine, notably *Oenococcus oeni* and others responsible for malolactic fermentation, can consume both free and sulfur dioxide-bound acetaldehyde, producing ethanol and acetic acid (Osborne et al. 2006). This acetaldehyde can be yeast-derived, suggesting a commensal relationship (Osborne et al. 2000). Bacterial metabolism is the primary reason that applications of MOx are separated into two phases before and after MLF (section 1.1.3), during which color intensity and stability have been observed to decrease, likely due to the prevention of acetaldehyde accumulation. When MLF is delayed, increased polymeric pigment formation has been observed (Burns and Osborne 2013, 2015), providing additional evidence to suggest the influence of microbes on an otherwise chemical process.

1.4 Controlling Wine Oxidation: Experimental Approaches

As with most other contemporary research, the study of wine oxidation has evolved to a great extent toward the use of "top-down" approaches involving large-scale, often untargeted analyses, to be related statistically to chemical and sensory phenomena. Extensive characterization of compositional parameters including color, metals, and various phenolic indices has been done to explore what chemical factors most influence oxygen consumption rates in wine (Ferreira et al. 2015). Linear sweep voltammetry has been used to capture wine's "oxidation signature," its profile of most readily oxidizable substances (Gonzalez et al. 2018), while electron paramagnetic spectroscopy measures its inventory of radical-quenching compounds likely to interrupt the oxidation cascade (Nikolantonaki et al. 2019). The increasingly popular chromatography-mass spectrometry "-omics" approach has led to the discovery of more and more markers of wine oxidation (Arapitsas et al. 2012) as well the characterization of a wine's pool of endogenous antioxidants

(Nikolantonaki et al. 2019). These technologies are powerful tools to identify key variables that may be used to predict and ultimately control wine oxidation.

However, in mutual support of such studies, experiments taking place in simpler model systems must be done to further test hypotheses in more controlled, chemically well-defined settings, in order to provide a clearer understanding of the fundamental chemistry underlying wine aging and oxidation. Much of the work presented hereafter constitutes such a "bottom-up" approach, the overall purpose of which has been to probe the various iron-catalyzed reactions in wine, in particular how specific aspects of wine composition influence the redox cycling of iron and, ultimately, the formation of the acetaldehyde.

Chapter 2 presents the development and validation of a spectrophotometric method for iron speciation in wine, one which quite literally controls the redox cycling of iron through the combined use of differentially selective chelating agents. The need for an easy, rapid, and inexpensive method, accessible in a commercial production setting, for the determination of iron(II):iron(III) ratios in red and white wine was addressed, though this method would come to be an integral part of the experiments taking place in model wine presented in Chapter 3 and 4.

This method was used in the experiments described in Chapter 3 to monitor iron(III) reduction in model wines of varied composition. Specifically, the effects of pH, copper, phenolic structure, and nucleophile availability on the rate of this reaction were evaluated and compared to their effects on the reciprocal process of oxygen consumption by iron(II). This assessment of the both halves of the redox cycle would provide indication as to which reaction is rate-determining for the remainder of the wine oxidation cascade.

The redox cycling of iron was further investigated in experiments pertaining to the fate of hydrogen peroxide and subsequent acetaldehyde production in anoxic model wine, presented in Chapter 4. The effects of pH and iron complexation by major wine acids (tartaric, malic, and citric acid) on the relative reaction rates of H_2O_2 with iron(II) and with sulfur dioxide were determined.

Chapter 5 presents a collaborative research project on the role of yeast in micro-oxygenation, to which an experiment involving the fermentation of synthetic must (again a controlled model system) was contributed to confirm the importance of residual sugar to acetaldehyde production during this process. In addition to

those aforementioned, yeast and residual sugar would be added to the “toolbox” of readily manipulable parameters at the disposal of winemakers to better control wine oxidation.

Chapter 2

A Production-Accessible Method: Spectrophotometric Iron Speciation in Wine Using Ferrozine and Ethylenediaminetetraacetic Acid

Published:

Nguyen TH and Waterhouse AL. 2019. A production-accessible method: Spectrophotometric iron speciation in wine using ferrozine and ethylenediaminetetraacetic acid. J Agric Food Chem 67:680-687.

2.1 Abstract

Wine oxidation is reported to be linked to the iron species present in the wine, but spectrophotometric speciation is plagued by unstable measurements due to alterations to the reduction potential of iron by complexing agents. Ferrozine raises the reduction potential of iron by complexing preferentially to iron(II), inducing the reduction of iron(III) during analysis, but here EDTA is added to chelate iron(III), thereby stabilizing iron against redox drift. Bisulfite addition allows the use of ferrozine for red wine analysis by mitigating color interference. Measurements agree with values from a previous method for iron(II) and from FAAS for total iron. Spike recoveries were in the range of 103.55-110.1%. The method is linear for iron concentrations in the range of 0.10-6.00 mg/L and offers good precision (CV 0.4-10.1%) and low limits of detection (0.02 mg/L) and quantification (0.06 mg/L). The method demonstrated changes to iron speciation during the oxygenation of red wines.

2.2 Introduction

The cascade of chemical reactions constituting wine oxidation is initiated by the reduction of oxygen coupled to the oxidation of phenolic compounds (Scheme 2.1). However, with two unpaired electrons, oxygen cannot react directly with phenols as reactions between triplet and singlet compounds are spin-forbidden (Green and Hill 1984, Singleton 1987). The catalysis of transition metal ions can overcome the initial energy barrier associated with electron transfer. With iron acting as a catalytic electron carrier between phenols and oxygen, the initial reactions of the oxidation pathway are characterized by the redox cycling of iron between its two oxidation states: iron(II) and iron(III) (Danilewicz 2003, 2007, 2011, 2013, Danilewicz and Wallbridge 2010, Powell and Taylor 1982, Waterhouse and Laurie 2006).

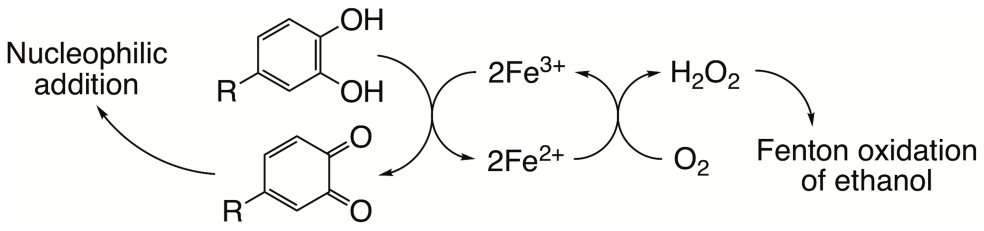

Scheme 2.1 Reduction of oxygen coupled to phenol oxidation via redox cycling of iron.

In acidic aqueous solutions, iron exists as a hexaaquo complex, although water can be displaced readily by other ligands which alter the reduction potential of iron (Danilewicz 2003, Danilewicz 2014). In wine, tartaric acid coordinates strongly with iron(III) while binding much more weakly to iron(II), thereby lowering the reduction potential of iron and displacing the equilibrium towards iron(III) (Danilewicz 2013, 2014, Timberlake 1964a, Yokoi et al. 1994). Iron(II) becomes a strong reductant in wine and the oxidation of iron(II) to iron(III) is a thermodynamically favorable process; the addition of electrons to oxygen from iron(II) readily occurs, generating hydrogen peroxide (H_2O_2) (Danilewicz 2003, du Toit et al. 2006, Waterhouse and Laurie 2006). Oxidation of iron(II) additionally catalyzes the Fenton reaction, in which hydrogen peroxide decomposes to yield the hydroxyl radical, a highly unstable species that quickly reacts with all substances present in solution, in proportion to their concentrations (Buxton et al. 1988, Elias and Waterhouse 2010, Fukuzawa et al. 1988). Given its relative abundance in wine, ethanol is a prime target for oxidation by the hydroxyl radical, and through a series of radical intermediates, it is eventually converted to

acetaldehyde (Elias and Waterhouse 2010, Joslyn and Comar 1941, Picariello et al. 2017). To allow the continued consumption of oxygen by catalytic levels of iron, it is necessary to regenerate iron(II). The reduction of iron(III) to iron(II) is coupled most commonly to the oxidation of phenols, yielding quinones, electrophiles that promptly react with nucleophilic species in wine such as thiols and other phenols (Blanchard et al. 2004, Oliveira et al. 2011, Nikolantonaki and Waterhouse 2012, Waterhouse et al. 2015). Reaction with bisulfite may also revert quinones back to their reduced phenol forms (Danilewicz 2016c).

The iron(II):iron(III) ratio in wine depends on the relative reaction rates of iron(II) with oxygen and of iron(III) with phenols (Danilewicz 2016b). While electrochemical measurement of the reduction potential of wine has been intended as an assessment of its redox status, such potentials have been found to be generated simply by the oxidation of ethanol at the electrode surface and not by the total redox processes in wine (Danilewicz 2012), and thus iron speciation has been proposed to better provide insight into the extent of oxidation or reduction in wine (Danilewicz 2018).

Several advanced instrumental methods for iron speciation have been developed, employing such technologies as adsorptive stripping voltammetry (Wang and Mannino 1989), flow-through fluorescent sensors (Pulido-Tofino et al. 2000), and ion-exchange chromatography coupled to atomic absorption spectroscopy (Ajlec and Stupar 1989), but given the cost and technical requirements of such methods, they are likely not accessible to wineries, while a spectrophotometric method would be more feasible.

Recent spectrophotometric methods have employed the complexing agents 2-(5-bromo-2-pyridylazo)-5-(diethylamino)-phenol (Br-PADAP), 2-(5-bromo-2-pyridylazo)-5-[N-propyl-N-(3-sulfopropyl)amino] phenol disodium salt dihydrate (Br-PAPS), 2,2'-dipyridylketone picolinoylhydrazone (DPKPH), and 3-(2-pyridyl)-5,6-diphenyl-1,2,4-triazine-*p,p*'-disulfonic acid monosodium salt (ferrozine), all of which form a colored complex with iron(II). The Br-PADAP method utilizes an acetate buffer of pH 5.5, as formation of the iron(II)-Br-PADAP complex occurs optimally at this pH (Ferreira et al. 2007). Similarly, DPKPH requires pH adjustment to 4.9 to maximize complexation (Lopez-Lopez et al. 2015). Such pH levels are significantly higher than typical wine pH (3.0-4.0), and changes to pH during analysis may affect iron speciation (Danilewicz 2016b, 2018). It is additionally worth noting that, unlike Br-PADAP, Br-PAPS, and ferrozine, DPKPH is not

commercially available and requires synthesis by condensation of 2,3-dipyridylketone and picolinoylhydrazide (Lopez-Lopez et al. 2015).

While the Br-PAPS and ferrozine methods avoid the issue of pH adjustment by analyzing unbuffered, undiluted wine samples, both complexing agents are iron(II)-selective. By stabilizing this oxidation state, these complexing agents increase the reduction potential of iron and render iron(III) an artificially strong oxidant. The consequence of preferential coordination with iron(II) has been observed as an upward drift in absorbance, indicating the gradual increase in iron(II) during analysis of a variety of sample matrices due to iron(III) reduction, including water and mineral systems in addition to wine (Anastacio et al. 2008, Danilewicz 2016b, 2018, Im et al. 2013, Verschoor and Molot 2013, Viollier et al. 2000). Br-PADAP and DPKPH are also iron(II)-selective complexing agents though this was not considered by the authors of either method; a 10 min reaction time is prescribed for Br-PADAP (Ferreira et al. 2007), during which some iron(III) would be reduced to iron(II), and no time is specified for DPKPH (Lopez-Lopez et al. 2015). On the other hand, the Br-PAPS and ferrozine methods are kinetic methods that rely on the reduction of iron(III) to iron(II) during analysis: the complexing agent is added to the wine sample, and the increase in absorbance is monitored at regular time intervals. A regression line is fitted to these data and extrapolated to time zero to obtain the absorbance at time of mixing, from which the original iron(II) concentration may be calculated (Danilewicz 2016b, 2018). While ferrozine has been used for iron speciation in white wines, red wine color interferes with measurement of the iron(II)-ferrozine complex at 562 nm (Danilewicz 2016b). In contrast, Br-PAPS forms a complex with iron(II) with an absorbance maximum at 740 nm, at which there is minimal interference from red wine color (Danilewicz 2018).

The aim of this study was to develop a simple spectrophotometric method for iron speciation in both white and red wines. Key criteria for the method include minimal disturbance of wine conditions, stabilization against redox drift of iron species during analysis, allowing for single-point measurements, and utilization of reagents and equipment accessible in a wine production environment.

2.3 Materials and Methods

2.3.1 Reagents, Model Wine, and Wine Samples. The ferrozine solution (3.5% m/v) was prepared in deionized water. The ethylenediaminetetraacetic acid (EDTA) (0.005% m/v), ascorbic acid (0.1% m/v), and sodium metabisulfite (1.0% m/v) solutions were prepared in model wine, which consisted of ethanol (12% v/v) in tartaric acid solution (4.0 g/L) adjusted to pH 3.5 with sodium hydroxide (5 N). The ascorbic acid and sodium metabisulfite solutions were prepared daily. Stock solutions of iron(II) (250.0 mg/L) from ferrous sulfate heptahydrate and iron(III) (250.0 mg/L) from ferric chloride hexahydrate were prepared in hydrochloric acid (0.1 N). Ferrozine, EDTA disodium salt dihydrate, ascorbic acid, tartaric acid, and ferric chloride hexahydrate were purchased from Sigma-Aldrich. Sodium metabisulfite, hydrochloric acid, and sodium hydroxide were purchased from Thermo Fisher Scientific. Ferrous sulfate heptahydrate and ethanol (200 proof, anhydrous) were purchased from VWR International. All chemicals used were of reagent grade.

White and red wine samples were either donated to or produced by the Department of Viticulture and Enology at the University of California, Davis. Analysis was not conducted immediately at the time of bottle/container opening and oxygen ingress was not controlled.

2.3.2 Procedures for Iron Speciation. An Agilent Technologies 8453 spectrophotometer was used for spectrophotometric measurements and was operated using 845x UV-Visible Chemstation software v. A.10.01[81]. Measurements were taken in disposable, semi-microvolume (3 mL), 1.0 cm pathlength, acrylic cuvettes from Sarstedt.

For the determination of iron(II) in white wine, 1000 μL of wine was transferred into a cuvette containing 10 μL ferrozine solution. The contents of the cuvette were mixed briefly, and 1500 μL EDTA solution was added immediately afterward. Absorbance measurements were taken 1 min after EDTA addition. For red wines, to minimize color interference, a smaller sample volume of 250 μL was used and 750 μL sodium metabisulfite solution was added after the addition of EDTA. Measurements were taken after absorbance stabilized following the complete bleaching of anthocyanins; stabilization required as much as 15 min for the red wines analyzed in this study.

For the determination of total iron, in a separate cuvette, EDTA in the analytical procedure was replaced with 1500 μL ascorbic acid solution. Measurements were taken after absorbance stabilized following the complete reduction of all iron(III) to iron(II); stabilization required as much as 30 min in this study. For red wines, sodium metabisulfite was added after ascorbic acid.

All absorbance measurements were taken at 562 nm against a blank (2.5 mL model wine, 10 μL ferrozine solution). Additionally, to correct for the background absorbance of each wine at 562 nm, cuvettes were prepared in triplicate containing wine samples without reagents. Model wine (1500 uL) accounted for the volume of EDTA or ascorbic acid solution otherwise added; the volume of ferrozine solution (10 μL) was considered negligible. For red wines, 750 μL sodium metabisulfite solution was included. Average background absorbances for each wine were subtracted from experimental values. These corrected absorbances were used to calculate iron(II) and total iron concentrations from the calibration curve. The concentration of iron(III) may be calculated by subtracting iron(II) from total iron.

2.3.3 Flame Atomic Absorption Spectroscopy (FAAS). A Varian SpectrAA 220 flame atomic absorption spectrometer was used for total iron measurements and was operated using SpectrAA 220 software v. 3.10. The iron hollow cathode lamp current was 5.0 mA. The analytical wavelength of 248.3 nm was used with a slit width of 0.2 nm; background correction was off. An air-acetylene flame was used with an air flowrate of 3.5 L/min, an acetylene flowrate of 1.5 L/min, and a burner height of 0.0 mm. The same standards used to calibrate the proposed iron speciation method were measured in triplicate to calibrate the spectrometer.

2.3.4 Method Evaluation. To check the linearity of the method, an external calibration curve was created by measuring iron(II) standards in the range of 0.1-6.0 mg/L in triplicate. The standards were prepared by adding appropriate volumes of freshly prepared 250.0 mg/L iron(II) stock solution into model wine already containing ferrozine and ascorbic acid, to ensure trace iron(III) was neither present nor allowed to form. The calibration curve was obtained by linear least squares regression using Microsoft Excel v. 16.14.

The use of EDTA in addition to ferrozine to stabilize iron against redox drift during analysis was first assessed by comparing the proposed method to the recent kinetic method for iron speciation in white wines

using only ferrozine, which serves to illustrate the reduction that occurs when using a single iron(II)-selective complexing agent (Danilewicz 2016b). The two methods were run in tandem to measure iron(II) in four white wines, and repeated measurements were taken as described for the kinetic method (below). The extent of stabilization using the proposed method was further evaluated by monitoring iron(II) concentrations in one white wine and one red wine every 10 min for 1 h following the addition of ferrozine and EDTA (and sodium metabisulfite in the case of the red wine). Additionally, EDTA solutions with concentrations in the range of 0.0025-0.01% were used to determine whether varying the ratio of the two complexing agents disrupts the stability of iron species during analysis.

Regarding the procedural modifications for the analysis of red wines, to determine whether using a smaller sample volume and adding sodium metabisulfite would affect iron speciation, the white wines were analyzed using the procedure proposed for red wines and results were compared to values from their analysis as white wines.

Recovery studies were done by spiking iron(II) and iron(III) (1 mg/L each) into two red wines. To prevent the oxidation of iron(II) upon spiking, oxygen was first removed from the wine samples (250 mL) by constant mixing with nitrogen gas for 30 min. Both iron(II) and total iron concentrations were measured using the proposed method immediately after spiking. Accuracy of the method in terms of total iron determination was assessed by comparing the results for all the wines to values obtained by FAAS.

All aforementioned comparisons were done by correlation and linear least squares regression analysis using Microsoft Excel v. 16.14 and agreement between methods was based on the calculated correlation coefficient as well as the linear regression equation. Results for individual wine samples measured by two methods were also compared by two-tailed, paired *t*-tests (α = 0.05).

Sampling was done in triplicate for all analyses. Precision of the method was assessed by calculating coefficients of variation (CV) for measured iron(II) and total iron concentrations; only the first in the series in cases of repeated iron(II) measurements over time were considered.

The limit of detection (LOD) and limit of quantification (LOQ) were determined based on the analysis of replicate blanks, according to IUPAC recommendations (Analytical Chemistry Division 1978). LOD was

calculated as 3(SD/*m*) and LOQ was calculated as 10(SD/*m*), where SD is the standard deviation of absorbance measurements for the blanks (*n* = 7) and *m* is the slope of the calibration curve.

2.3.5 Iron(II) Determination with Ferrozine Only. The previous kinetic method in which only ferrozine is used for iron(II) determination in white wines was performed with minor modifications to the published procedure (Danilewicz 2016b). Use of nitrogen gas during sampling was omitted as characterizing the intact iron(II):iron(III) ratio of specific wines in different containers with different closures was not the purpose of this study. Sample and reagent volumes were reduced such that the procedure could take place directly in cuvettes as opposed to separate reaction tubes, though proportions were unchanged: wine (2500 μL) was transferred into a cuvette and mixed with 12.5 μL ferrozine (3.5%) before absorbance measurements at 562 nm. Repeated measurements were taken 1 min after ferrozine addition every minute for 6 min and a linear least squares regression line was fitted to these data and extrapolated to time zero to obtain the original iron(II) concentration at time of mixing. Absorbance measurements were taken against a blank consisting of model wine and ferrozine, and background absorbances for each wine were used to correct experimental values. Disposable acrylic cuvettes were used instead of quartz cuvettes.

2.3.6 Oxygenation of Red Wines. The proposed method was used to monitor changes in iron speciation during the oxygenation of four red wines. Aliquots of each wine (100 mL) were transferred into 250 mL Erlenmeyer flasks and shaken continuously for 3 h on an Innova 2300 platform shaker set to 150 rpm. Samples were taken at time zero, at every 15 min for the first hour, and at every 30 min for the second and third hours.

2.4 Results and Discussion

2.4.1 Comparison to Previous Ferrozine Method. The particular manner in which ferrozine was used in the proposed method was derived from the previous method for iron speciation in white wine: a small volume, relative to the wine sample, of concentrated ferrozine solution (3.5% m/v) is used to ensure the prevailing iron(II):iron(III) ratio remains undisturbed while providing excess ferrozine. The author of the previous method surmised a larger reagent volume would dilute the sample and alter its pH, potentially resulting in inaccurate iron speciation (Danilewicz 2016b). It has been proposed the protonation states of

Table 2.1 Basic chemical parameters and determination of iron(II) and total iron for white and red wines used in method validation (n=3).

			initial iron(II) (mg/L)		total iron (mg/L)	
wine	**pH**	**ethanol (% v/v)**	**previous method**	**proposed method**	**FAAS**	**proposed method**
2012 Pinot grigio	3.27	12.03	1.74 ± 0.01	1.77 ± 0.02	2.92 ± 0.06	2.90 ± 0.07
2014 white blend	3.04	14.43	0.91 ± 0.01	0.95 ± 0.02	1.49 ± 0.02*	1.71 ± 0.02*
2015 Chardonnay	3.37	13.86	0.72 ± 0.02	0.72 ± 0.01	2.66 ± 0.07	2.86 ± 0.01
2015 Sauvignon blanc	3.73	13.83	1.62 ± 0.03	1.58 ± 0.03	1.98 ± 0.02*	2.16 ± 0.03*
2016 Petite Syrah	3.80	13.96		1.83 ± 0.05	2.24 ± 0.01	2.37 ± 0.05
2016 red blend A	3.99	14.58		3.10 ± 0.08	3.37 ± 0.04	3.42 ± 0.01
2016 red blend B	4.01	14.21		0.76 ± 0.04	1.12 ± 0.02	1.19 ± 0.11
2012 Cabernet sauvignon	3.67	13.17		1.45 ± 0.15	2.40 ± 0.01	2.47 ± 0.06

*significantly different via two-tailed, paired t-test ($\alpha = 0.05$)

Table 2.2 Linear regression equations and correlation coefficients for comparisons between methods.

measurement	**method *x***	**method *y***	**linear least squares regression equation**	**correlation coefficient**
iron(II) in white wines	previous	proposed (whites)	$y = 0.9765x + 0.0344$	0.9980
total iron in all wines	FAAS	proposed	$y = 0.9525x + 0.2205$	0.9942
iron(II) in white wines	proposed (whites)	proposed (reds)	$y = 1.0398x - 0.0342$	0.9997

iron ligands, e.g. tartaric acid, would be altered, thereby changing the reduction potential of iron and affecting speciation (Danilewicz 2018). However, the data here suggests after formation of the iron(II)-ferrozine complex, dilution does not necessarily change a sample's iron(II):iron(III) ratio, provided the diluent is model wine at pH 3.5 containing EDTA to chelate the other species, iron(III). This is evident in the agreement between the two methods for the analysis of iron(II) in the four white wines (Table 2.1), based on the linear least squares regression equation and correlation coefficient for the two data sets (Table 2.2). Results for each wine were not found to be significantly different via *t*-test ($p > 0.05$).

While use of the kinetic method resulted in an upward drift in iron(II) concentration during analysis as expected, the addition of EDTA after ferrozine per the proposed method appeared to prevent the reduction of iron(III) (Figure 2.1). As can be seen for the 2012 Pinot grigio, the concentration of iron(II) increased steadily over 6 min using ferrozine only but was stable when both ferrozine and EDTA were used; this difference between the two methods was observed for all four white wines analyzed. Given the change in iron(II) concentration that can occur with ferrozine alone, EDTA must be added immediately after sample mixing with ferrozine, to avoid any significant reduction of iron(III). Chelation of iron(III) by EDTA stabilizes iron speciation, making extrapolation of repeated measurements to time zero per the kinetic method unnecessary. It is additionally worth noting while the calibration curve for the proposed method was linear up to 6.00 mg/L iron(II), that of the previous method was unexpectedly nonlinear past 2.00 mg/L (Figure 2.2). Calibration of the older method was performed according to the original publication, which presented the relationship $y = 0.4952x + 0.0156$ for iron(II) concentrations in the range of 0.50-4.00 mg/L,

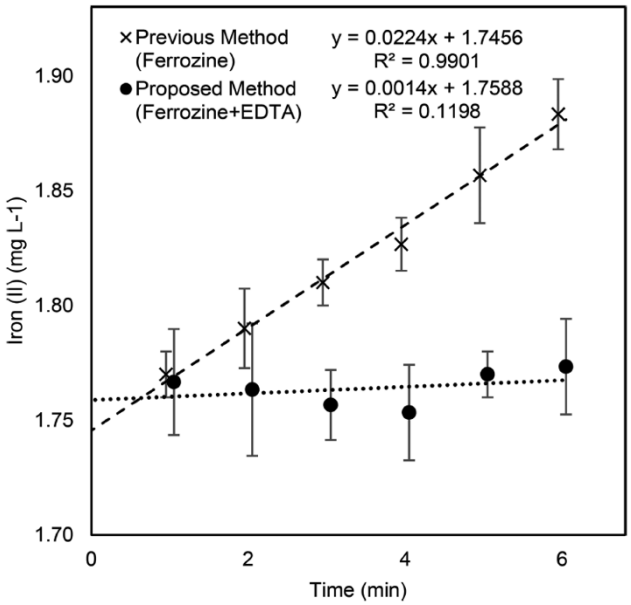

Figure 2.1 Iron(II) concentration during analysis of the 2012 Pinot grigio using both the previous ferrozine method and proposed method; error bars indicate one standard deviation above and below the mean (n=3). Shown are the linear least-squares regression lines extrapolated to time zero for both methods.

where *y* is absorbance at 562 nm and *x* is the concentration of iron(II) (Danilewicz 2016b), though the same linearity could not be replicated in the present study likely due to the use of disposable acrylic cuvettes as opposed to quartz cuvettes. According to this equation, an iron concentration of 4.00 mg/L should result in an absorbance measurement of 1.9964 AU, though this is beyond the recommended linear range for typical spectrophotometers. Using acrylic cuvettes, the linear range of the ferrozine-only method was, however, sufficient for the analysis of the white wines in this study, none of which contained iron(II) at concentrations surpassing 2.00 mg/L. However, recent studies have found modern wines typically contain 1-6 mg/L total iron (Danilewicz 2016b, 2018, Ferreira et al. 2007, Lopez-Lopez et al. 2015), and with the proposed method, 6.00 mg/L iron(II) yielded an average absorbance of 1.0286 AU. Because a smaller volume of wine is used, relative to the previous method, and additionally diluted with reagent solutions, the proposed method offers an extended linear range and is better suited for wineries where plastic cuvettes and/or less sensitive spectrophotometers may be used.

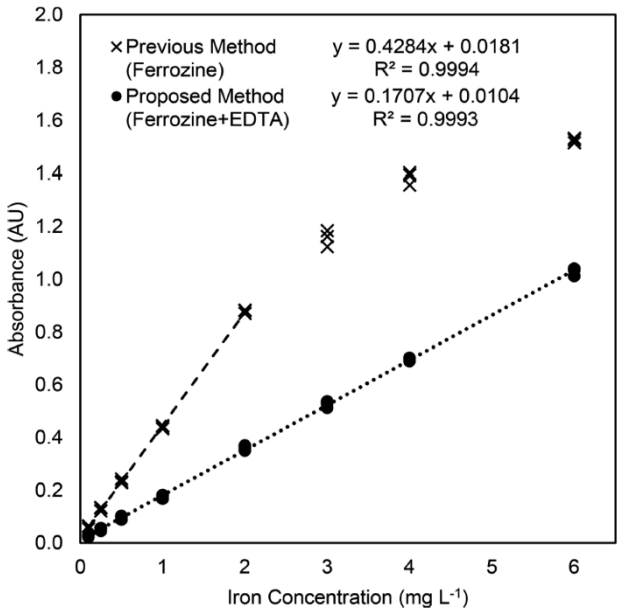

Figure 2.2 Calibration curves for the previous ferrozine method and proposed method generated by measuring external iron(II) standards with concentrations in the range of 0.01-6.00 mg/L (*n*=3).

2.4.2 Complexation with EDTA. Ferrozine has been found to complex with iron at a 3:1 molar ratio (Stookey 1970), while EDTA is a hexadentate chelating agent that complexes iron at a 1:1 molar ratio (McGee and Diosady 2018), requiring two moles fewer than ferrozine to complex iron. For the proposed method, the EDTA solution was prepared with a concentration (0.005%) that would provide the capacity to bind an equivalent amount of iron as ferrozine; EDTA is available at a ratio of 1:3 with ferrozine.

Following complexation with both ferrozine and EDTA, iron(II) concentrations were found to be stable in the white and red wine samples monitored over the course of 1 h, thus analysis is not strictly time-sensitive and multiple samples may be prepared as necessary prior to measurement. Tests using 0.0025%, 0.01%,

and 0.05% solutions of EDTA (constituting 1:6, 2:3, and 20:1 ratios with ferrozine respectively) showed varying the concentration in this range had no effect on the stability of iron speciation over 1 h. The exact ratio of ferrozine and EDTA to their respective iron species: iron(II) and iron(III), depends entirely on the extent of oxidation or reduction of the wine sample, thus the data suggests that both complexing agents must simply be provided in excess. Using the 0.005% solution provides EDTA at an approximate molar ratio of 2:1 with iron with regards to the highest calibration standard concentration (6 mg/L). However, it is possible that other ratios of EDTA:ferrozine beyond those evaluated here could result in one complexing agent negating the effects of the other, subsequently inducing instability of iron speciation.

In contrast to ferrozine, EDTA favors complexation with iron(III), thereby lowering the reduction potential of iron (Ilan and Czapski 1977, Welch et al. 2002). The stability observed when the two complexing agents are in excess suggests change to the reduction potential of iron by either complexing agent is negated by the other. Although electrochemical determination of the reduction potential of complexed iron in wine and wine-like systems in the presence of oxygen is stifled by the oxidation of ethanol at the electrode surface (Danilewicz 2012), such measurements could take place in future studies in anoxic conditions (Ferreira et al. 2018) or perhaps in an acidified aqueous matrix free of confounding electroactive constituents like ethanol. Furthermore, it is possible the stability constants for the iron(II)-ferrozine complex and the iron(III)-EDTA complex are comparable in a wine matrix, though these values also remain to be determined quantitatively.

Stability conferred by EDTA may alternatively be explained in terms of the loss of reactivity of iron(III) with phenols. Reduction of iron(III) by a phenolic compound requires coordination between the two species, forming an unstable complex within which electron transfer occurs (Danilewicz et al. 2008, Hynes and O'Coinceanainn 2001, Powell and Taylor 1982). In a study evaluating the effect of iron chelation on complex formation with phenols in black tea, it was found that the number of coordinating donor atoms in the chelating agent predicted the prevention of iron-phenol complexation. EDTA and other hexadentate ligands, by occupying all six coordination sites of iron, were found to be the most effective at preventing complex formation (McGee and Diosady 2018).

Interference of iron(III) on the measurement of iron(II) using ferrozine is not unique to wine and has been observed in a number of iron speciation studies on water and mineral samples. It has been proposed dissolved organic carbon induces the reduction of iron(III) in the presence of ferrozine (Verschoor and Molot 2013, Viollier et al. 2000) or the iron(III)-ferrozine complex is light-sensitive and undergoes photochemical reduction (Anastacio et al. 2008), although reduction has been observed even in the absence of light (Im et al. 2013). EDTA may be an effective masking agent to aid iron speciation in environmental samples as well, though this remains to be tested. While the pH of such samples would be higher than that of wine, metal complexes with EDTA would be expected to be more stable at higher pH as complexation occurs predominantly with the deprotonated form of EDTA. Similarly, the reaction rate of ferrozine with iron(II) has been found to increase with higher pH (Thompsen and Mottola 1984). Regardless of the mechanism, the addition of EDTA slows the reduction of iron(III) such that no reaction was detected during time intervals much longer than would be required for analysis.

2.4.3 Procedure for Red Wines. Color compounds in red wine have an absorbance maximum at 520 nm, though the peak can tail well past 600 nm, interfering with spectrophotometric measurement of the iron(II)-ferrozine complex at 562 nm. In a kinetic method similar to the previous ferrozine method, the complexing agent Br-PAPS has been used for iron speciation in red wines, as the iron(II)-Br-PAPS complex is measured at 740 nm and avoids the issue of red wine color interference (Danilewicz 2018). However, this method was not used as a reference in validating the accuracy of the proposed procedure because Br-PAPS is not a well-established complexing agent for iron analysis, having been used to determine other metals in other sample matrices, particularly zinc in serum (Homsher and Zak 1985, Ohyoshi et al. 1999). Furthermore, the use of Br-PAPS in measuring total iron in wine was shown to be in poor agreement with measurements obtained by FAAS. Presented in the publication was the linear regression equation $y = 0.8288x + 0.3718$, where x is total iron by FAAS and y is total iron measured using Br-PAPS (Danilewicz 2018), suggesting significant proportional and additive interferences. Nonetheless, future studies may investigate whether Br-PAPS may be used in combination with EDTA to stabilize iron speciation in the same manner as ferrozine.

The addition of bisulfite, as sodium metabisulfite, is proposed here as a means of reducing red wine color interference, allowing the use of ferrozine for iron analysis in red wines. Although no direct comparison to

another method for iron(II) determination in red wines was conducted, the white wines were analyzed using the procedure for red wines to demonstrate bisulfite addition has no direct effect on iron speciation. Results from the analysis of the white wines using the procedure for red wines were in agreement with results from their analysis as white wines (Table 2.2), suggesting that reducing the sample volume and adding sodium metabisulfite, as proposed for red wine analysis, does not affect iron speciation. Results for each wine were not found to be significantly different via *t*-test ($p > 0.05$).

Bisulfite has an extensive role in the wine oxidation pathway, reacting with quinones to regenerate their reduced phenol form or quenching hydrogen peroxide to preclude the Fenton reaction (Danilewicz 2016c). While it is possible such reactions could indirectly affect the iron(II):iron(III) ratio in wine, the results of this study suggest iron complexation with ferrozine and EDTA prevents changes to this ratio otherwise potentiated by the addition of bisulfite, further attesting to the stability of iron speciation conferred by the use of both complexing agents.

While bisulfite renders monomeric anthocyanins colorless, pyranoanthocyanins and polymeric pigments also contributing to absorbance in this range are resistant to such bleaching (Somers and Evans 1977). Therefore, the extent to which bisulfite addition can mitigate red wine color interference depends on the chemical composition and age of the wine sample; bleaching would be most effective in young red wines with higher levels of monomeric anthocyanins. However, interference in older wines due to pyranoanthocyanins and polymeric pigments is expected to be minimal because derived pigments undergo a hypsochromic shift in absorbance to a lower wavelength away from 562 nm (Bakker et al. 1997).

2.4.4 Comparison to FAAS. The use of ascorbic acid with ferrozine for total iron analysis yielded results in agreement with values obtained by FAAS (Tables 2.1 and 2.2), indicating the ascorbic acid was effective in reducing all iron to iron(II). For the red wines, the strong correlation suggests bisulfite addition to a smaller sample volume was an effective means of improving accuracy. While the intercept of the linear regression equation comparing the proposed method to FAAS is +0.2205, only two white wines (the 2014 white blend and 2015 Sauvignon blanc) were found via *t*-test to differ significantly in terms of total iron measured by the two methods ($p < 0.05$). Such deviations from FAAS are likely not a result of the proposed

method but may rather be explained by the formation of colored ferrozine complexes with metals other than iron, such as copper, magnesium and calcium (Stookey 1970), that may be found in particular wines at interfering levels.

2.4.5 Analytical Characteristics. Precision as CV was in the range of 1.1-10.1% for iron(II) measurements and 0.4-9.6% for total iron measurements. LOD and LOQ were found to be 0.02 mg/L and 0.06 mg/L respectively, well below typical iron concentrations in wine. Recoveries for iron(II) and total iron in the two red wine samples spiked with both iron(II) and iron(III) (1 mg/L each) were in the range of 103.5-110.1% (Table 2.3). The results suggest added iron(III) did not interfere with measurement of iron(II) and that oxidation of iron(II) was avoided by purging oxygen from the samples with nitrogen prior to spiking. Furthermore, total iron recoveries indicate the complete reduction of iron(III) to iron(II) by ascorbic acid.

Table 2.3 Recoveries of iron(II) and iron(III) spikes (1 mg/L each) in red wine samples (*n*=3).

	iron(II) (mg/L)			total iron(mg/L)		
wine	**initial**	**measured**	**recovery (%)**	**initial**	**measured**	**recovery (%)**
2016 red blend A	2.18 ± 0.09	3.24 ± 0.16	106.0	3.41 ± 0.04	5.48 ± 0.11	103.5
2016 red blend B	0.66 ± 0.04	1.75 ± 0.03	109.3	1.23 ± 0.04	3.43 ± 0.06	110.1

2.4.6 Method Demonstration. While previous studies have investigated the effects of oxygen exposure by saturating wine with air, it was thought continuous aeration in ambient conditions for this study would better simulate winery operations. The proposed method was used successfully during the oxygenation of red wine samples to demonstrate the method's fitness for purpose: to monitor changes to iron speciation over time. Oxygenation of these wines and the measurement of iron(II) was not done immediately at bottle opening and the extent of oxygen ingress prior was not controlled, thus the proportion of iron initially present as iron(II) was variable among the wines (58.8-90.8%).

The responsiveness of iron species to oxygenation (Figure 2.3) indicates the utility of iron speciation as a means of assessing the extent of oxygen ingress during cellar operations, storage, etc. (Danilewicz 2016b, 2018). While this can be assessed simply by measuring dissolved oxygen, iron speciation would serve as a

more direct measure of the potential of a wine to oxidize, given iron(III), not oxygen, reacts with phenols to trigger the wine oxidation pathway. While oxygenation was used in the present study to quickly induce measurable change in the iron(II):iron(III) ratio, reduction of iron should also be measurable using the proposed method. It is uncertain how quickly the iron(II):iron(III) ratio of wine would increase at low oxygen levels, though tracking an increase in iron(II) may be used to assess the reductive capacity of a wine that could be developed in the future. This method can thus provide winemakers with data to probe the extent of oxidation or reduction in their wines, particularly in the context of bottling, aging, and oxidative processes, e.g. micro-oxygenation and pumpovers.

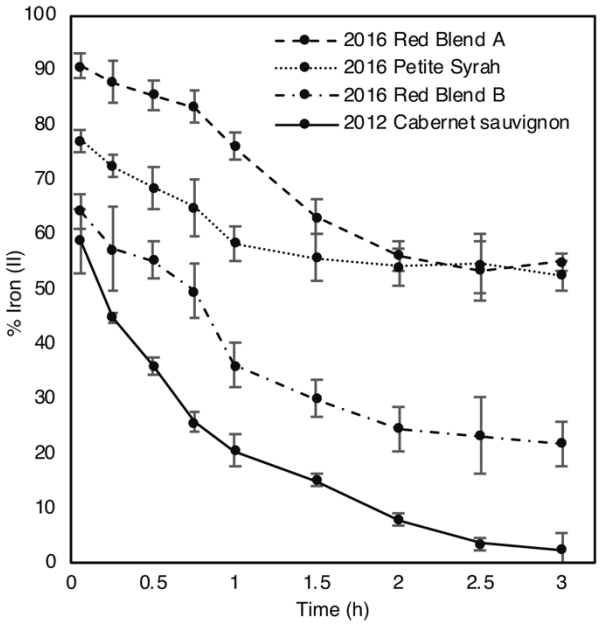

Figure 2.3 Change in the percentage of iron as iron(II) in four red wines during oxygenation; error bars indicate one standard deviation above and below the mean (*n*=3).

For three out of the four red wines, the decline in iron(II) with oxygenation appeared to plateau within 3 h, well before complete oxidation to iron(III). Similar declines in iron(II) have been observed for red and white wines saturated with air, though plateaus were reached after at least 40 h in the case of the white wines (Danilewicz 2016b, 2018). For the 2012 Cabernet sauvignon in the present study, oxidation appeared to go to completion, with only 2.4% of the iron present as iron(II) by 3 h. Given the current understanding of wine oxidation, it is possible the reductive phenols in the 2012 Cabernet sauvignon, older than the other wines studied and stored in a plastic bottle, were no longer present at sufficiently high concentrations to counter the oxidation of iron(II) to iron(III) by oxygen. Thus, this method may provide a means for further inquiry into the role of iron and phenols in wine oxidation; variability in the reactivity of wine phenols with iron, and the implications this may have on wine oxidation overall, remains an active area of investigation.

Chapter 3

Redox Cycling of Iron: Effects of Chemical Composition on Reaction Rates with Phenols and Oxygen in Model Wine

Published:

Nguyen TH and Waterhouse AL. 2021. Redox cycling of iron: Effects of chemical composition on reaction rates with phenols and oxygen in model wine. Am J Enol Vitic 72:209-216.

3.1 Abstract

Wine oxidation is mediated by the redox cycling of iron between two oxidation states: the oxidation of iron(II) by oxygen and reduction of iron(III) by phenols. The effects of phenolic structure, pH, and copper on the rates of these reactions were evaluated in model wine. In the absence of a nucleophile, pyrogallol exhibited greater reactivity with iron(III) than 4-methylcatechol. However, both compounds ultimately required aid from the nucleophile benzenesulfinic acid for unrestricted reduction of iron(III) to occur, illustrating the differential structure-dependent reactivities of phenols and the importance of nucleophiles to oxidation. It was hypothesized that the rate of oxygen consumption depends on the rate at which iron(II) is recycled from iron(III), though this was not found to be the case. While the rate of iron(III) reduction by 4-methylcatechol in the presence of benzenesulfinic acid decreased at higher pH, oxygen consumption was faster with increases in pH. Furthermore, copper had no effect on the rate of iron(III) reduction but significantly increased the rate of oxygen consumption, indicating the two reactions may not occur synchronously despite being coupled through iron. Pseudo-first order rate constants for oxygen consumption were much lower than those for iron(III) reduction except when nucleophiles were absent (unlikely in wine), suggesting that iron(II) oxidation is the rate-determining reaction for the wine oxidation pathway. Therefore, the rate at which wine ages is likely limited by oxygen ingress, not chemical composition. However, the overall capacity of wine for oxidation may still depend on constituent phenols and nucleophiles, and a method to assess these factors is of interest.

3.2 Introduction

The cascade of chemical reactions that occurs during wine aging starts with the oxidation of phenolic compounds into quinones coupled to the reduction of oxygen into hydrogen peroxide (Scheme 3.1) (Danilewicz 2003, Waterhouse and Laurie 2006). It is now well-established that phenols are oxidized through iron, not by oxygen directly. While phenols are singlet compounds, molecular oxygen is a diradical existing in a paramagnetic, triplet ground state, thus a direct reaction is spin-forbidden (Green and Hill 1984, Singleton 1987). The reaction cannot occur without the catalysis of transition metals, particularly iron, which circumvent the kinetic energy barrier associated with electron transfer (Miller et al. 1990). Studies in model wine have demonstrated oxygen consumption by phenols cannot occur without the inclusion of iron (Danilewicz 2007, 2011, Danilewicz and Wallbridge 2010). Furthermore, slowing of oxidation reactions in model and real wines has been observed with the addition of potassium ferrocyanide and other chelating agents, providing additional evidence for the central role of iron in wine oxidation (Danilewicz and Wallbridge 2010, Kreitman et al. 2013a, Nguyen and Waterhouse 2019).

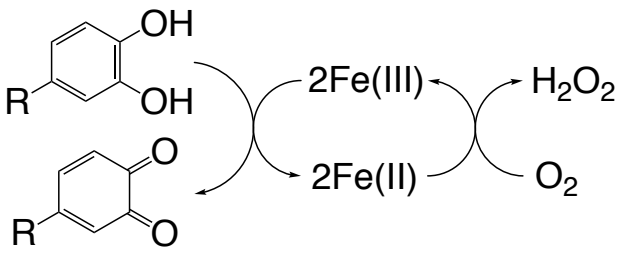

Scheme 3.1 Phenol oxidation coupled to the reduction of oxygen via redox cycling of iron.

With iron acting as an electron carrier between phenols and oxygen, the initial reactions of wine oxidation are characterized by the redox cycling of iron between two oxidation states: iron(II) and iron(III). Evidence for the redox cycling of iron stems primarily from studies in which oxygen consumption was monitored in air-saturated model wine. Oxygen consumption occurred with iron(II) in proportion to the concentration of iron(II) used, but not with iron(III). Following this initial phase of oxygen uptake attributable to iron(II) oxidation, consumption continued only with the reduction of iron(III) to regenerate the necessary iron(II) (Danilewicz 2011, Danilewicz and Wallbridge 2010, Danilewicz et al. 2008). In real wines, iron(III) has been found to accumulate following exposure to excess oxygen, although iron(II) becomes the predominant species during aging (Danilewicz 2016b, 2018, Nguyen and Waterhouse 2019), which suggests that

reduction by phenols occurs in typical storage conditions. These findings illustrate the key intermediary function of iron in the reaction between wine phenols and oxygen.

While oxygen consumption by iron(II) oxidation has been well studied, much less is known about the reciprocal process of iron(III) reduction by which wine phenols are oxidized. The rate at which this iron-phenol reaction occurs and the effect of chemical composition on this rate are unknown, as an evaluation of this reaction has never been attempted in wine. Iron speciation studies using excess oxygen to drive the oxidation of iron(II) showed that in most cases, the iron(II):iron(III) ratio stabilized before complete oxidation to iron(III) occurred (Danilewicz 2016b, 2018, Nguyen and Waterhouse 2019); therefore, wine phenols should be able to reduce iron(III) at an observable rate at least matching that of oxidation to effectively maintain a non-zero level of iron(II). Studying this reaction would furnish a more complete understanding of wine oxidation and potentially explain in part the differences observed among in the ageability of wines, i.e. their capacity to process oxygen and consequently undergo chemical changes during aging. Phenols are the primary substrate for wine oxidation, though wines can vary tremendously in phenolic content and composition. Reduction potentials vary among different phenolic compounds (Danilewicz 2003, 2012, Kilmartin et al. 2001, 2002), and studies conducted in non-wine matrices have demonstrated that the structure of phenolic compounds can govern their ability to complex with and reduce iron(III) (Mira et al. 2002, Moran et al. 1997).

In addition to evaluating the effects of phenolic structure on the rate of iron(III) reduction in wine conditions, this investigation also aimed to examine the relationship between iron(III) reduction and oxygen consumption. High pH wines are thought to oxidize more readily than low pH wines (Rossi and Singleton 1966, Singleton 1987), and oxygen consumption has been found to occur more quickly in model wine at pH 6.97 than at pH 3.6 (Danilewicz 2011), though such an evaluation within the range of typical wine pH (3.0 to 4.0) has not been performed. Copper is another factor that accelerates oxygen uptake and is thought to catalyze the reaction between iron(II) and oxygen, though the precise mechanism of this interaction is uncertain (Danilewicz 2003, 2013, Danilewicz and Wallbridge 2010). Given the cyclic nature of iron's role in the wine oxidation mechanism, pH and copper may affect the recycling of iron(II) from iron(III) by phenols, thereby indirectly dictating the rate of oxygen consumption as a consequence. It was hypothesized the rate

at which oxygen is consumed would depend on the rate at which iron(II) is replenished by phenols, thus conditions that accelerate iron(III) reduction would also accelerate oxygen consumption. To test this hypothesis, we evaluated and compared the kinetics of these two processes to ascertain which reaction is rate-determining for the wine oxidation pathway.

3.3 Materials and Methods

3.3.1 Chemicals and Reagents. Iron(III) chloride hexahydrate, L-(+)-tartaric acid, 3-(2-pyridyl)-5,6-diphenyl-1,2,4-triazine-p,p'-disulfonic acid monosodium salt (ferrozine), and ethylenediaminetetraacetic acid (EDTA) disodium salt dihydrate were purchased from Sigma-Aldrich. L-ascorbic acid and 4-methylcatechol were purchased from Aldrich Chemical Co., Inc. Sodium hydroxide and copper(II) sulfate pentahydrate were purchased from Fisher Scientific. Pyrogallol was purchased from HM Chemical Co., Ltd. Benzenesulfinic acid sodium salt was purchased from Acros Organics. Ethanol (200 proof) was purchased from Decon Labs. All chemicals used were of reagent grade.

Solutions of sodium hydroxide (5 N), iron(III) chloride (10.0 mM), copper(II) sulfate (1.0 mM), and ferrozine (3.5% m/v) were prepared in water. The EDTA (0.005% m/v) and ascorbic acid (0.1% m/v) solutions were prepared in model wine, which consisted of ethanol (12% v/v) and tartaric acid (8 g/L) in water, adjusted to pH 3.5 using sodium hydroxide (5 N). Deionized water purified using a Milli-Q Synthesis A10 system from Millipore was used in the preparation of all solutions.

3.3.2 Reduction of Iron(III). Model wines were prepared as above, though additional components were included and pH was adjusted according to the experimental treatments described below. The prepared wines were portioned (100 mL aliquots) into 125 mL glass serum bottles from Sigma-Aldrich. The bottles were fashioned with SP-PSt3-NAU oxygen sensors, which allowed for use of a Fibox 3 trace oxygen meter from PreSens to noninvasively monitor dissolved oxygen levels. The bottles were wrapped in black electrical tape to exclude light and sealed with aluminum crimp caps with polytetrafluoroethylene/butyl septa from Agilent Technologies, through which further sample manipulations could take place.

Nitrogen gas from Praxair was used to purge the samples of oxygen and was delivered through bottle septa via deflected point, 22-gauge stainless steel needles from Cadence Science; secondary outlet needles

allowed air to escape. When anoxic conditions were achieved (<0.06 mg/L dissolved oxygen), iron(III) was added (0.1 mM) to start the reaction by injecting 1 mL of iron(III) chloride solution (10 mM). Extraction of samples for iron speciation (1.0 mL) was done using needle and syringe and took place periodically over 3 h to track the reduction of iron(III) to iron(II). Oxygen levels were monitored to verify the integrity of septa in preventing oxygen ingress throughout sampling. Experiments took place at room temperature (22.2 ± 0.4 °C) and were conducted in triplicate.

3.3.2.1 Effects of Phenolic Structure and Benzenesulfinic Acid. Either 4-methylcatechol or pyrogallol were included during model wine preparation at 1.0 mM, with and without equimolar benzenesulfinic acid. The pH of these wines was adjusted to 3.5 using sodium hydroxide (5 N).

3.3.2.2 Effects of pH and Copper. The model wine system of 4-methylcatechol (1.0 mM) and benzenesulfinic acid (1.0 mM) was further studied at pH 3.0 and 4.0, in addition to pH 3.5. At each of these three pH levels, samples were prepared with and without copper (0.01 mM). Copper additions took place by injecting 1 mL of copper(II) sulfate solution (1.0 mM) through bottle septa immediately prior to the injection of iron(III).

3.3.3 Oxygen Consumption. Model wines were prepared with 4-methylcatechol (1.0 mM), benzenesulfinic acid (1.0 mM), and iron(III) (0.1 mM) as described above at pH 3.0, 3.5, and 4.0, with and without copper (0.01 mM). The wines were saturated with air and transferred into 300 mL biological oxygen demand bottles (DWK Life Sciences Wheaton) leaving no headspace. The samples were prepared in triplicate and stored in the dark at room temperature (22.2 ± 0.4 °C). Dissolved oxygen levels were measured periodically over several days via PreSens sensors and oxygen meter to track consumption.

3.3.4 Spectrophotometric Iron Speciation. Upon sample extraction, analysis was performed using a previously described spectrophotometric method for iron speciation in wine (Nguyen and Waterhouse 2019), using the procedures for analysis of white wines. An Agilent Technologies 8453 spectrophotometer was used for measurements and was operated using 845x UV-visible Chemstation software v. A.10.01[81]. Measurements were taken in disposable, semi-microvolume (3.0 mL), 1.0 cm pathlength, acrylic cuvettes from Sarstedt.

For the determination of iron(II), the samples (1.0 mL) were transferred into cuvettes containing 10 µL ferrozine (3.5% m/v) and mixed briefly, immediately after which 1500 µL EDTA (0.005% m/v) was added. For total iron analysis (performed once initially in a separate cuvette to verify iron had been correctly added to each sample at 0.1 mM), 1500 µL ascorbic acid (0.1% m/v) was used in place of EDTA. All absorbance measurements were taken at 562 nm against a model wine blank. Concentrations were calculated using an external calibration curve generated from a series of iron(II) standards in model wine (0.001 to 0.1 mM) measured in triplicate. Iron(III) levels were calculated by subtracting iron(II) from total iron.

3.3.5 Reaction Order and Rate Constant Determination. Reaction orders for iron(III) reduction and oxygen consumption were determined by plotting traces of these processes over time. All replicate data from each experimental treatment was included for linear least-squares regression analysis, done using Microsoft Excel v. 16.14. Rate constants (k) were calculated from the slope of lines best fitted to the data on the basis of maximizing coefficients of determination (R^2).

3.4 Results and Discussion

3.4.1 Differential Phenolic Reactivity with Iron(III). The level of iron used here (0.1 mM) approximates the global average concentration of iron in wine (5.5 mg/L) (Danilewicz 2007). The model phenols, 4-methylcatechol or pyrogallol, were included at 1.0 mM to ensure a molar excess relative to iron while also approximating the typical total phenolic content of white wines. Anoxic conditions were maintained throughout to enable monitoring of iron(III) reduction without interference from iron(II) oxidation.

In model wine at pH 3.5, 4-methylcatechol was unable to reduce iron(III) to any significant extent without aid from a nucleophile, with only 0.004 mM iron(II) detected by the end of the experiment (Figure 3.1). Pyrogallol reduced iron(III) to a greater extent, though iron(II) levels also appeared to plateau in the absence of a nucleophile and reached 0.033 mM by the end of the experiment. In tartrate buffer at pH 3.5, the reduction potential ($E_{3.5}$) of the iron(III)/iron(II) couple is 360 mV (Danilewicz 2003, Green and Parkins 1961), while $E_{3.5}$ values for the quinone/4-methylcatechol and quinone/pyrogallol couples are 547 and

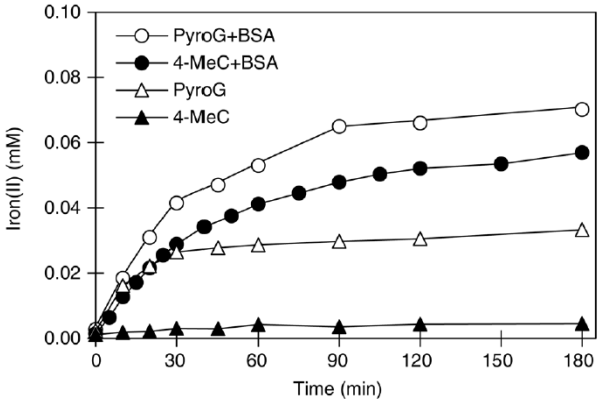

Figure 3.1 Iron(II) formation from iron(III) (0.1 mM) in anoxic model wine (12% ethanol v/v, 8 g/L tartaric acid, <0.06 mg/L dissolved oxygen) with 4-methylcatechol (4-MeC) or pyrogallol (PyroG) (1.0 mM) in the absence and presence of equimolar benzenesulfinic acid (BSA) at pH 3.5. Standard deviations at each timepoint did not exceed 0.002 mM iron(II) (n=3).

474 mV respectively. These values were calculated from data derived from polarographic measurements done in phosphate buffer at pH 6.72 (Horner and Geyer 1965), based on the knowledge that the reduction potential of phenolic compounds decreases by 59 mV per pH unit increase (Danilewicz 2003, 2012, Kilmartin et al. 2001). At pH 3.5, the cell potential (or potential difference, $\Delta E_{3.5}$) for the reduction of iron(III) is therefore -187 mV for 4-methylcatechol and -114 mV for pyrogallol. Negative values correspond to a positive change in Gibbs free energy (Equation 3.1), thus neither reaction is spontaneous in the forward direction, as evidenced here. In this equation, ΔG is the change in Gibbs free energy, n is number of electrons transferred, and F is the Faraday constant.

$$\Delta G = -nF\Delta E \qquad \text{(Equation 3.1)}$$

$$\Delta E = \frac{RT}{nF} \ln K_{eq} \qquad \text{(Equation 3.2)}$$

Iron(II) levels began to plateau at 30 min; therefore, concentrations at this timepoint were used to estimate equilibrium constants (K_{eq}) for the reduction of iron(III) by 4-methylcatechol (Reaction 3.1) and pyrogallol (Reaction 3.2) in the absence of benzenesulfinic acid. The stoichiometry of these reactions presumes two moles of iron(III) are reduced for each mole of either phenol oxidized. The Nernst equation (Equation 3.2) was used to calculate $\Delta E_{3.5}$ for these reactions from their observed K_{eq} values. In this equation, R is the gas constant and T is absolute temperature, while n and F are defined as above. Using 360 mV as $E_{3.5}$ for iron(III)/iron(II), values for the quinone/ 4-methylcatechol and quinone/pyrogallol couples may then be calculated from $\Delta E_{3.5}$ for

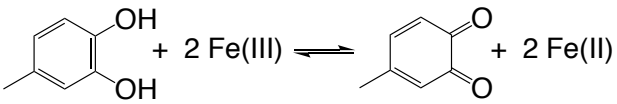

$K_{eq} = 1.56 \times 10^{-6}$ $\Delta E_{3.5} = -172$ mV

Reaction 3.1 Oxidation of 4-methylcatechol by iron(III).

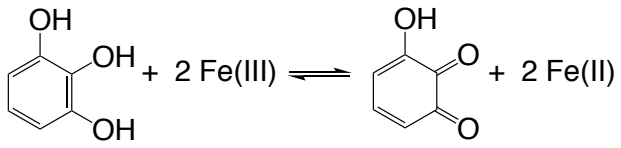

$K_{eq} = 1.74 \times 10^{-3}$ $\Delta E_{3.5} = -172$ mV

Reaction 3.2 Oxidation of pyrogallol by iron(III).

Reactions 3.1 and 3.2: the experimentally determined values here for $E_{3.5}$ are 532 mV for quinone/4-methylcatechol and 442 mV for quinone/pyrogallol. It should be noted the equilibrium constants used in calculating these reduction potentials were estimates, thus while these values are comparable to the aforementioned calculated values from polarography, discrepancies may be explained by the instability of quinones preventing true equilibrium between oxidation and reduction (Kilmartin et al. 2001).

In both cases when benzenesulfinic acid was included, iron(III) reduction was unrestricted (Figure 3.1). Other studies have demonstrated oxygen consumption in model wines cannot occur without the presence of a nucleophile to react with quinones as they are produced, thereby allowing phenol oxidation to occur in the thermodynamically disfavored forward direction per Le Chatelier's principle (Danilewicz 2003, 2011, Danilewicz and Wallbridge 2010, Danilewicz et al. 2008). The observations here reaffirm the function of nucleophiles in wine oxidation to aid phenols in providing the requisite iron(II) for oxygen consumption. Benzenesulfinic acid is not found naturally in wine but was used here as a model nucleophile, as has been done in previous studies to trap quinones (Cheynier et al. 1989, Danilewicz et al. 2008). The concentration used, equimolar to 4-methylcatechol or pyrogallol (1.0 mM), ensured all potential quinones could be effectively captured. Different wine nucleophiles, including glutathione, thiols, phloroglucinol (representing the A-ring of flavonoids), and amino acids, have been found to react at different rates with the quinone of 4-methylcatechol in model wine (Nikolantonaki and Waterhouse 2012). Notably, sulfur dioxide reacts more slowly than benzenesulfinic acid (Danilewicz et al. 2008). The ability of nucleophiles to trap quinones may be a factor in determining the rate of iron redox cycling (Danilewicz 2011). Therefore, results may differ if a different nucleophile and concentration had been used; future studies should investigate this possibility.

The greater reactivity of pyrogallol in comparison to 4-methylcatechol in the presence and absence of benzenesulfinic acid suggests phenolic structure has a significant effect on the rate of iron(III) reduction regardless of the nucleophile. The lower reduction potential of pyrogallol means it more readily loses electrons to iron(III), attributable to its third hydroxyl group, which confers additional stability to the

semiquinone radical intermediate formed prior to the quinone (Waterhouse and Laurie 2006). Furthermore, electron transfer from phenols to iron(III) requires the formation of a transient iron(III)-phenolate complex, from which the oxidized semiquinone/quinone and reduced iron(II) are subsequently released (Hynes and O'Coinceanainn 2001, Mentasti and Pelizzetti 1973, Perron and Brumaghim 2009). The third hydroxyl group of pyrogallol likely also aids in the formation of this complex with iron(III).

However, wine ageability may not be a matter of kinetics. If reactions were monitored for a much longer period of time (Figure 3.1), the difference between the reaction rates of pyrogallol and 4-methylcatechol would become immaterial, as both would eventually reduce the same amount of iron(III) provided a nucleophile such as benzenesulfinic acid is available. While pyrogallol serves as a model for 1,2,3-trihydroxy phenols (e.g. epigallocatechin and myricetin), and 4-methylcatechol serves as a model for ortho-dihydroxy phenols (e.g. caffeic acid and catechin), not represented here are monohydroxy, meta-dihydroxy, and methoxy-substituted phenols which are not as readily oxidized due to their inability to form stable semiquinones (Waterhouse and Laurie 2006). Cyclic and linear sweep voltammetry have been used to distinguish such phenolic fractions in wine based on their oxidizability. Findings have shown readily oxidized phenols constitute only a portion of the total phenolic content in wines (Kilmartin et al. 2001, 2002, Ugliano 2016), thus measures of total phenolic content (e.g. Folin-Ciocalteu assay, absorbance at 280 nm) likely do not reflect the oxidative capacity of wines.

Phenolic reactivity may still be diagnostic of wine age and ageability. Voltammetric analysis of wines has revealed anodic peak current intensities at certain voltages decrease with age and/or oxygen exposure, suggesting the exhaustion of oxidizable substrate (Gonzalez et al. 2018, Kilmartin et al. 2002, Martins et al. 2008, Rodrigues et al. 2007). Attending expressly to the reaction of phenols in the oxidation pathway, their ability to reduce iron(III) may similarly reflect wine age, as findings from a recent iron speciation study showed that while the majority of wines evaluated under continuous aerial oxygenation were able to maintain a non-zero level of iron(II), one much older wine that had been stored in a plastic bottle was found unable to prevent the complete oxidation of iron(II) to iron(III) (Nguyen and Waterhouse 2019). However, the results here with regard to the effects of benzenesulfinic acid suggest the loss of phenolic reactivity could also be attributed to the depletion of nucleophiles, which evidently can play a similarly significant a role as phenolic

compounds in wine oxidation. Therefore, if wine age and ageability are to be evaluated quantitatively, accounting for the differential reactivity of phenolic compounds and their dependence on nucleophiles remains a challenge. A measurement of wine's reactivity with iron, similar in principle to the ferric reducing antioxidant power assay (Benzie and Strain 1996, Katalinic et al. 2004), warrants further investigation as a potential means of assessing oxidizability.

3.4.2 Iron(III) Reduction Rates. Despite the ten-fold molar excess of 4-methylcatechol relative to iron(III), reduction of iron(III) in the presence of benzenesulfinic acid could not be neatly characterized as a pseudo-first order reaction with respect to iron(III) based on linear regression analysis of the decline in iron(III) over time; the reaction also did not fit zeroth or second order kinetics. However, the natural log graphs of iron(III) reduction exhibited two distinct linear phases, as shown for pH 3.5 (Figure 3.2), which suggests that the reduction of iron(III) here is biexponential. Such kinetics may be attributed to two processes occurring together upon the addition of iron(III) to the system: while 4-methylcatechol can initially reduce iron(III) at a particular rate, complexation of iron(III) by tartrate gradually decelerates this reaction. Given electron transfer from 4-methylcatechol to iron(III) is predicated upon complex formation, its rate of reaction with iron(III) is likely dampened by competition from tartrate for the coordination sites of iron(III). Separate rate constants (k1 and k2) were calculated for the two phases of iron(III) reduction for each experimental treatment under the presumption of pseudo-first order kinetics for the individual phases (Table 3.1).

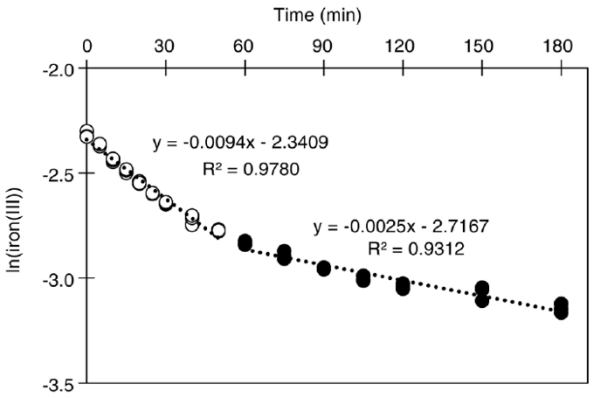

Figure 3.2 Natural log of iron(III) reduction (0.1 mM) in anoxic model wine (12% ethanol v/v, 8 g/L tartaric acid, <0.06 mg/L dissolved oxygen) with 4-methylcatechol (1.0 mM) and benzenesulfinic acid (1.0 mM) at pH 3.5 (n=3).

It is worth noting that the reaction between benzenesulfinic acid and the quinone of 4-methylcatechol produces an adduct with regenerated dihydroxy functionality (Reaction 3.3) (Danilewicz et al. 2008) that is capable of reacting again with iron(III). The effect of the benzenesulfinate group on the reactivity of this

adduct is unclear, though the effect here on the observed rate of iron(III) reduction is expected to be insignificant because the original 4-methylcatechol is present at a much higher concentration relative to the adduct. Electron-withdrawing or sterically bulky nucleophiles in wine would produce less reactive adducts, the buildup of which over time may contribute to the loss of ageability.

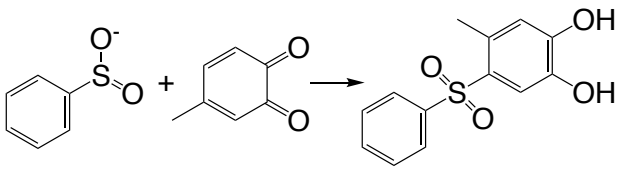

Reaction 3.3 Adduct formation from benzenesulfinic acid and 4-methylcatehol.

Table 3.1 Pseudo-first order rate constants (1/min) for iron(III) reduction and oxygen consumption in model wine (12% ethanol v/v, 8 g/L tartaric acid) containing 4-methylcatechol (1.0 mM) and benzenesulfinic acid (1.0 mM). k1 and k2 are the respective rate constants for the first and second phases of iron(III) reduction caused by tartrate complexation.

pH	Copper (mM)	Iron(III) Reduction			Oxygen Consumption
		k1	k2	(k1+k2)/2	k
3.0	--	1.7E-02	4.7E-03	1.1E-02	7.5E-05
	0.01	1.6E-02	3.1E-03	9.5E-03	3.9E-04
3.5	--	9.4E-03	2.5E-03	6.0E-03	1.4E-04
	0.01	1.0E-02	3.0E-03	6.6E-03	5.5E-04
4.0	--	7.5E-03	2.4E-03	5.0E-03	2.9E-04
	0.01	7.6E-03	2.5E-03	5.1E-03	7.5E-04

The reduction potential of quinone/phenol couples decreases as pH increases because quinone formation entails the loss of both electrons and protons (Danilewicz 2003, 2012, Kilmartin et al. 2001). Furthermore, the anionic phenolate forms of phenolic compounds, more prevalent in alkaline conditions, are thought to be more susceptible to oxidation than their protonated conjugates (Rossi and Singleton 1966, Singleton 1987). Based on this information, electron transfer to iron(III) was expected to occur more quickly with higher pH, though this was not found to be the case: the rate of iron(III) reduction by 4-methylcatechol in the presence of benzenesulfinic acid was lower at pH 4.0 than at pH 3.0 (Table 3.1, Figure 3.3). These results suggest the proportion of phenolates is not significant to wine oxidation in this pH range. While the

reduction potential for the quinone/ 4-methylcatechol couple decreases by 59 mV per pH unit increase, that of the iron(III)/iron(II) couple decreases by 130 mV per pH unit increase (Green and Parkins 1961). Due to increased deprotonation of tartaric acid into tartrate, which preferentially stabilizes iron(III) over iron(II) (Danilewicz 2014, Timberlake 1964a), ΔE for the reaction becomes increasingly negative with higher pH. Reduction potentials appear to predict reaction rates for pH-dependent redox reactions (Michaelis and Smythe 1931, Smythe 1931), though they are a thermodynamic property and should not be used to explain reaction rates, which describe kinetics.

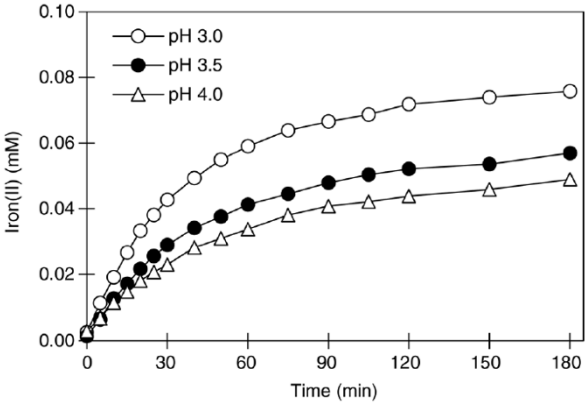

Figure 3.3 Iron(II) formation from iron(III) (0.1 mM) in anoxic model wine (12% ethanol v/v, 8 g/L tartaric acid, <0.06 dissolved oxygen) with 4-methylcatechol (1.0 mM) and benzenesulfinic acid (1.0 mM) at various pH. Standard deviations at each time point did not exceed 0.002 mM iron(II) (n=3).

While phenolates do become more abundant with higher pH, the effective concentration of iron(III) may be lowered due to tartrate complexation. Dimeric and trimeric iron(III)-tartrate complexes, which are more prevalent with higher pH (Timberlake 1964a, Yokoi et al. 1994), may be particularly effective at blocking phenols from complexing and reacting with iron(III). Furthermore, the occurrence of intra-complex electron transfer has been found to be pH-dependent. While mono (1:1) iron(III)-phenolate complexes predominate in acidic conditions (pH < 4.0) are redox-active, the bis (1:2) and tris (1:3) complexes arising in more basic conditions appear to be stable against redox decomposition (Avdeef et al. 1978, Hider et al. 2001, Perron and Brumaghim 2009, Powell and Taylor 1982). The stability of such complexes in alkaline conditions provides the basis for the ferric chloride test for phenols, as used in the Adams-Harbertson assay for tannin quantification in wine (Harbertson et al. 2003), and may explain in part the diminished rate of iron(III) reduction observed at higher pH.

The level of copper used here (0.01 mM) equates to 0.6 mg/L and constitutes an extreme scenario in which the legal limit for residual copper in wine (0.5 mg/L), as defined in the US Code of Federal Regulations (§24.246), has been exceeded. The inclusion of copper at this concentration did not discernibly affect the

rate of iron(III) reduction at all three pH levels (Table 3.1), despite previous studies showing that copper increased rates of oxygen consumption (Danilewicz 2013, Danilewicz and Wallbridge 2010).

3.4.3 Oxygen Consumption Rates. In monitoring oxygen levels in air-saturated model wines of the same compositions as above, rates of oxygen consumption increased with higher pH and with the inclusion of copper (Table 3.1), disproving our hypothesis that rates of oxygen consumption and phenol oxidation are linked. These two processes may be coupled by the redox cycling of iron but do not necessarily occur synchronously. Faster oxygen consumption observed with higher pH may be attributed to iron(II) oxidation independent of its recycling from iron(III) by phenols. Although tartrate forms more stable complexes with iron(III), complexes with iron(II) also become more abundant as pH increases. The extraction of an electron from an electrically neutral iron(II)-tartrate complex is far less energetically demanding than the oxidation of a free iron(II) cation (Michaelis and Smythe 1931, Smythe 1931). With regards to the effects of copper, these findings indicate it facilitates the reaction between iron(II) and oxygen, as has been suggested previously, but not the reaction between iron(III) and phenols. The precise mechanism by which copper catalyzes the oxidation of iron(II) has yet to be determined, although copper may also participate in redox cycling by coupling iron(II) oxidation to the reduction of oxygen, or it may form a cationic copper(I)-dioxygen intermediate that more readily oxidizes iron(II) (Danilewicz 2007). The formation of a binuclear iron-copper complex capable of reacting more rapidly with oxygen is also possible (Danilewicz and Wallbridge 2010). In previous studies attempting to correlate rates of oxygen consumption with the chemical compositions of red, white, and rosé wines, pH and copper consistently exhibited a positive relationship with oxygen consumption. Interestingly, correlations with most other parameters, notably aspects of phenolic content and composition, were inconsistent or negative (Carrascon et al. 2017, 2018, Ferreira et al. 2015).

As has been reported previously in white wines (Gonzalez et al. 2018), oxygen consumption here appeared to follow pseudo-first order kinetics, despite addition of iron to the model wines in the form of oxidized iron(III) at a concentration not in excess relative to the initial concentration of oxygen at air-saturation. In the abovementioned correlational studies employing repeated air-saturation cycles (Carrascon et al. 2017, Ferreira et al. 2015), reaction order was not determined but the kinetics of oxygen uptake were consistent upon each saturation, which, according to the study authors, implies that iron(III) is “spontaneously”

reduced at the end of each cycle. However, the direct oxidation of iron(II) by oxygen is not the only means by which oxygen is consumed in the wine oxidation pathway. After formation of hydrogen peroxide and the Fenton oxidation of ethanol, oxygen can add to the intermediate 1-hydroxyethyl radical to form the 1-hydroxyethylperoxyl radical, which ultimately decomposes to yield acetaldehyde (Elias and Waterhouse 2010). Given the catalytic role of iron(II) in the Fenton reaction, this secondary point of entry for oxygen does still constitute the oxidation of a molar equivalent of iron(II), albeit indirectly. The effects of wine composition on the rates of these reactions remain to be elucidated.

The results here in the model system of 4-methylcatechol and benzenesulfinic acid confirm a supply of iron(II) can be effectively maintained so as not to limit the rate of oxygen consumption: rate constants for iron(III) reduction were significantly higher than those for oxygen consumption in all cases (Table 3.1). While the effect of different nucleophiles on the rate of iron(III) reduction is unclear, sulfur dioxide significantly decreases the rate of oxygen consumption. The difference in rate constants would be even more apparent, as the quenching of hydrogen peroxide by sulfur dioxide would eliminate post-Fenton reaction oxygen consumption and increase the availability of iron(II). Together with our results, this suggests iron(II) oxidation is the rate-determining reaction for the wine oxidation pathway. However, the ability of wine to reduce iron(III) likely declines as it ages, whether by exhaustion of phenols or of nucleophiles, such that it eventually limits the rate of oxygen consumption.

The relative rates of iron oxidation and reduction may explain the poor correlation noted previously between oxygen consumption and wine composition, as well as the high iron(II):iron(III) ratios (Danilewicz 2016b, 2018, Nguyen and Waterhouse 2019) and low oxygen levels (Castellari et al. 2004, del Alamo-Sanza and Nevares 2014, 2018, Vidal et al. 2017) commonly observed for wines in storage. Evidently, wine effectively maintains reductive conditions, and oxygen is very rarely in constant excess (e.g. defective closures or packaging). It follows that wine is constantly primed to receive more oxygen and therefore ages at a rate limited by oxygen ingress and not by the reactions therein (Danilewicz 2018).

The outcome of oxidation varies among wines, given the accumulation of different chemical products responsible for changes to color, flavor, and mouthfeel is a function of initial composition. However,

variability in the rate at which wines undergo such changes may be attributed largely to differences in oxygen ingress, which initiates iron(II) oxidation and determines the rate for the remainder of the pathway. Given that oxygen is seldom in constant excess during winemaking and aging, future studies pertaining to wine ageability should focus on maximum quantity of oxygen consumption, perhaps before a particular chemical or sensory threshold is reached, rather than on rate of oxygen consumption.

Chapter 4

Controlling the Fate of Hydrogen Peroxide in Wine through Complexation of Iron by Wine Acids

4.1 Abstract

At a key branchpoint in the wine oxidation pathway, hydrogen peroxide may react either with iron(II), leading to the Fenton oxidation of ethanol into acetaldehyde, or with sulfur dioxide, precluding oxidation. The fate of H_2O_2 was investigated in anoxic model wines with varied pH (3.0 and 4.0) and acid composition (tartaric, malic, citric, and a 12:12:1 blend) to determine the effects these parameters have on the relative reaction rates of H_2O_2 with iron(II) and SO_2. In the absence of SO_2, anoxic conditions allowed the stoichiometric production of acetaldehyde from H_2O_2. Decomposition of H_2O_2 followed pseudo-first order kinetics and iron(II):iron(III) ratios never approached zero, despite iron(II) being limiting, indicating the efficient redox cycling of iron in anoxia; the effects of oxygen warrant investigation. Initial rates of acetaldehyde production and declines in iron(II):iron(III) ratios were positively correlated (Pearson's r = 0.940). Acetaldehyde production occurred more quickly at pH 4.0 than at pH 3.0, attributable to increased complexation of iron by the wine acids, as well as the pH-sensitive mechanism by which the 1-hydroxyethyl radical intermediate is converted to acetaldehyde. Acetaldehyde production and changes to iron(II):iron(III) ratios occurred most rapidly in the model wine buffered with citric acid, while the relative effects of tartaric and malic acid were pH-dependent, likely due to differences in the stabilities of their complexes with iron. The inclusion of SO_2 significantly reduced acetaldehyde formation and diminished the differential effects of these acids and pH. Results suggest viticultural and enological practices, as they pertain to the management of wine acidity, may have significant repercussions on the kinetics of wine oxidation.

4.2 Introduction

Oxygen ingress, whether during cellar operations or aging, changes the chemical profile of wine, consequently altering sensory attributes such as color, flavor, and mouthfeel. The cascade of chemical reactions constituting wine oxidation begins with the reduction of oxygen coupled to the oxidation of phenols through the redox cycling of iron between two oxidation states: iron(II) and iron(III) (Danilewicz 2003, 2007, 2011, 2013). Findings from a recent study conducted in model wine suggest the rate-determining reaction for the wine oxidation pathway is iron(II) oxidation (Nguyen and Waterhouse 2021); therefore, the rate of oxygen ingress likely dictates the rate of aging overall (Danilewicz 2018). Despite this, different wines subject to the same oxidative conditions will often vary in the extent to which they develop oxidized character and in the rate at which they do so. One explanation may lie "downstream" at a key branchpoint in the oxidation pathway.

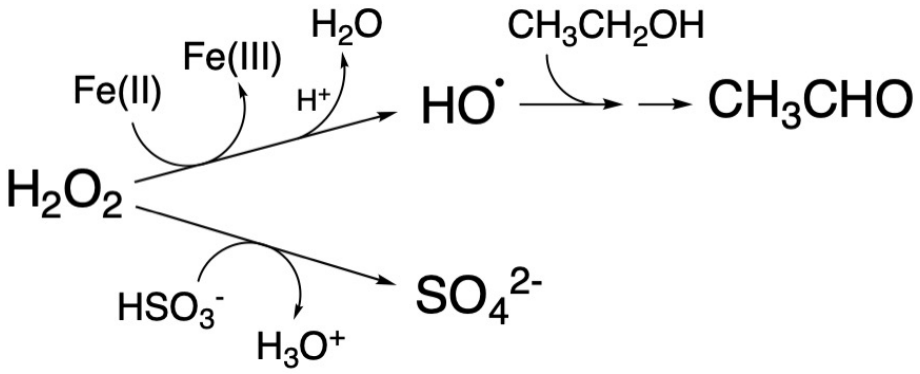

Scheme 4.1 Branchpoint for hydrogen peroxide in the wine oxidation pathway: Fenton oxidation of ethanol (top) or quenching by bisulfite (bottom).

As iron(III) is reduced to iron(II), the loss of electrons from phenols generates quinones, electrophiles which react with nucleophilic species found in wine, namely thiols and other phenols (Nikolantonaki and Waterhouse 2012). The reciprocal oxidation of iron(II) to iron(III) provides the electrons to convert oxygen into hydrogen peroxide (H_2O_2) (Waterhouse and Laurie 2006), which can react in one of two ways: decomposition by iron(II) to the hydroxyl radical ($HO^{\bullet}$) in the Fenton reaction, or quenching by sulfur dioxide (SO_2, as bisulfite, HSO_3^-) to yield sulfate (SO_4^{2-}) (Elias and Waterhouse 2010) (Scheme 4.1). Hydroxyl radicals are highly unstable species which react immediately with any substances present in solution in proportion

to their concentrations (Buxton et al. 1988). Given its relative abundance in wine, ethanol (CH_3CH_2OH) is a prime target for oxidation, and through a series of radical intermediates is converted into acetaldehyde (CH_3CHO) (Elias et al. 2009). In addition to impacting wine aroma, acetaldehyde can react with flavonoids, such as anthocyanins and flava-3-ols, to produce pigments and pyranoanthocyanins, as well as ethylidene-bridged polymers (de Freitas and Mateus 2011, Drinkine et al. 2007, Mateus et al. 2002). In its capacity as an antioxidant, SO_2 protects wine from this oxidative cascade of reactions essentially by competing against iron(II) for H_2O_2. Dissolved oxygen levels and catechol content have been shown to control this branchpoint in tartrate- and phosphate-buffered model wines (Elias and Waterhouse 2010), though the potential effects of other factors such as pH and iron complexation have not been investigated.

Wine ageability is commonly discussed in terms of its sensory properties, with acidity often touted as a key predictor of an age-worthy wine. Additions of tartaric, malic, and citric acid to Aglianico wine were recently found to alter the outcome of oxidation, each variably altering parameters such as hue and astringency (Picariello et al. 2019). One mechanism by which these acids may exert their influence on wine oxidation is through complexation of iron, which determines the reduction potential of iron and consequently its ability to redox cycle and function as a catalyst. The prevailing pH further modulates iron's reactivity by controlling the protonation states of these chelators (Danilewicz 2003, 2014, Green and Parkins 1961).

It is hypothesized that complexation of iron by the organic acids found in wine, by controlling iron's reduction potential, influences whether H_2O_2 reacts in the Fenton oxidation of ethanol or is quenched by SO_2. However, the precise nature and direction of this effect is uncertain, as conflicting information regarding the role and function of acids is presented in the published literature, most of which has been derived from studies taking place in non-wine matrices. In studies pertaining to the degradation of organic matter in natural surface waters and fungal rot, respectively, fulvic acid and oxalic acid were found to increase the rate of H_2O_2 decomposition in the Fenton reaction (Voelker and Sulzberger 1996, Park et al. 1997). It has been proposed that complexation of iron(II) facilitates its oxidation by counterbalancing its positive charge (Smythe 1931). However, the opposite effect of acids on the Fenton reaction has also been reported: for the purposes of geological remediation, phytic, citric, and malonic acid have been found to moderate the decomposition of H_2O_2 such that it can better penetrate through the earth to reach subsurface

contaminants (Watts et al. 2007). It is possible that occupation of the coordination sites of iron(II) protects it against oxidation (Kolthoff and Medalia 1949a), effectively lowering the concentration available to react with H_2O_2. It has also been proposed that complexation of the oxidized iron(III) form hinders its reduction (Kreitman et al. 2013a), thereby limiting the regeneration of iron(II) needed for the Fenton reaction to proceed.

The purpose of this investigation was to determine the effects of pH and acid composition on the fate of H_2O_2 added to several anoxic model wine systems. This was done to approximate conditions in which oxygen ingress is rate-limiting, and oxygen is presumably quickly reduced to H_2O_2. Differential acetaldehyde formation and changes to the iron(II):iron(III) ratio in these wines are reported.

4.3 Materials and Methods

4.3.1 Chemicals and Reagents. L-(+)-tartaric acid (≥99.7%, food grade), L-(-)-malic acid (≥99%, ReagentPlus), citric acid (99%), 3-(2-pyridyl)-5,6-diphenyl-1,2,4-triazine-p,p'-disulfonic acid monosodium salt hydrate (ferrozine, 97%), ethylenediaminetetraacetic acid (EDTA) disodium salt dihydrate (99.0-101.0%, ACS reagent), potassium metabisulfite (≥98%), sodium hydroxide, hydrochloric acid, and sulfuric acid were purchased from Sigma-Aldrich. Acetonitrile (Optima LC-MS), formic acid (Optima LC-MS), and hydrogen peroxide (3% w/v, certified) were purchased from Fisher Scientific. Acetaldehyde (99.5%, ACS reagent) and 2,4-dinitrophenylhydrazine (30% water w/w) were purchased from Spectrum Chemical. The 2,4-dinitrophenylhydrazine was purified by recrystallization from acetonitrile according to US EPA Method 8315A (SW-846) (1996). Ferrous sulfate heptahydrate (ACS reagent) was purchased from Macron Fine Chemicals and ethanol (200 proof) was purchased from Decon Labs. Deionized water purified using a Milli-Q Synthesis A10 system (Millipore) was used in the preparation of all solutions unless otherwise noted.

4.3.2 Model Wine Preparation and Experimental Procedures. Model wines were prepared with 12% (v/v) ethanol. With regards to acid content, experimental treatments were as follows: 50 mM tartaric acid, 50 mM malic acid, 50 mM citric acid, or a 12:12:1 blend of these acids totaling 50 mM. The pH of these wines was adjusted to either 3.0 or 4.0 using sodium hydroxide (5 N).

4.3.2.1 Reactions in the Absence of Sulfur Dioxide. For each experimental treatment combination of acid and pH level, model wine was portioned (100 mL aliquots) into 250 mL Erlenmeyer flasks. The wines were stirred continuously with nitrogen gas from Praxair (industrial grade, 99.995%) dispersed via bubbling stones for the duration of each experiment. Dissolved oxygen was monitored using a dipping probe (DP-PSt3) and Fibox 3 LCD trace V7 oxygen meter from PreSens (Precision Sensing GmbH). When anoxic conditions were achieved (<0.1 mg/L dissolved oxygen), iron(II) was added at 100 μM from a 50 mM stock solution (in 0.1 N hydrochloric acid to stabilize against oxidation). Then H_2O_2 was added at 600 μM from the 3% stock solution, the concentration of which was confirmed spectroscopically at 240 nm using an extinction coefficient of 40 M^{-1} cm^{-1} (Elias and Waterhouse 2010). Experiments took place at room temperature (22.6 ± 0.2 °C) and were conducted in triplicate. Acetaldehyde analysis and iron speciation were conducted once prior to H_2O_2 addition, then afterward over the course of 360 s.

4.3.2.2 Reactions in the Presence of Sulfur Dioxide. Model wines were prepared and experiments were performed as above, but with the inclusion of SO_2 at 600 μM using a freshly prepared 75 mM stock solution from potassium metabisulfite. The addition of SO_2 took place after iron(II) addition and before H_2O_2 addition. Iron speciation was conducted once prior to H_2O_2 addition, then afterward at 30 and 90 s. Acetaldehyde analysis was conducted once prior to H_2O_2 addition, then only once again at 90 s.

4.3.3 Acetaldehyde Analysis. Acetaldehyde was analyzed as its 2,4-dinitrophenylhydrazone derivative by high-performance liquid chromatography (HPLC) (Han et al. 2015), with minor modifications to the published procedure. Samples (200 μL) were dispensed into 2 mL HPLC vials (Thermo Scientific) already containing 40 μL SO_2 (1140 mg/L, freshly prepared from potassium metabisulfite) to immediately quench H_2O_2 reactions, after which 40 μL of sulfuric acid (25% v/v) and 280 μL 2,4-dinitrophenylhydrazine reagent (in acetonitrile, saturated) were added. The vials were placed into a 65 °C water bath for 20 min for derivatization. Samples were then diluted 1:1 with formic acid (0.5% v/v) and filtered through 0.45 μm polytetrafluoroethylene, 13 mm, syringe tip filters (VWR International).

Analysis was conducted using an HP 1100 series HPLC from Agilent Technologies coupled to a diode array detector. A Zorbax Rapid Resolution HT SB-C18 1.8 μm particle size, 4.6 x 100 mm column was used for

separation. HPLC conditions were as follows: injection volume 15 µL, flowrate 0.75 mL/min, column temperature 35 °C. Mobile phases A (0.5% formic acid v/v) and B (acetonitrile) were used with the following gradient elution protocol: 35% B at 0 min, 60% B at 8 min, 95% B at 13 min (2 min hold), 35% B at 16 min (4 min hold); total runtime was 20 min. Detection took place at 365 nm. Agilent ChemStation software v. A.10.02[1757] was used for HPLC operation and peak integration.

Quantitation was done using an external calibration curve from a series of acetaldehyde standards (10-1000 µM) in model wine (12% ethanol v/v, 50 mM tartaric acid, pH 3.5), prepared in triplicate. Due to the presence of trace acetaldehyde in model wine, all standard peak areas were corrected using a model wine blank. Experimental acetaldehyde concentrations were similarly adjusted by subtracting the acetaldehyde detected at time zero (prior to H_2O_2 addition), such that measurements at time zero were normalized to 0 µM acetaldehyde for all experimental treatments; therefore, subsequent concentrations reported here indicate the acetaldehyde *produced* following H_2O_2 addition.

4.3.4 Iron Speciation. Iron(II) levels were determined according to a previously described spectrophotometric method for iron speciation in wine (Nguyen and Waterhouse 2019), using the procedures for white wine analysis with minor modifications. Samples (1000 µL) were dispensed into disposable, 4.5 mL, 1.0 cm pathlength, acrylic cuvettes (Fisher Scientific) containing 10 µL ferrozine (3.5% m/v), immediately after which 1500 µL EDTA (0.005% m/v) was added and mixed. Absorbance measurements were taken at 562 nm against a model wine blank (12% ethanol v/v, 50 mM tartaric acid, pH 3.5, with ferrozine and EDTA as above) using an Agilent Technologies 8453 spectrophotometer, operated using 845 UV-Visible ChemStation software v. A.10.01[81]. Quantitation was done using an external calibration curve from a series of iron(II) standards (1-100 µM) in model wine, analyzed in triplicate. The molar extinction coefficient here for iron(II)-ferrozine was checked against published values (Danilewicz 2016b, Stookey 1970). Analysis at time zero (prior to H_2O_2 addition) confirmed the addition of 100 µM iron, present at the start of each experiment entirely as iron(II) (± 2 µM).

4.3.5 Reaction Rate Determinations. Concentrations of H_2O_2 were calculated based on acetaldehyde production ($[H_2O_2]$ = 600 µM – [acetaldehyde]) for the purposes of reaction order and rate constant

determination (in the absence of SO_2), which was done by linear least-squares regression analysis of H_2O_2 traces over time using Microsoft Excel v. 16.14. Initial rates of acetaldehyde production and change to the iron(II):iron(III) ratio were calculated as the slope between concentrations at time zero and the next analytical timepoint; the absolute value of the slope was used for the apparent rate of change to iron speciation given the net decrease in iron(II) with oxidation.

4.3.6 Statistical Analysis. Comparisons of acetaldehyde production (rates in the absence of SO_2, concentrations in the presence of SO_2) between experimental treatments were performed using Welch's *t*-test (α = 0.05). Rates of change to the iron(II):iron(III) ratio were also compared between treatments in the same manner. Relationships between acetaldehyde production and apparent iron(II) oxidation rates were assessed by calculating Pearson's correlation coefficient (Pearson's *r*). These analyses were done using Microsoft Excel v. 16.14.

4.4 Results and Discussion

4.4.1 Iron Redox Cycling and Acetaldehyde Production. A recent investigation into the redox cycling of iron in model wine revealed rates of iron(III) reduction to be at least an order of magnitude greater than rates of oxygen consumption under wine-relevant conditions, suggesting a supply of iron(II) can effectively be maintained so as not to limit the consumption of oxygen (Nguyen and Waterhouse 2020). Along with the high iron(II):iron(III) ratios (Danilewicz 2016b, 2018, Nguyen and Waterhouse 2019) and low oxygen levels commonly observed for real wines in storage (Castellari et al. 2004, del Alamo-Sanza and Nevares 2014, 2018, Vidal et al. 2017), this supports the notion that the rate of wine oxidation is limited by oxygen ingress (Danilewicz 2018). For the present study, anoxic conditions (<0.1 mg/L dissolved oxygen) and hydrogen peroxide addition were employed to approximate such aging scenarios in which what oxygen enters wine is readily reduced into H_2O_2. Furthermore, as was observed by Elias and Waterhouse (2010) in similar model wine systems, the absence of oxygen enabled the stoichiometric production of acetaldehyde from H_2O_2.

Across all experimental treatments here in the absence of sulfur dioxide, peak concentrations of acetaldehyde ranged from 596 to 637 μM (Figure 4.1), indicating the complete reaction of H_2O_2 (600 μM) despite the much lower concentration of iron(II) initially available (100 μM). This iron level approximates

the global average iron concentration in wine (Danilewicz 2007), and the molar ratio of 1:6 for iron(II) to H_2O_2, used previously by Elias and Waterhouse (2010), closely approximates the ratio of 0.147 found to be optimal for hydroxyl radical formation in salicylic acid solution at pH 3.0-4.0 (Chang et al. 2008). It should be noted, however, that the concentration of H_2O_2 used here for the sake of experimentation equates to the instantaneous consumption and reduction of 19.2 mg/L oxygen, far more than is possible under real wine aging conditions.

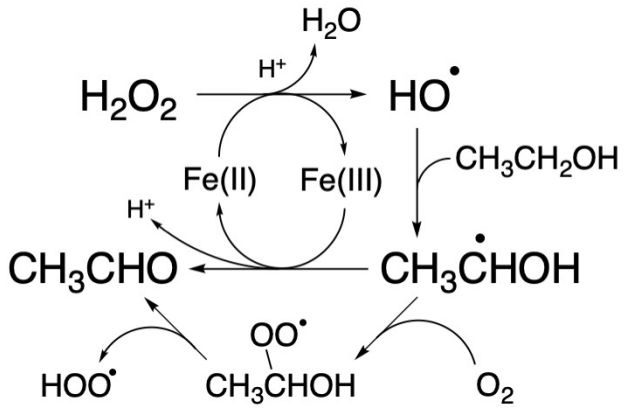

Scheme 4.2 Fenton oxidation of ethanol in the presence and absence of oxygen.

The slight declines in acetaldehyde observed by 360 s may be attributed to volatilization, given the samples were stirred continuously with nitrogen throughout the course of the experiment. In the presence of oxygen, the 1-hydroxyethyl radical (CH_3•CHOH) produced upon the oxidation of ethanol by the Fenton-derived hydroxyl radical is thought to react with oxygen to form the 1-hydroxyethylperoxyl radical (CH_3CH[-OO•]OH), which presumably decomposes to yield acetaldehyde and a hydroperoxyl radical (HOO•). It has been proposed this reaction pathway precludes the regeneration of iron(II) required for the continued decomposition of H_2O_2 in the Fenton reaction (Scheme 4.2). The absence of oxygen allows the 1-hydroxyethyl radical to instead rapidly reduce iron(III) to iron(II), allowing total H_2O_2 consumption and conversion to acetaldehyde (Elias and Waterhouse 2010, Kolthoff and Medalia 1949a, 1949b). The recycling of iron by the 1-hydroxyethyl radical is further evidenced by the non-zero iron(II):iron(III) ratios observed throughout the course of acetaldehyde formation; iron(II) was never completely oxidized to iron(III) in all cases despite the six-fold excess of H_2O_2 (Figure 4.2).

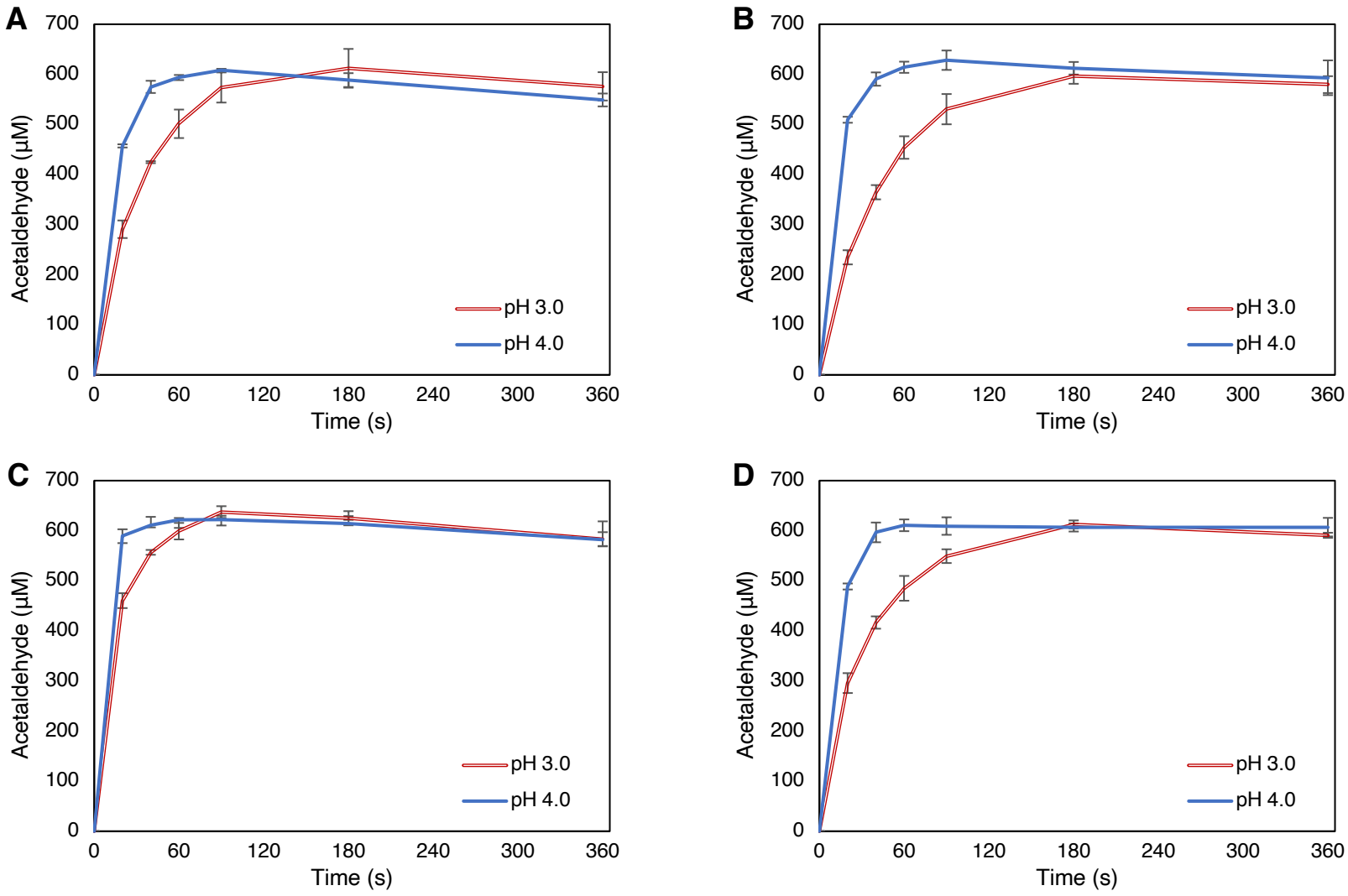

Figure 4.1 Acetaldehyde formation following the addition of 600 µM hydrogen peroxide to model wines (12% ethanol v/v) buffered with 50 mM tartaric acid (A), malic acid (B), citric acid (C), and a 12:12:1 acid blend (D), at pH 3.0 and 4.0, in the absence of sulfur dioxide; error bars indicate one standard deviation above and below the mean at each timepoint (*n*=3).

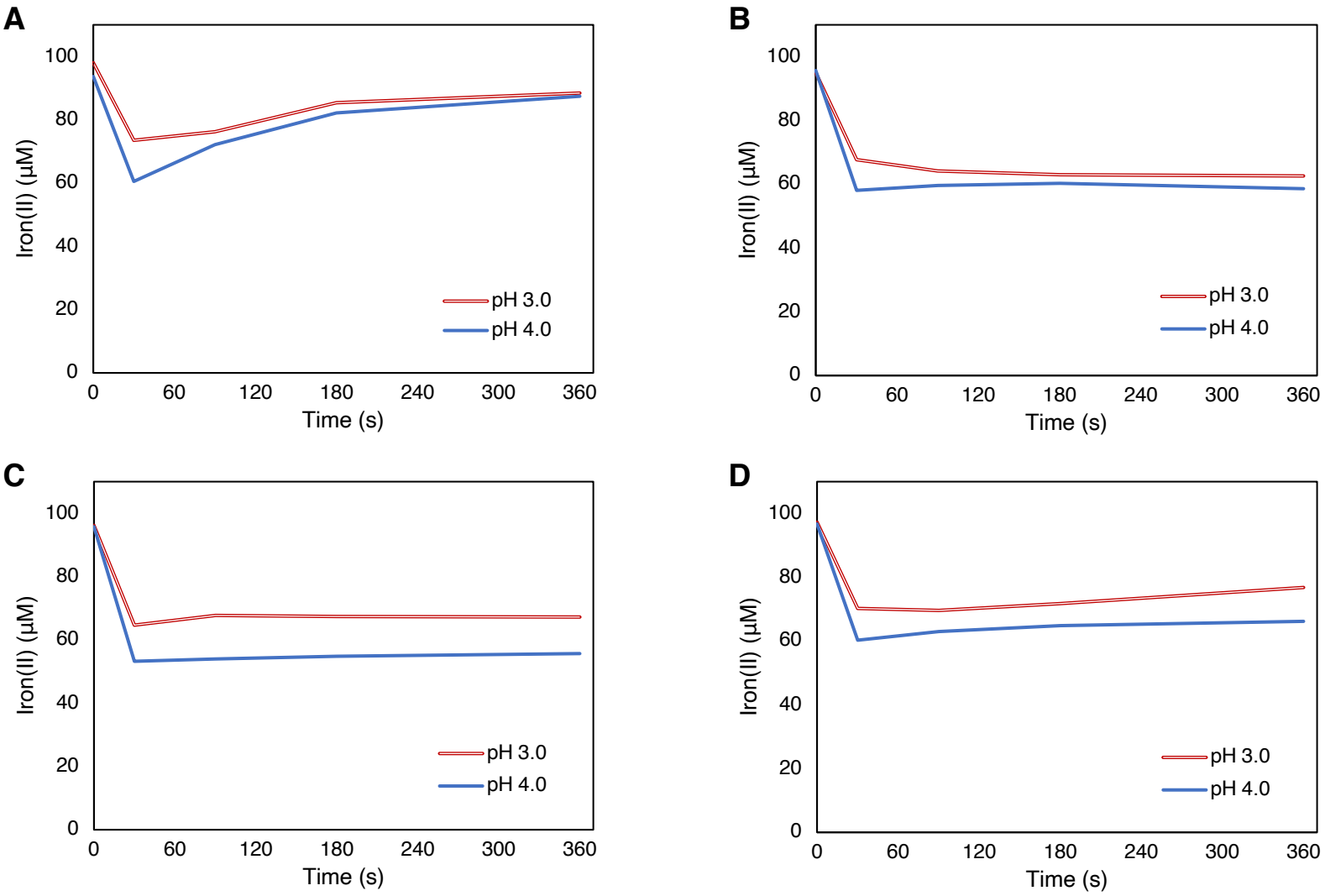

Figure 4.2 Changes to iron(II) levels following the addition of 600 µM hydrogen peroxide to model wines (12% ethanol v/v) buffered with 50 mM tartaric acid (A), malic acid (B), citric acid (C), and a 12:12:1 acid blend (D) at pH 3.0 and 4.0, in the absence of sulfur dioxide; standard deviations at each timepoint (not shown) were no more than 3 µM (n=3).

Loss of H_2O_2, calculated from the production of acetaldehyde (H_2O_2 was not directly monitored), followed pseudo-first order kinetics (Table 4.1) with respect to H_2O_2 despite the concentration of iron(II) being limiting. This again is indicative of iron redox cycling (Tachiev et al. 2000), and such kinetics have also been observed elsewhere in applications of Fenton oxidation for the degradation of dyes and remediation of industrial wastewater (Wang 2008, Xu et al. 2012).

Table 4.1 Pseudo-first order rate constants (1/s) for hydrogen peroxide consumption for each model wine (12% ethanol v/v, 50 mM acid) and pH level, in the absence of sulfur dioxide.

Wine	pH 3.0	pH 4.0
Tartrate	2.92E-02	8.15E-02
Malate	2.19E-02	9.14E-02
Citrate	6.90E-02	1.43E-01
12:12:1 Blend	2.71E-02	8.67E-02

However, the level of iron(II), following the initial drop from H_2O_2 addition, returned to 87-88% of original levels only in the model wine buffered with tartaric acid. In the malate and citrate wines, the proportion of iron as iron(II) remained steady at 53-68% for the remainder of the reaction. Iron(II) appeared to return somewhat in the wine containing with the blend of acids, though to a lesser extent than in the tartrate wine (reaching only 66-77%), suggesting the mitigating influence of malic and citric acid on iron(III) reduction. The direct oxidation of tartaric acid by iron(III) is possible, where other organic acids have been found to resist such oxidation (Fenton 1894, Coleman et al. 2020). Photochemical oxidation is another possibility (Clark et al. 2011), given light was not excluded during experiments. Furthermore, malate and citrate are known to form more stable complexes with iron(III) (Timberlake 1964a, 1964b), an additional factor which may help explain the relatively low iron(II) recovery in the wines buffered with these acids.

Production of acetaldehyde from H_2O_2 went to completion despite this incomplete recycling of iron. Trace levels of oxygen may be a small factor, either directly oxidizing iron(II) or allowing the 1-hydroxyethyl radical to produce acetaldehyde without reduction of iron(III) (Elias and Waterhouse 2010). It is also possible the 1-hydroxyethyl radical forms acetaldehyde by some other means yet to be determined. It is worth noting, however, that this “missing” iron(II) would account for only a small portion of the H_2O_2 added and acetaldehyde produced (1-8% of the 600 µM across treatments).

As noted by Elias and Waterhouse (2010), concentrations of oxygen in wine will vary between air-saturation and virtually zero under real winemaking and storage conditions, and results here would likely differ if dissolved oxygen levels were modified. Future studies should investigate the Fenton oxidation of ethanol over a range of oxygen levels, as this is expected to alter the rate and outcome of this process.

4.4.2 Effects of pH. Rate constants for H_2O_2 decomposition were higher at pH 4.0 than at pH 3.0 in all the model wines. A comparison of the initial rates of acetaldehyde production among treatments makes clear the effects of pH on ethanol oxidation: the reaction was significantly faster at pH 4.0 than at pH 3.0 in all the model wines ($p < 0.05$) (Figure 4.3). The dependence of the Fenton reaction on pH has been well-established in non-wine matrices. In the absence of other ligands, when water occupies the coordination sites of iron, the rate of reaction increases above pH 3 to a plateau at approximately pH 4, an effect attributable to ionization of the coordinated water (Pignatello et al. 2006, Wells and Salam 1968). Complexation can facilitate the oxidation of iron(II) by attenuating its positive charge and lowering its reduction potential; the removal of an electron from a neutral complex is energetically less demanding than from a free cation (Smythe 1931). This pH-dependent effect has been widely observed for non-water ligands as well, which generally increase the solubility of iron, precluding the precipitation of iron hydroxides and permitting Fenton chemistry in more basic conditions (Michaelis and Friedheim 1931, Tachiev et al. 2000).

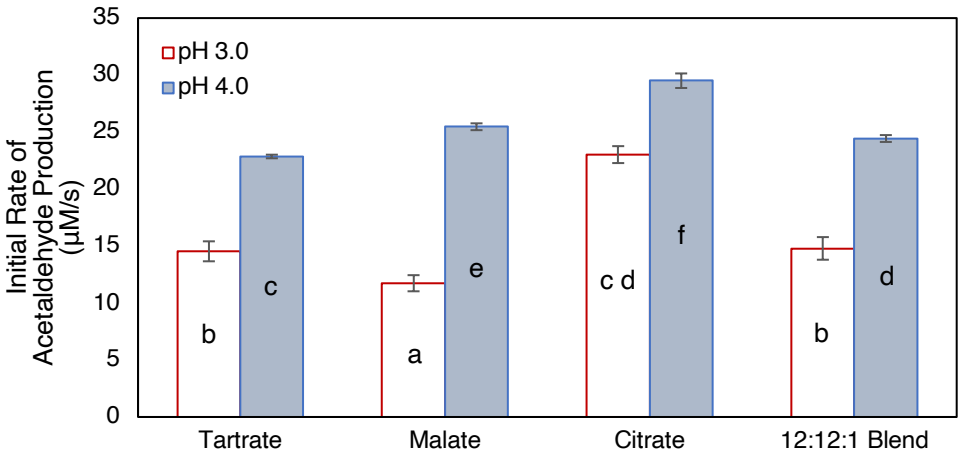

Figure 4.3 Initial rates of acetaldehyde production upon the addition of 600 µM hydrogen peroxide across all model wines (12% ethanol v/v, 50 mM acid), at pH 3.0 and 4.0, in the absence of sulfur dioxide; error bars indicate one standard deviation above and below each mean (n=3). Different letters indicate significant differences between treatments ($p<0.05$).

Furthermore, chelators in which oxygen atoms serve as ligands, such as the carboxylic acids found in grapes and wine, preferentially stabilize the oxidized iron(III) form of iron (Welch et al. 2002). Their carboxylate forms are hard bases (Pearson 1963), and the prevailing pH governs the protonation states of these compounds and therefore the abundance of their complexes with iron, circumstances which may be conceptualized as a competition between iron and hydrogen ions for the binding sites of the chelating agent (Danilewicz 2014, Michaelis and Friedheim 1931, Voelker and Sulzberger 1996). Additionally, the manner of complexation with iron is also a function of pH, with dimeric (2:2) and trimeric (3:3) forms arising at higher pH levels, further affecting the reduction potential of iron (Danilewicz 2014, Timberlake 1964a, 1964b). As observed here, rates of H_2O_2 decomposition by iron have been found to increase with pH in aqueous solutions of fulvic acid (Voelker and Sulzberger 1996) and oxalic acid (Park et al. 1997), as well as tartaric acid (Oh et al. 2016). Additionally, the preference for iron(III) over iron(II) was seen here in the lower iron(II):iron(III) ratios at pH 4.0 in comparison to ratios at pH 3.0.

As described above, the production of acetaldehyde involves the redox cycling of iron, not just the oxidation of iron(II) but the reduction of iron(III) as well, thus the effects of pH on the latter must also be considered. As neither iron(II) nor iron(III) comes to dominate over the course of acetaldehyde formation, it is fair to assume that rates of iron oxidation and reduction are comparable under these conditions. Given the preferential stabilization of iron(III) by the organic acids employed here, their role in iron(III) reduction is likely minimal. An explanation for increased rates of iron(III) reduction (and redox cycling overall) with higher pH, independent of iron complexation, may lie in the mechanism of 1-hydroxyethyl radical oxidation: a proton must be lost, presumably to water or hydroxide, in order to produce acetaldehyde.

High pH wines are commonly believed to deteriorate faster than more acidic wines, possibly due to an increased proportion of phenolic compounds present in their more oxidizable phenolate forms (Rossi and Singleton 1966, Singleton 1987). Oxygen consumption rates in wine have been found to increase with higher pH (Danilewicz 2011, Nguyen and Waterhouse 2021), an effect that can be similarly attributed to iron complexation as described above. The findings here add yet another layer to our understanding of the effects of pH on wine oxidation: the rate of acetaldehyde production from the reaction of iron and H_2O_2 increases through the range of typical wine pH (3.0-4.0). Following this, the rate at which acetaldehyde then

reacts with phenolic compounds is also pH-dependent. The condensation and polymerization reactions which sequester acetaldehyde, effectively rendering it nonvolatile and masking “oxidized” aroma, occur more readily at lower pH (Dueñas et al. 2006, Pissarra et al. 2003). The importance of pH in managing wine oxidation is clear.

4.4.3 Effects of the Complexing Acid. While the model wines buffered with tartaric acid, malic acid, and the blend of acids exhibited similar rates, that buffered with citric acid converted H_2O_2 into acetaldehyde much more quickly at both pH levels ($p < 0.05$). This was unexpected as citric acid is added to wine as not only as an acidulant but also a preservative, thought to stabilize wine against browning and haze formation by chelating transition metals such as iron (Margalit 2012, Vivela 2019, Zoecklein 1995). Moreover, the addition of citric acid to Aglianico wine was found recently to result in less Fenton-induced acetaldehyde formation, in comparison to tartaric or malic acid additions (Picariello et al. 2020). In contrast, however, as observed here, the enhanced reactivity of iron with H_2O_2 when complexed with citrate, as opposed to tartrate or malate, has been demonstrated for the Fenton degradation of cyclohexane in phosphate buffer (Farinelli et al. 2020).

Of the three acids evaluated, citric acid forms the most stable complexes with iron (Timberlake 1964a, 1964b), and iron(III)-selective chelating agents have been shown to exert a short-term pro-oxidant effect. In evaluating the impact of different chelators on the oxidative stability of model wine exposed to air, Kreitman et al. (2013a) demonstrated that EDTA and phytic acid, both iron(III)-selective like citric acid, induced 1-hydroxyethyl radical and acetaldehyde formation, likely by promoting iron(II) oxidation, though this effect diminished as the timeframe of their experiments was extended from hours to days. It was hypothesized that the redox cycling of iron eventually slows as the iron(II):iron(III) ratio decreases, and increased binding of iron(III) comes to limit further reactions (Kreitman et al. 2013a). Therefore, it is possible that the effect of citric acid on acetaldehyde formation observed here would decline if oxidation were to continue. For the aforementioned experiments in Aglianico, H_2O_2 was added at 1.25 mM, more than double the concentration used here (600 μM), and analysis of acetaldehyde took place after several days (Picariello et al. 2020), during which acetaldehyde could be consumed in secondary reactions with other wine constituents (Es-Safi et al. 1999, Peterson and Waterhouse 2016, Timberlake and Bridle 1976).

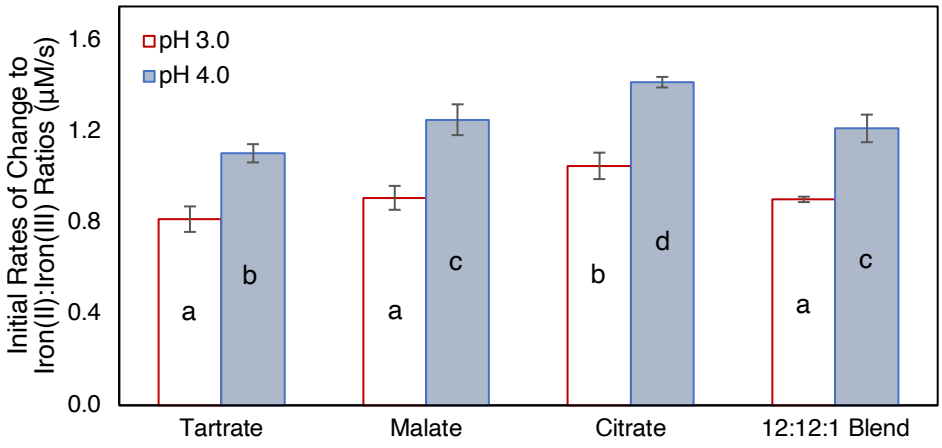

Figure 4.4 Initial rates of change to iron(II):iron(III) ratios upon the addition of 600 µM hydrogen peroxide across all model wines (12% ethanol v/v, 50 mM acid), at pH 3.0 and 4.0, in the absence of sulfur dioxide; error bars indicate one standard deviation above and below each mean (n=3). Different letters indicate significant differences between treatments (p<0.05).

The relatively high rate of acetaldehyde production in the citrate model wine at both pH levels was reflected in changes to its iron(II):iron(III) ratio: lower levels of iron(II) were achieved more quickly with citric acid than with tartaric and malic acid (Figure 4.4). Across all experimental treatments, initial rates of net iron(II) oxidation and initial rates of acetaldehyde production exhibited a positive, linear correlation (Figure 4.5) (Pearson's r = 0.940).

The relatively low rate of acetaldehyde production in the malate wine at pH 3.0 paralleled the more gradual manner in which its iron(II):iron(III) ratio decreased. At this pH, acetaldehyde formation was slowest in the malate wine, though at pH 4.0 its rate surpassed that of the tartrate and acid-blend wines (p < 0.05). Timberlake (1964b) observed an apparent switch in the relative efficacies of tartaric acid and malic acid as iron chelating agents at approximately pH 3.3. Interestingly, this lies between the first dissociation constants of tartaric

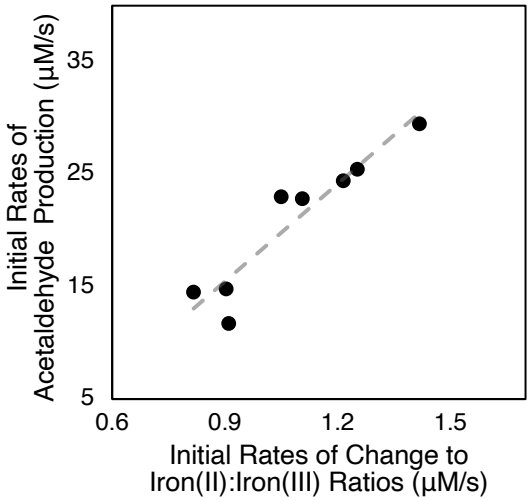

Figure 4.5 Relationship between initial rates of acetaldehyde production and changes to iron speciation.

acid (pK_{a1} = 2.98) and malic acid (pK_{a1} = 3.40) (Waterhouse et al. 2016). Tridentate chelation of iron by two carboxylate groups and one hydroxyl group has been proposed for these acids, leaving one additional non-chelating hydroxyl group for tartrate, the inductive effect from which softens the basicity of tartrate (Timberlake 1964b). This may explain the observations here: at pH 3.0 malic acid is deprotonated to a lesser extent than tartaric acid, but at pH 4.0 has sufficient negative charge to effectively chelate iron, without suffering the inductive effect from an additional hydroxyl group as tartrate does.

The effects of malic acid and citric acid were apparent in the acid-blend wine, the rate of acetaldehyde production in which was similar to that of the tartaric wine at pH 3.0 but significantly higher at pH 4.0 ($p < 0.05$). Tartaric, malic, and citric acid were included in this blend at a ratio of 12:12:1 to model a more realistic wine acid profile. The weighted average of initial acetaldehyde production rates across the tartaric, malic, and citric wines calculated using this ratio was 13.5 μM/s at pH 3.0 and 24.4 μM/s at pH 4.0, closely matching the initial acetaldehyde production rates in the acid-blend wine at pH 3.0 and 4.0: 14.8 μM/s and 24.4 μM/s respectively. Unsurprisingly, analysis of the data from iron speciation in the same manner yielded similar findings: the weighted average of initial rates of net iron(II) oxidation was 0.87 μM/s at pH 3.0 and 1.19 μM/s at pH 4.0, while rates for the blend were 0.90 μM/s at pH 3.0 and 1.21 μM/s at pH 4.0.

While not evaluated here, the effects of acid concentration are expected to be minimal, as these acids are consistently in overwhelming excess relative to iron; acid concentrations are at least two orders of magnitude greater than iron concentrations in wine. However, these results do illustrate the importance of the relative proportions of these acids to the kinetics of oxidation reactions, effects additionally modulated by pH. Enological practices, such as acidulation by acid addition, or deacidification by precipitation with potassium/calcium carbonate salts, may therefore affect wine oxidation. Furthermore, the ratio of tartaric to malic acid can vary among grape varieties and with the climate in which they are cultivated and ripened (Amerine 1964, Picariello et al. 2019); harvest dates likely have an impact as well (Kliewer et al. 1967).

Microbial activity also alters the acid composition of wine, with succinic acid being produced by yeast, and lactic acid and acetic acid coming primarily from bacteria. As to be expected given its structure, succinate forms complexes with iron comparable to those of malate (Gorman and Clydesdale 1984), though its effect

in wine is likely negligible given its pK_{a1} value of 4.21 (Waterhouse et al. 2016). Acetic acid has a similarly high pK_{a1} of 4.76, and being a monodentate complexing agent, forms relatively weak complexes with iron. In fact, acetate complexation of iron fails to bring iron's reduction potential down to below that of oxygen; model wine buffered with acetic acid was found incapable of consuming oxygen (Danilewicz 2014). As a monocarboxylic acid, lactic acid would likely behave similarly to acetic acid. However, the production of lactic acid through malolactic fermentation may be of consequence, given this process constitutes the loss of malic acid and an increase in pH (Bartowsky and Pretorius 2009). Lactic acid bacteria are also known to metabolize citric acid (Lonvaud-Funel 1999).

4.4.4 Fenton Oxidation in the Presence of Sulfur Dioxide. Experiments were conducted as above, but with the inclusion of 600 μM sulfur dioxide, equimolar to the H_2O_2 added. Based on previous findings (Elias and Waterhouse 2010), this would create a scenario in which iron and SO_2 must compete for H_2O_2, and acetaldehyde formation is only partially prevented by SO_2. Furthermore, this level of SO_2 equates to 38.4 mg/L, a reasonable concentration not dissimilar to typical levels employed in commercial practice. Because acetaldehyde formation in the absence of SO_2 peaked at approximately 90 s in the experiments discussed above, the timeframe here was shortened to avoid the evaporative loss of what little acetaldehyde is formed; acetaldehyde analysis was conducted only once at 90 s.

The levels of acetaldehyde produced in the presence of SO_2 were approximately 1/6 the concentrations of acetaldehyde produced in the absence of SO_2 (Figure 4.6). The highest acetaldehyde concentrations (121-133 μM) were observed in the model wines buffered with citric acid ($p < 0.05$); this is in agreement with the faster rates of acetaldehyde production in the citrate wines in the absence of SO_2. By forming the most stable complexes with iron (Timberlake 1964b), citric acid evidently increases the competitiveness of iron for H_2O_2. While differences between the tartaric, malic, and acid-blend wines were apparent in the absence of SO_2, levels of acetaldehyde among them here were not significantly different.

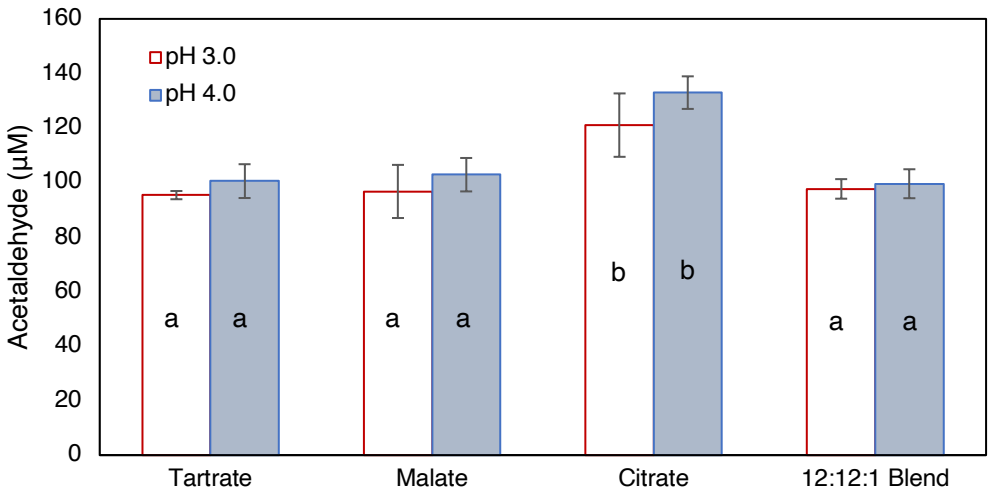

Figure 4.6. Acetaldehyde measured 90 s after the addition of 600 μM hydrogen peroxide across all model wines (12% ethanol v/v, 50 mM acid), at pH 3.0 and 4.0, in the presence of sulfur dioxide (600 μM); error bars indicate one standard deviation above and below each mean (n=3). Different letters indicate significant differences between treatments (p<0.05).

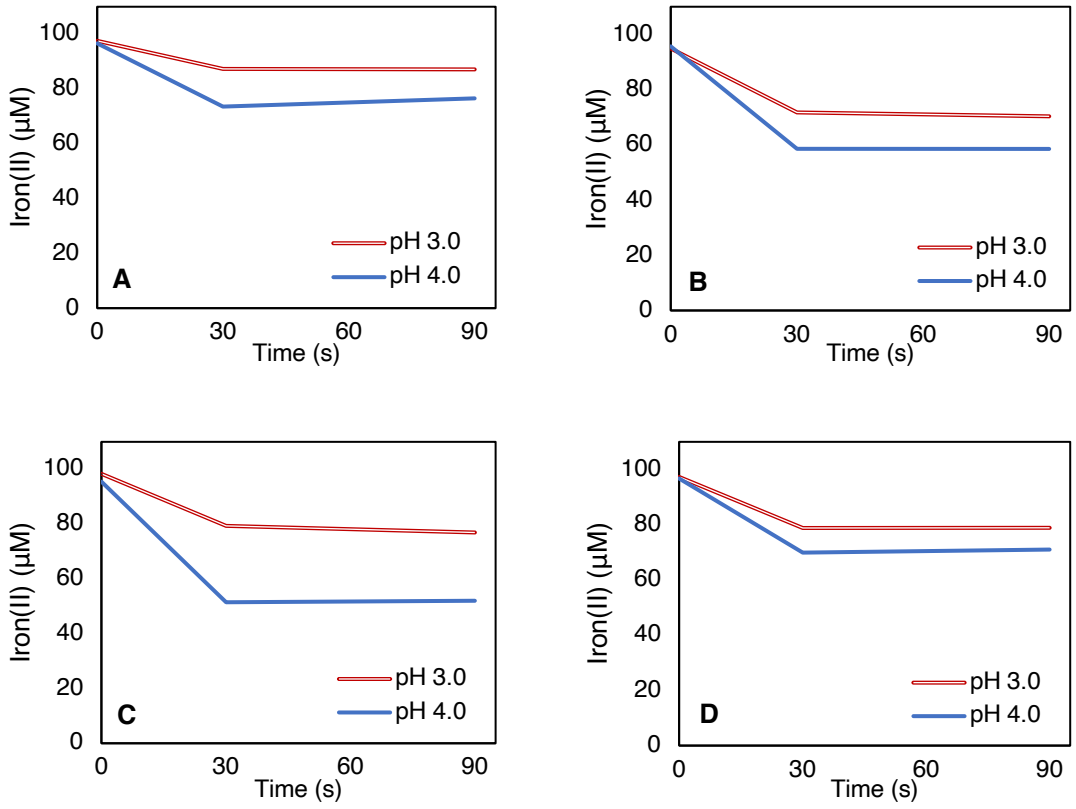

Figure 4.7 Changes to iron(II) levels over 90 s after the addition of 600 μM hydrogen peroxide to model wines (12% ethanol v/v) buffered with 50 mM tartaric acid (A), malic acid (B), citric acid (C), and a 12:12:1 acid blend (D), at pH 3.0 and 4.0, in the presence of sulfur dioxide (600 μM); standard deviations at each timepoint (not shown) were no more than 3 μM (n=3).

Iron(II):iron(III) ratios over 90 s were similar to those observed in the absence of SO_2, with a sharp decline occurring initially with the addition of H_2O_2 followed by steadier phase of redox cycling (Figure 4.7). Ratios were similar to those in the absence of SO_2 for the malate and citrate model wines but were slightly higher in the presence of SO_2 for the tartrate and acid-blend wines, again reflecting the relative weakness of iron(III) complexation by tartrate. While no significant recovery of iron(II) could be discerned, as was seen for the tartrate and acid-blend wines in the absence of SO_2, the non-zero iron(II):iron(III) ratios observed across all treatments again indicate the redox cycling of iron. Acetaldehyde formation and initial rates of net iron(II) oxidation were positively correlated, though this correlation was weaker in the presence of SO_2 (Pearson's r = 0.604).

Sulfur dioxide exists in a pH-dependent equilibrium (pK_{a1} = 1.81, pK_{a2} = 7.0), with bisulfite being the most abundant species at wine pH. Bisulfite is considered the antioxidant form, as it not only reacts with H_2O_2, but other oxidation products as well, namely quinones and aldehydes. The mechanism by which it quenches H_2O_2 is sensitive to pH, slowing in rate as pH increases above 1.5 (McArdle and Hoffman 1983). While not statistically significant (p > 0.05), a slight pH effect on acetaldehyde formation was observed here across all the model wines, which may be explained in part by the pH-dependent equilibrium and reactivity of SO_2. However, in light of results from the experiments conducted in the absence of SO_2, this pH effect may also be attributed to differences in the protonation states of the organic acids, and consequently their abilities to complex with iron and govern its reactivity.

These findings provide additional evidence for the importance of managing wine acidity and pH in controlling wine oxidation, particularly with regards to the efficacy of SO_2 as an antioxidant. Results are expected to differ if other concentrations of H_2O_2 and SO_2 were used, with differences between experimental treatments likely becoming more apparent with lower SO_2 levels; future studies should address this possibility. Furthermore, the effects of other potential iron complexing agents in wine, namely polyphenols, polysaccharides, and proteins (Karadjova et al. 2002), as well as the impact of SO_2 adducts with anthocyanins, sugars, and carbonyl compounds (Beech et al. 1979, Burroughs and Sparks 1973), warrants investigation. These compositional parameters may additionally control the fate of H_2O_2 in wine.

Chapter 5

Yeast Induce Acetaldehyde in Wine Micro-oxygenation Treatments

Published:

Ji J, Henschen CW, **Nguyen TH***, Ma L, and Waterhouse AL. 2020. Yeast induce acetaldehyde in wine micro-oxygenation treatments. J Agric Food Chem 68:15216-15227.

*Contributions include the residual sugar experiment (sections 5.3.5 and 5.4.3) and editing throughout.

5.1 Abstract

Micro-oxygenation (MOx) is a common technique used to stabilize color and reduce harsh astringency in red wines. Here, we investigated the role of residual sugar, phenolic compounds, SO_2, and yeast on the oxidation of wine in three studies. In a MOx experiment, populations of yeasts emerged after the loss of SO_2, and this was associated with sharp increases in oxygen consumption and acetaldehyde production. No acetaldehyde production was observed without the presence of yeast. In an oxygen saturation experiment, unfiltered wines, in particular those with more than 3 g/L residual sugar, consumed oxygen more quickly and produced more acetaldehyde than filtered wines. In a final experiment, the reincorporation of oxygen and glucose immediately after the completion of fermentation of an otherwise dry synthetic wine resulted in significant acetaldehyde production. These experiments highlighted the importance of yeast metabolism in determining a wine's response to MOx, and findings suggest that the role of chemical oxidation to produce acetaldehyde during MOx may be relatively insignificant. It appears that control of microbial populations and residual sugar levels may be key to managing MOx treatments in winemaking, and production scale experiments should be conducted.

5.2 Introduction

Oxidation is a key chemical process affecting the development of wine (Danilewicz 2012, Waterhouse and Laurie 2006). Excessive oxidation leads to most wines losing their freshness followed by a decline in general quality. However, it is commonly believed that a small amount of oxygen can benefit most red wines, in particular by improving fruit flavors, increasing complexity, reducing excessive astringency, and deepening and stabilizing color (Danilewicz 2003, Ma et al. 2018, 2019, Waterhouse and Laurie 2006). At almost every stage of the winemaking process, form pre-fermentation to bottle aging, there has been no consensus regarding what might be considered optimal oxygen exposure (Petrozziello et al. 2018, Picariello et al. 2020, Ugliano 2013).

There are many traditional techniques that control wine exposure to oxygen at various stages, including aerative pumpovers, traditional barrel aging, and bottling under cork, as well as modern techniques such as micro-oxygenation (MOx) (Cano-López et al. 2008, 2010, Cejudo-Bastante et al. 2011b, Durner et al. 2015, Gómez-Plaza and Cano-López 2011, Sáenz-Navajas et al. 2018). MOx refers to the slow introduction of small amounts oxygen into wine with discrete timing, typically applied between primary fermentation and bottling. It simulates the oxidation that normally occurs with traditional equipment which does not provide the hermetic exclusion of oxygen as do the stainless-steel tanks more commonly used today. With appropriate control, MOx can yield wines that are often preferred by consumers.

The MOx process is initiated when oxygen oxidizes iron(II) to iron(III), producing the hydroperoxyl radical. This may then be reduced to hydrogen peroxide either by further reaction with iron(II) or by electron transfer from catechols. The stepwise oxidation of catechols first generates semiquinones and then quinones; quinones may also be produced by the direct oxidation of catechols by iron(III) (Danilewicz 2016, 2018, Waterhouse and Laurie 2006). The generated H_2O_2 then decomposes in the Fenton reaction to yield the hydroxyl radical, which reacts with the most abundant organic compound in wine, ethanol, to produce acetaldehyde (Singleton 1987). Therefore, quinones and acetaldehyde can be considered the primary oxidation products in wine. Due to the instability of quinones (Ma and Waterhouse 2018, Nikolantonaki and

Waterhouse 2012), the formation of acetaldehyde is considered an important marker for oxidation (Es-Safi et al. 1999, Timberlake and Bridle 1976).

There are many components that should be measured in order to understand the influence of wine composition on oxygen consumption and the production of acetaldehyde. Phenolic compounds are a principal substrate for the interaction between oxygen and wine (Singleton 1987), and thus would be considered a major factor in predicting wine's response to oxygen. It has been reported that oxygen consumption is greater in red wines than in white wines due to higher concentrations of phenolic compounds in red wines (Rossi and Singleton 1966, Waterhouse and Laurie 2006). However, another study found phenolic content and composition were negatively correlated with oxygen consumption rates in 15 bottled wines following saturation with air (Ferreira et al. 2015). These contradictory findings suggest there are other important factors influencing oxygen consumption that have not yet been considered.

Sulfur dioxide is an important antioxidant in wine, which functions primarily by consuming the products of oxidation. It can serve as a nucleophile, adding to quinones, or as a reducing agent to convert quinones back to their original phenol forms; both processes replenish the pool of phenolic compounds that serve as substrate for oxidation (Danilewicz 2007, 2016, Singleton 1987). SO_2 can also quench H_2O_2 and prevent the formation of acetaldehyde, or act as a nucleophile to acetaldehyde and form a tightly bound adduct. In a manner, SO_2 actually facilitates oxidation, as the consumption of these oxidation products shifts equilibria toward their production. Consequently, SO_2 is generally consumed in tandem with the consumption of oxygen (Danilewicz et al. 2008, Danilewicz and Wallbridge 2010).

However, in some cases it has been observed that rapid oxygen consumption can occur with little change in SO_2 levels in red wines (Ferreira et al. 2015), indicating that some mechanisms other than the aformentioned chemical reactions of oxygen with SO_2 could be responsible for the oxygen consumption. Yeast are known to be stimulated by oxygen, consuming it through several pathways including aerobic respiration, lipid metabolism, metal ion uptake, and fatty acid synthesis (Rosenfeld and Beauvoit 2003). *Brettanomyces* are associated particularly with the post-fermentation or aging period of alcoholic beverages, including wine (Bisson 2010). The activity of *Saccharomyces cerevisiae* in the post-fermentation

environment is well documented in sherry production, where the strains are distinct from those that perform primary fermentation (Esteve-Zarzoso et al. 2001). Sherry is well known to have high levels of acetaldehyde from the biochemical oxidation of ethanol (Esteve-Zarzoso et al. 2001), so it is possible that yeast is involved in the production of acetaldehyde in other wines post-fermentation, but few studies have addressed this possibility (Han et al. 2017). It has yet to be determined whether oxygen can enhance the growth of yeast after fermentation, and how yeast might affect oxygen consumption and/or acetaldehyde production during MOx.

Here we investigated the factors that influence how wines respond to MOx treatments. This series of experiments focused on oxygen consumption, acetaldehyde production, and the role of chemical and microbial parameters such as residual sugar, phenolic compounds, SO_2, and yeast. It was hypothesized that yeast and residual sugar are needed for acetaldehyde production, a desired outcome of MOx.

5.3 Materials and Methods

5.3.1 Chemicals and Reagents Catechin, sulfuric acid, and 2,4-dinitrophenylhydrazine reagent were purchased from Sigma-Aldrich, Inc. Sodium bisulfite and formic acid were purchased from Acros Organics. Methanol and acetonitrile were purchased from Fisher Bioreagents, Fisher Scientific. Potassium metabisulfite was purchased from Thermo Fisher Scientific. Vanillin was purchased from Alfa Aesar. Water was purified using a Milli-Q system (Millipore). All chemicals were of analytical grade or of the highest available purity.

5.3.2 Initial Wine Analysis. Ethanol was analyzed using an Anton-Paar Alcolyzer, pH was determined via pH meter, titratable acidity was determined by autotitration with sodium hydroxide to an endpoint of pH 8.2, residual sugar and malic acid were determined by enzymatic analysis, and volatile acidity (as acetic acid) was determined by gas chromatography. Free and total SO_2 were measured using the aeration-oxidation method (Iland et al. 2004). Total iron and copper were analyzed by microwave plasma atomic emission spectroscopy (Agilent Technologies).

5.3.3 MOx Experiment. The base wine used for the MOx experiment was produced by Woodbridge Winery (Acampo, CA, USA) from *Vitis vinifera* cv. Merlot grapes, from the 2015 vintage. Chemical parameters for

the wine were as follows: pH 3.60, 5.3 g/L titratable acidity, 14.21% (v/v) ethanol, 0.01 g/L malic acid, 0.60 g/L volatile acidity, 23.8 mg/L free SO_2, 51.3 mg/L total SO_2, 4.56 mg/L iron, 0.051 mg/L copper, and 3.00 g/L residual sugar.

The Merlot wine was divided into eight treatment groups based on MOx status, filtration, and SO_2 addition. Filtered wines were filtered first through pads with 1.5 μm and 0.7 μm nominal pore sizes (Filtrox) and then through three membranes with 1.0 μm nominal, 1.0 μm/0.5 μm dual-stage nominal, and 0.45 μm absolute pore sizes (EMD Millipore) on the first day of the experiment. The dissolved oxygen level was recorded as 597 μg/L after pad filtration and 730 μg/L after membrane filtration. SO_2 additions (30 mg/L) were made using potassium metabisulfite dissolved in warm water prior to sealing the tanks. This protocol gave eight experimental treatment combinations, coded as follows: F_SO_2_M (Filtered, SO_2 added, MOx); F_NoSO_2_M (Filtered, No SO_2 added, MOx); UF_SO_2_M (Unfiltered, SO_2 added, MOx); UF_NoSO_2_M (Unfiltered, No SO_2 added, MOx); F_SO_2_UM (Filtered, SO_2 added, No MOx); F_NoSO_2_UM (Filtered, No SO_2 added, No MOx); UF_SO_2_UM (Unfiltered, SO_2 added, No MOx); UF_NoSO_2_UM (Unfiltered, No SO_2 added, No MOx). All treatments were conducted in duplicate, in randomly assigned 25 L stainless-steel tanks sanitized with 70% ethanol. The wines were stored at 19.1 ± 0.2 ^{o}C for the duration of the experiment.

The MOx system used was identical to those described previous reports (Gambuti et al. 2015, Sáenz-Navajas et al. 2018). Fluorinated ethylene-propylene tubing (108.9 cm) was used in each MOx apparatus. At the start of the experiment, all external fittings were tested for leaks using Snoop Leak Detector (Swagelok). For the duration of the experiment, oxygen was introduced to the MOx tanks at 15 mg/L/month (confirmed initially in deoxygenated water) by setting the pressure inside the system to 68 psi.

All pieces of equipment that came in contact with the wine were sanitized with 70% (v/v) ethanol prior to use. As previously described (Gambuti et al. 2015, Sáenz-Navajas et al. 2018), dissolved oxygen was measured using a Fibox 3 LCD-trace V7 oxygen meter (PreSens Precision Sensing GmbH) daily in MOx tanks and every 28 days in non-MOx tanks. Samples for microbial tests were taken at the start of the experiment and at 14, 28, 40 and 49 days. Sampling protocols for the analysis of chemical variables are given in their respective subsections of section 5.4.1. The duration of the experiment was 49 days.

Table 5.1 Initial chemical parameters of the wines used for the oxygen saturation experiment.

Wine	Code	Ethanol (% v/v)	pH	Titratable acidity (g/L)	Residual sugar (g/L)	Malic acid (g/L)	Volatile acidity (g/L)	Free SO_2 (mg/L)	Total SO_2 (mg/L)	Iron (mg/L)	Copper (mg/L)
Cabernet Sauvignon #1	CS1	14.43	3.66	5.4	0.36	0.27	0.60	5.96	49.8	4.03	0.017
Cabernet Sauvignon #2	CS2	14.35	3.74	5.3	0.24	0.18	0.48	8.92	43.2	4.22	0.100
Cabernet Sauvignon #3	CS3	13.13	3.68	5.5	3.52	0.10	0.51	8.18	52.8	3.75	0.006
Cabernet Sauvignon #4	CS4	12.41	3.68	5.4	1.68	0.15	0.58	10.4	45.4	3.47	0.019
Cabernet Sauvignon /Merlot blend	CM	14.14	3.65	5.4	1.34	0.14	0.56	11.2	26	4.19	0.006
Merlot #1	ME1	13.90	3.46	6.3	1.91	0.07	0.63	18.6	59.5	4.08	0.029
Merlot #2	ME2	13.97	3.61	5.4	3.63	0.01	0.56	7.44	49.1	5.16	0.039
Alicante Bouschet	AB	12.33	3.59	6.1	0.15	0.07	1.07	32.7	79.6	2.43	0.016
Tannat	TN	11.48	3.5	6.3	0.54	0.08	0.60	10.4	52.8	3.62	0.031
Rubired	RR	13.07	3.68	6.2	0.36	0.34	0.46	20.1	40.9	2.32	0.093

5.3.4 Oxygen Saturation Experiment. Ten wines were obtained for the oxygen saturation study from Woodbridge Winery (Table 5.1). All wines were from the 2015 vintage, made from various *Vitis vinifera* cultivars.

At the start of the experiment, wines were divided into filtered and unfiltered treatments. Filtered treatments were first clarified by centrifugation for 15 minutes at 10,000 g using a Sorvall RC 5B Plus centrifuge (Thermo Fisher Scientific). The wines were then passed through successive 47 mm filter membranes with 0.8 μm absolute and 0.45 μm absolute pore sizes (EMD Millipore) by vacuum.

To saturate the wines with oxygen, excess wine was placed in a 500 mL volumetric flask, and zero grade air (Airgas) was introduced to the samples using a bubbling stone. Dissolved oxygen was measured constantly using a Fibox 3 LCD-trace V7 oxygen meter (PreSens Precision Sensing GmbH) with a dipping probe. When the dissolved oxygen level stabilized at saturation, wine was added to 300 mL biological oxygen demand (BOD) bottles (Wheaton) such that there was zero headspace. Prior to the experiment, a Presens PST3 oxygen-sensing dot (Nomacorc LLC) was installed in each bottle. All bottles, flasks, and other pieces of equipment that came in contact with the wine were sanitized with 70% (v/v) ethanol prior to use. Bottles were stored in the dark at 19.1 ± 0.2 ^{o}C for the duration of the experiment. Dissolved oxygen measurements were recorded at filling, at three additional points in the first 24 h, and subsequently once per day. The experimental endpoint for each bottle was defined as having been reached when dissolved oxygen levels were less than 0.5 mg/L. At this point, the stopper was removed, and chemical and microbiological analyses were performed.

5.3.5 Residual Sugar Experiment. Synthetic wine used in the final experiment on the effects of residual sugar was fermented from the synthetic medium Triple M (for “minimal must medium”) (Spiropoulos et al. 2000). This medium was prepared from three stock solutions (A, B, and C), stable when kept separate, which were modified from the original recipe as follows. Solution A was prepared with 440 mg/mL D-glucose and 440 mg/mL D-fructose (Thermo Fisher Scientific); a 2.5 mg/mL solution of ergosterol (Sigma-Aldrich) in 25% (v/v) Tween 80 (Thermo Fisher Scientific) in 95% (v/v) ethanol was added to solution A at 1.6% (v/v) just prior to the combination of all three solutions (A, B, and C). Solution B was 30 mg/mL tartaric acid,

15 mg/mL malic acid, and 2.5 mg/mL anhydrous citric acid (Thermo Fisher Scientific). Solution C was 8.4 mg/mL Difco amino acid- and ammonium sulfate-free yeast nutrient base, 10 mg/mL vitamin-free amino acids (BD Biosciences), 0.03 mg/mL myo-inositol, 1 mg/mL anhydrous calcium chloride, 4 mg/mL L-arginine hydrochloride, 5 mg/mL L-proline, 0.5 mg/mL L-tryptophan, and 5 mg/mL ammonium phosphate (Thermo Fisher Scientific). All solutions were prepared in autoclaved Milli-Q water unless otherwise stated. The three solutions were combined as follows: 25% A, 20% B, 20% C, and 35% (v/v) water, resulting in a sugar concentration measuring 22.4 ^{o}Brix. The pH of the medium was adjusted to 3.25 with potassium hydroxide. It was then sterile-filtered through a Corning 0.45 μm bottle-top filter (Sigma-Aldrich) and used immediately. *Saccharomyces cerevisiae* strain EC1118 from the UC Davis Department of Viticulture and Enology Culture Collection was used for fermentation, which took place at 22.2 ± 0.4 ^{o}C. At the end of fermentation, chemical parameters for the wine were as follows: pH 3.24, 7.5 g/L titratable acidity, 13.51% (v/v) ethanol, and 0.01 g/L residual sugar. Yeast cell density was 1.33 x 10^{8} CFU/mL and the concentration of acetaldehyde was 70.4 mg/L.

The synthetic wine was divided into treatment groups based on glucose addition (3 g/L) and oxygenation. Each was performed in duplicate in autoclaved 60 mL BOD bottles (Wheaton). BOD bottles for the oxygenated test samples contained 40 mL of wine such that 20 mL of headspace remained, while those for non-oxygenated test samples were filled completely, leaving no headspace. This gave four treatment combinations coded as follows: Glu_Ox (glucose added, oxygenated), nGlu_Ox (no glucose added, oxygenated), Glu_nOx (glucose added, not oxygenated), and nGlu_nOx (no glucose, not oxygenated). All were placed onto an Innova 2300 platform shaker (New Brunswick Scientific) set to 110 rpm. The experiment took place at 22.2 ± 0.4 ^{o}C. The bottles were opened after 10 days for the quantification of acetaldehyde and yeast. Residual sugar analysis was also conducted to verify the consumption of the added glucose.

5.3.6 Experimental Analytical Procedures

5.3.6.1 Sulfur Dioxide Analysis. All measurements were conducted on the day of sampling using the aeration-oxidation method (Iland et al. 2004).

5.3.6.2 Residual Sugar Analysis. Residual sugar was determined by enzymatic analysis based on the formation or consumption of nicotinamide adenine dinucleotide (NAD^+) or its reduced form (NADH), using a Gallery automated photometric analyzer (Thermo Fisher Scientific).

5.3.6.3 Acetaldehyde Analysis. Acetaldehyde was analyzed using an adapted high-performance liquid chromatography (HPLC) procedure (Han et al. 2015). Briefly, 100 µL of each wine sample were dispensed into a vial, followed by additions of 20 µL of 1120 mg/L SO_2 solution, 20 µL of 25% (v/v) sulfuric acid, and 140 µL of 2,4-dinitrophenylhydrazine reagent (in acetonitrile, saturated). After mixing, vials were placed in a 65 °C water bath for 15 min for derivatization, then cooled to room temperature. Samples were diluted 1:1 with 0.5% formic acid before analysis. The acetaldehyde hydrazone was quantified using a HP 1100 series HPLC coupled to a diode array detector (Agilent Technologies); peaks were analyzed at 365 nm. A Zorbax Rapid Resolution HT SB-C18, 1.8 µm particle size, 4.6 x 100 mm column (Agilent Technologies) was used for separation. The HPLC conditions were as follows: injection volume 15 µL, flow rate 0.75 mL/min, column temperature 35 °C. Mobile phases A (0.5% formic acid) and B (acetonitrile) were used with the following gradient elution protocol: 35% B at 0 min, 60% B at 8 min, 95% B at 13 min (2 min hold), 35% B at 16 min (4 min hold); total runtime was 20 min. For quantification, a standard curve was created at each analytical time point from an acetaldehyde-hydrazone standard (Supelco Inc.).

5.3.6.4 Phenolic Analysis. The adapted vanillin-reactive flavan assay (Sun et al. 1998) was performed to quantify phenolic compounds that react with aldehydes. Briefly, 200 µL of diluted wine (1/10) in methanol (Fisher Scientific) was added to black microcentrifuge tubes in order to exclude light in the subsequent reaction. Vanillin (500 µL, 2% in methanol) or 500 µL pure methanol was added to the tubes. After 5 min, tubes were placed on ice before adding 500 µL of 9 N sulfuric acid in methanol. The reaction was allowed to occur for 15 min at 30 °C, after which absorbance at 500 nm was measured using an Agilent 8453 UV-Vis spectrophotometer. The difference between absorbance readings with and without vanillin were taken as the final values, used to calculate the concentration of vanillin-reactive flavans from a calibration curve in (+)-catechin equivalents.

Monomeric pigments, small polymeric pigments, and large polymeric pigments were quantified using the Adams-Harbertson assay (Harbertson et al. 2003), for which three absorbances readings at 520 nm were taken. For Reading 1, Buffer A (1 mL, 200 mM acetic acid, 170 mM NaCl, pH 4.9 adjusted with NaOH) was combined with 250 µL wine and 250 µL model wine (12% ethanol, 5 g/L tartaric acid, pH 3.3 adjusted with NaOH) in a plastic cuvette, after which absorbance at 520 nm was measured. For Reading 2, potassium metabisulfite (120 µL 0.36 M) was added to the first cuvette, and the absorbance was measured again after 10 min. For Reading 3, Buffer B (1 mL, 200 mM acetic acid, 170 mM NaCl, 1 g/L ovalbumin, pH 4.9 adjusted with NaOH) was combined with 250 µL wine and 250 µL model wine in a microcentrifuge tube, gently shaken for 15 min, then centrifuged at 14,000 g for 2 min. The supernatant (1 mL) and 80 µL of 0.36 M potassium metabisulfite were then added to a plastic cuvette and allowed to react for 10 min before the third absorbance measurement. "Small polymeric pigments" were defined by Reading 3, "large polymeric pigments" were defined by Reading 3 subtracted from Reading 2, and "monomeric pigments" were defined by Reading 2 subtracted from Reading 1. All measurements were given in absorbance units and multiplied by two to account for the 1:1 dilutions with model wine.

5.3.6.5 Microbiological Analysis. To quantify viable yeast and bacteria, samples were plated on Wallerstein Laboratory Nutrient (WLN) media for yeast and 50% de Man, Rogosa, and Sharpe (MRS) media for bacteria. Samples were also analyzed qualitatively under a microscope prior to plating. WLN plates were prepared by mixing WL broth dehydrated culture media according to manufacturer's instructions with 1.8% Bacto agar (BD Biosciences), autoclaving, and pouring into square gridded Petri dishes (Thermo Fisher Scientific). Half-strength MRS plates were prepared by mixing MRS broth dehydrated culture media at half the manufacturer's recommended concentration with 1.8% Bacto agar (BD Biosciences), autoclaving, and pouring into square gridded petri dishes. For samples with suspected yeast populations, Delvocid (DSM) was added to the 50% MRS media at 25 mg/L after autoclaving to suppress fungal growth. The plating procedure was as follows: wine samples were diluted 1/10 serially in sterile 2 mL microcentrifuge tubes to make five dilutions in addition to the original sample. Plates were divided into six lanes per plate. Ten microliters of each wine dilution were added to each lane with the plate resting at an angle, such that the sample ran down each lane in a straight line. Both types of plates (WLN and 50% MRS) were prepared in

duplicate for each wine sample. After drying, plates were incubated at 30 °C. Growth was assessed after 2-3 days for WLN plates and after 7-10 days for 50% MRS plates. Colonies were counted in the lane that contained 20-200 colonies, except in cases where no lanes contained 20 colonies or more. Colonies were analyzed under a microscope to determine cell morphology.

Yeast species were identified according to the following procedure. A colony from each population was removed from each plate and placed in a sterile 1.5 mL microcentrifuge tube, after which 555 µL extraction reagent containing 74% ethanol, 240 mM NaOH (Thermo Fisher Scientific), and 2.7 mM EDTA (Sigma-Aldrich) was added to the tube. The sample was chilled at -80 °C for 10 min, then immediately heated at 80 °C for 10 min. The sample was then centrifuged at 141,000 g for 10 min, and the pellet was suspended in an aqueous solution containing 50 mM Tris-HCl (Promega), 0.1 mM EDTA (Sigma-Aldrich), 1% Triton X-100 (US Biological), and 0.5% Tween 20 (Thermo Fisher Scientific). Subsequently, a polymerase chain reaction (PCR) was performed using the extracted DNA with forward primer NL1 (sequence: 5'-GCATATCAATAAGCGGAGGAAAAG-3'), reverse primer NL4 (sequence: 5'-GGTCCGTGTTTCAAGAGGG-3'), with the following conditions: first an initial melting at 94 °C for 10 min, then 30 cycles of melting at 94 °C for 45 s, annealing at 55 °C for 30 s, and extending at 72 °C for 60 s, followed by a final extension at 72 °C for 4 min. The amplified products of PCR were confirmed by gel electrophoresis, and purified using a QIAquick PCR purification kit (Qiagen). Species were identified using the Basic Local Alignment Search Tool (BLAST) (National Center for Biotechnology Information), with at least 97% sequence match.

5.3.7 Statistical Analysis. Statistics were carried out on experimental replicates, and calculations were performed with R Studio v. 0.99.903 and Prism 7. Pairwise comparisons were conducted by *t*-test and global *p* values were obtained by ANOVA. The level of significance was defined by $\alpha = 0.05$ unless stated otherwise.

5.4 Results and Discussion

5.4.1 MOx Study

5.4.1.1 Oxygen. Dissolved oxygen measurements for the MOx tanks over the course of the experiment are shown in Figure 5.1A. Consumed oxygen levels (Figure 5.1B) were calculated by subtracting the oxygen accumulated from the amounts delivered (0.5 mg/L/day x days). Each curve was divided into three stages based on an approximately linear rate of accumulation or consumption. The first part of the curve ("initial rate," IR) was highly variable, perhaps because the wines had to equilibrate with the small amount of headspace in each tank. Oxygen accumulation during this initial phase was relatively fast, with rates much higher than the rest of the experiment, though oxygen concentrations often fluctuated for each wine. Therefore, linear estimates of IR were imprecise. The second part of the curve ("secondary rate," SR) was fairly constant and comprised the majority of the experimental timeframe. However, "tertiary rates" (TR) then varied significantly among different treatments: filtered samples exhibited a TR of oxygen accumulation lower or similar to their SR, while unfiltered samples exhibited a rapid consumption of oxygen to a final level of zero.

To further investigate differences in IR, SR and TR with SO_2 and/or filtration, the oxygen consumption rates at different stages were calculated (Figure 5.1C-E). There were no significant differences in IR, SR, and TR attributable to initial SO_2 levels, and no significant effects of filtration on IR and SR ($p > 0.05$). However, the TR of oxygen consumption was much higher in the unfiltered samples than in the filtered samples ($p < 0.05$). Since the presence of yeast is the major difference between the filtered and unfiltered samples, these results indicated that yeast had a significant influence on the final stage of oxygen consumption in our experiment.

5.4.1.2 Sulfur Dioxide Consumption. Free SO_2 was measured at the start of the experiment and at 7, 14, 21, 28, 33, 40, and 47 days (Figure 5.2A). Total SO_2 was measured at the start of the experiment and at 28, 40, and 47 days (Figure 5.2B). The sharp drop in dissolved oxygen levels corresponded closely to the depletion of total SO_2, emphasizing the importance of bound SO_2. This contradicts previous findings which suggest that free SO_2 is the more consequential fraction (Gambuti et al. 2015, Tao et al. 2007).

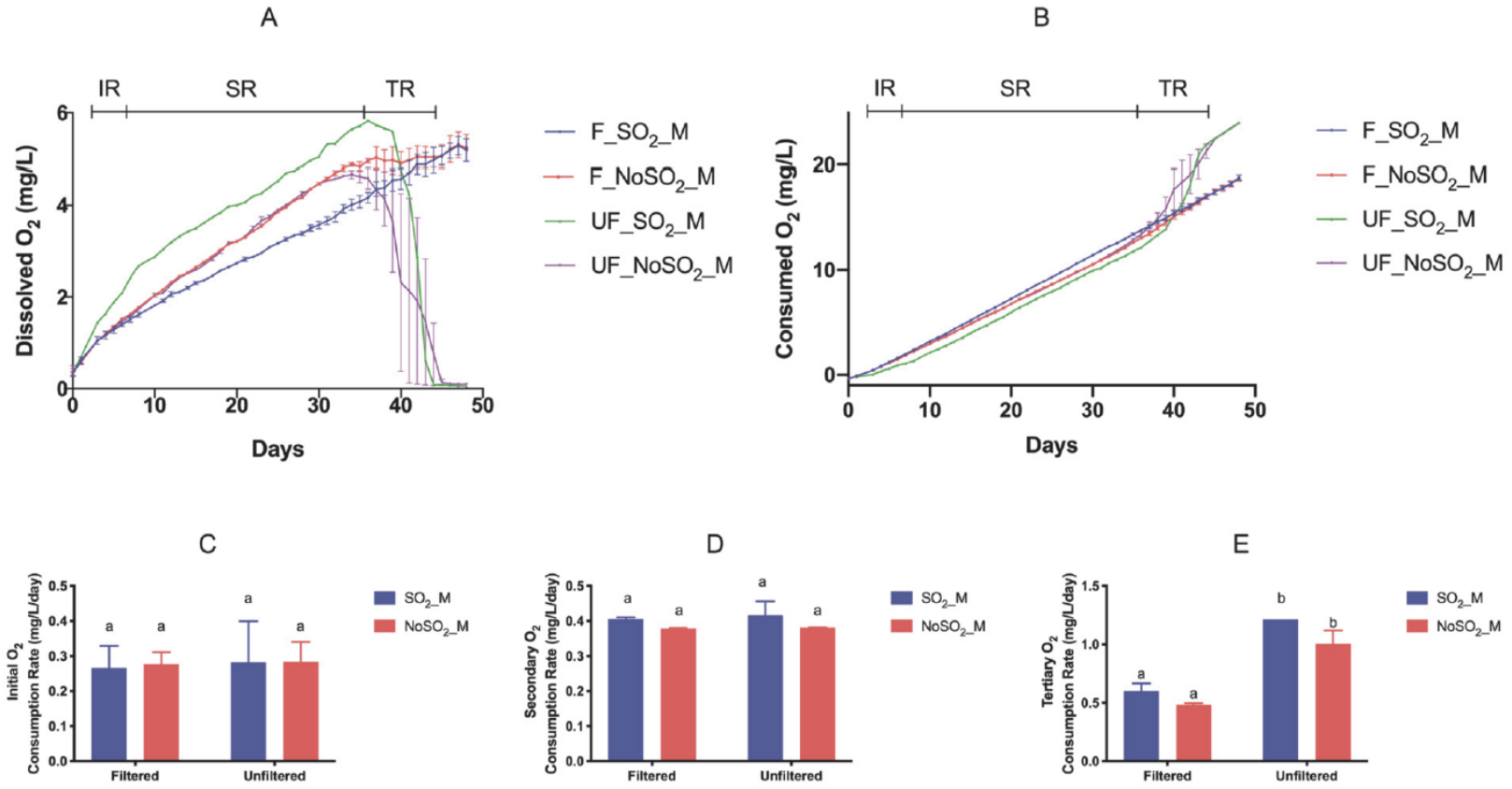

Figure 5.1 Dissolved oxygen (A) and consumed oxygen (B) levels in micro-oxygenated tanks over the course of the MOx experiment. Changes exhibited initial (IR), secondary (SR), and tertiary (TR) rates (C, D, and E respectively); different lowercase letters indicate significant differences between treatments (p<0.05).

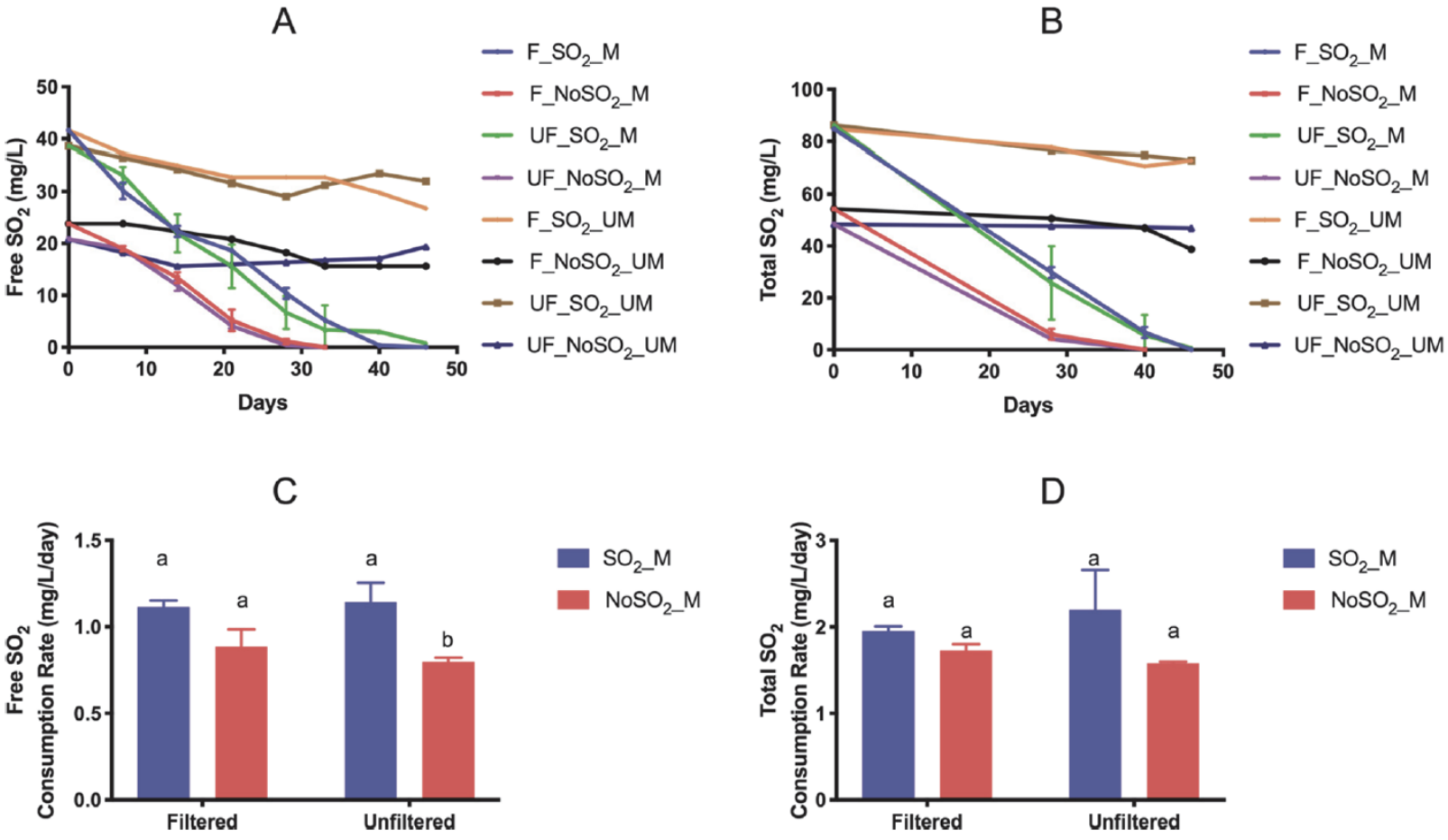

Figure 5.2 Free SO_2 (A) and total SO_2 (B) concentrations for all treatments over the course of the MOx experiment. Rates of free SO_2 (C) and total SO_2 (D) consumption; different lowercase letters indicate significant differences between treatments ($p<0.05$).

Concentrations of free and total SO_2 declined linearly in MOx tanks compared to non-MOx tanks over the course of the experiment. Linear free SO_2 consumption rates were calculated over the first 21 days of the experiment for samples without added SO_2 and the first 28 days for samples with added SO_2 (Figure 5.2C). Total SO_2 consumption rates were calculated over the first 28 days for samples without added SO_2, and the first 40 days for samples with added SO_2 (Figure 5.2D). For the unfiltered wines that underwent MOx, samples with SO_2 added had a higher free SO_2 consumption rate compared to the samples without added SO_2 ($p < 0.05$) though the difference is small. Rates of total SO_2 consumption did not vary between tanks with and without added SO_2. Overall, it would appear that filtration did not significantly affect SO_2 consumption.

5.4.1.3 Microbiological Data. All culturable yeast populations were positively identified as *Saccharomyces cerevisiae* by amplification and sequencing. All of these populations also had similar cell and colony morphology. No culturable bacteria was observed in any of the samples from this experiment.

Yeast counts for treatment groups at each time point during the experiment are shown in Figure 5.3A. No yeast populations could be detected by plating at the start of the experiment, including the unfiltered treatments, and sparse cells could only be observed under a microscope after centrifugation. In the UF_NoSO_2_M and UF_SO_2_M tanks, yeast began to appear 40 days after the start of oxygenation, and the population grew to 2.13×10^5 and 3.78×10^5 CFU/mL, respectively, by the final time point. At 49 days, yeast levels of UF_NoSO_2_M and UF_SO_2_M tanks were significantly higher than the other tanks, indicating the effect of filtration on the yeast counts. It is extremely unlikely that yeast was introduced to the wine from an exogenous source during the experiment, because tanks were sealed off from the atmosphere and sampling needles were sterilized with ethanol before use. Therefore, it appears that a small population of *S. cerevisiae* was present in the wine the whole time, but not in significant viable numbers until the conditions became more favorable (the presence of oxygen and absence of SO_2). Either the number of cells was simply too low to be detected by plating or the population was predominately in a viable but non-culturable state. Importantly, the appearance of these yeast populations coincides with the reduction of free and total SO_2 to negligible levels and the onset of rapid oxygen consumption. It should be noted that no yeasts developed in the filtered treatments or in the unfiltered non-MOx treatments, the latter of which maintained higher

SO_2 levels. Although numerous previous studies have demonstrated the stimulatory effect of oxygen on *Saccharomyces* growth and metabolism, they have focused on primary fermentation when fermentable sugars are still abundant (Rosenfeld and Beauvoit 2003). Few studies have demonstrated the apparent stimulation of yeast population growth by oxygen from a non-culturable state post-fermentation.

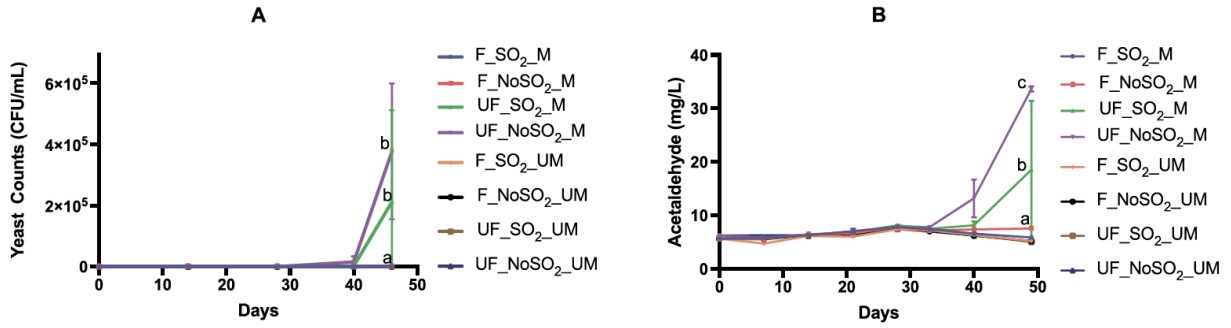

Figure 5.3 *Saccharomyces cerevisiae* cell counts by plating (A), and total acetaldehyde concentrations (B) over the course of the MOx experiment; different lowercase letters represent time points at which certain treatments were significantly different ($p<0.05$).

5.4.1.4 Acetaldehyde Production. Acetaldehyde was analyzed at the start of the experiment and at 7, 14, 21, 28, 33, 40, and 49 days (Figure 5.3B). The scale of the acetaldehyde production was similar to previous observations, as the concentrations rose from ~5 mg/L to ~35 mg/L over a period of approximately 2 weeks. This mirrored oxygen consumption, as observed previously by Gambuti et al. (2015), with the beginning of the spike in acetaldehyde coinciding with the sharp decrease in dissolved oxygen levels. Yeast populations grew to the order of 10^5 CFU/mL in this experiment, much lower than what is observed during primary fermentation, though acetaldehyde production was observed even when cell counts were at such a low level. Therefore, relatively small yeast populations are capable of causing large chemical changes in micro-oxygenated wines. In addition, these treatments produced acetaldehyde at extremely efficient rates, with more than one mole of acetaldehyde formed for each mole of oxygen consumed. Substantial accumulation of acetaldehyde was observed at the end of the experiment for the UF_NoSO$_2$_M and UF_SO$_2$_M tanks, which differed significantly from all other treatment/time combinations and from each other ($p < 0.05$). These differences coincided with the appearance of yeast in the UF_NoSO$_2$_M and UF_SO$_2$_M tanks, indicating the suppressive effect of filtration on acetaldehyde production, the latter being positively correlated to yeast cell density.

5.4.1.5 Phenolics. The vanillin-reactive flavan assay adapted from Sun et al. (1998) was used to quantify phenolic compounds that react with aldehydes at the start of the experiment and at 7, 21, 33, and 49 days (Figure 5.4A). The concentration of these compounds appeared to decrease during the first 7 days before returning to initial levels at 21 days, after which levels declined through the remainder of the experiment. Initial and final measurements were significantly different ($p < 0.05$) for every treatment, but no significant differences were discovered between treatments ($p > 0.05$), suggesting that this assay is not diagnostic of the formation of aldehydes, given the high acetaldehyde samples had effectively the same response to vanillin as the others.

Monomeric pigments, small polymeric pigments, and large polymeric pigments were quantified using the Adams-Harbertson assay at the start of the experiment and at 7, 14, 21, 28, 33, 40, and 49 days. However, only monomeric pigments, those susceptible to sulfite bleaching, showed meaningful changes in this experiment (Figure 5.4B). Monomeric pigments generally increased over the first 40 days in the wines that underwent MOx before decreasing afterward. Concentrations for the filtered MOx and unfiltered SO_2 MOx treatment groups were significantly different from initial levels by the 28-day time point onward. Monomeric pigments in the UF_NoSO_2_M wines reached significantly different concentrations at the 40-day time point only, largely because the initial readings in this group were higher than all other groups ($p < 0.05$). Monomeric pigments in the non-MOx group were significantly different from initial measurements at the 33-day and 40-day points, but these differences were no longer apparent by the end of the experiment; concentrations in the UM wines much lower than in the MOx wines at the 40-day and 49-day points. Overall, there seemed to be a small positive effect of MOx on monomeric pigments. Small polymeric pigments generally decreased during the first 28 days (Figure 5.4C). Concentrations in the filtered MOX and unfiltered SO_2 treatment groups then returned to the initial levels, while concentrations in the unfiltered SO_2 and non-MOx treatment groups surpassed initial levels by the end of the experiment. No significant main effects were found for treatment ($p > 0.05$) with regards to small polymeric pigments, but there was a significant treatment-time interaction effect ($p < 0.05$). For large polymeric pigments, all main effects and interactions were not significant ($p > 0.05$, Figure 5.4D).

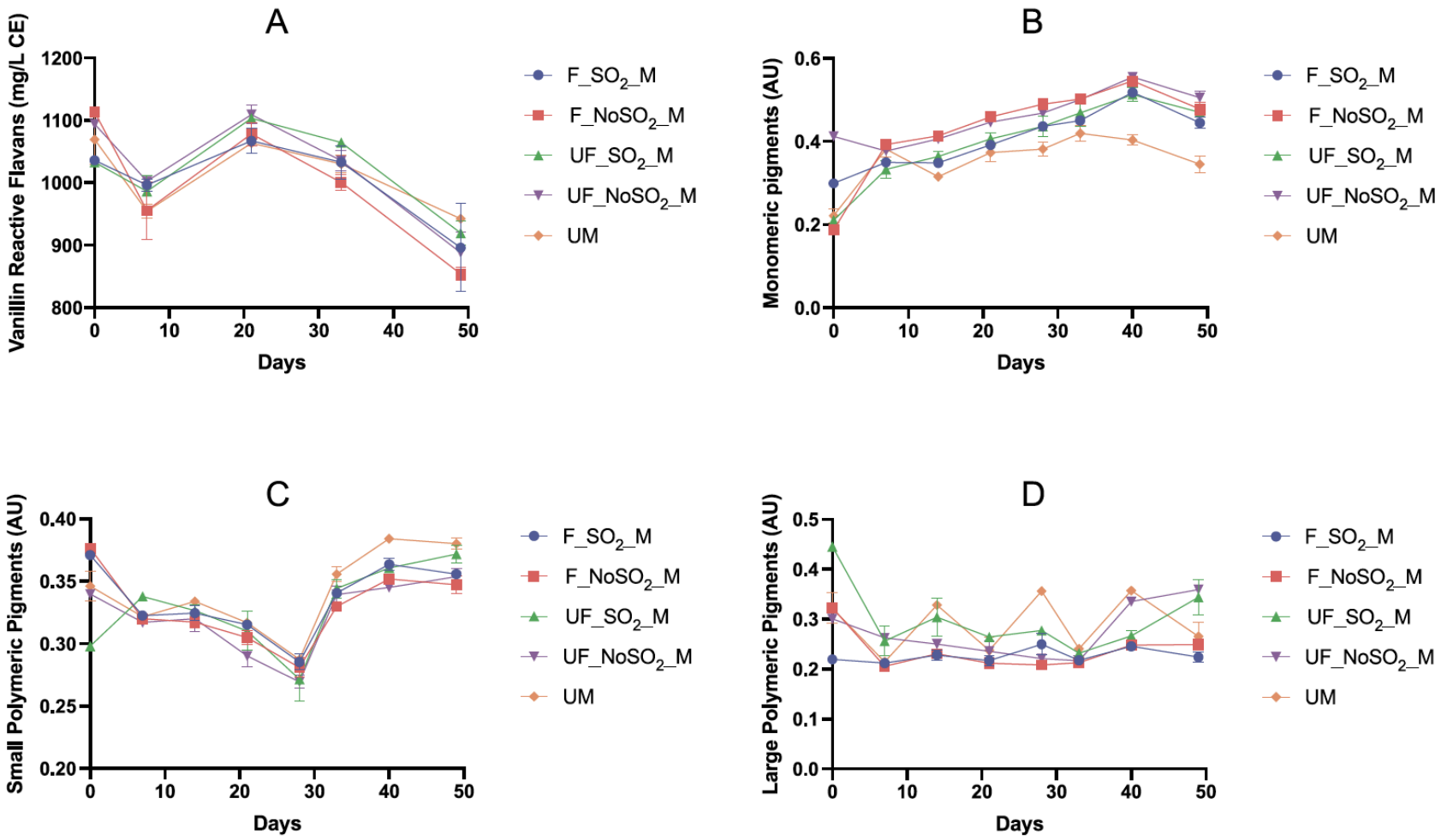

Figure 5.4 Vanillin-reactive flavans (A), monomeric pigments (B), small polymeric pigments (C), and large polymeric pigments (D) over the course of the MOx experiment.

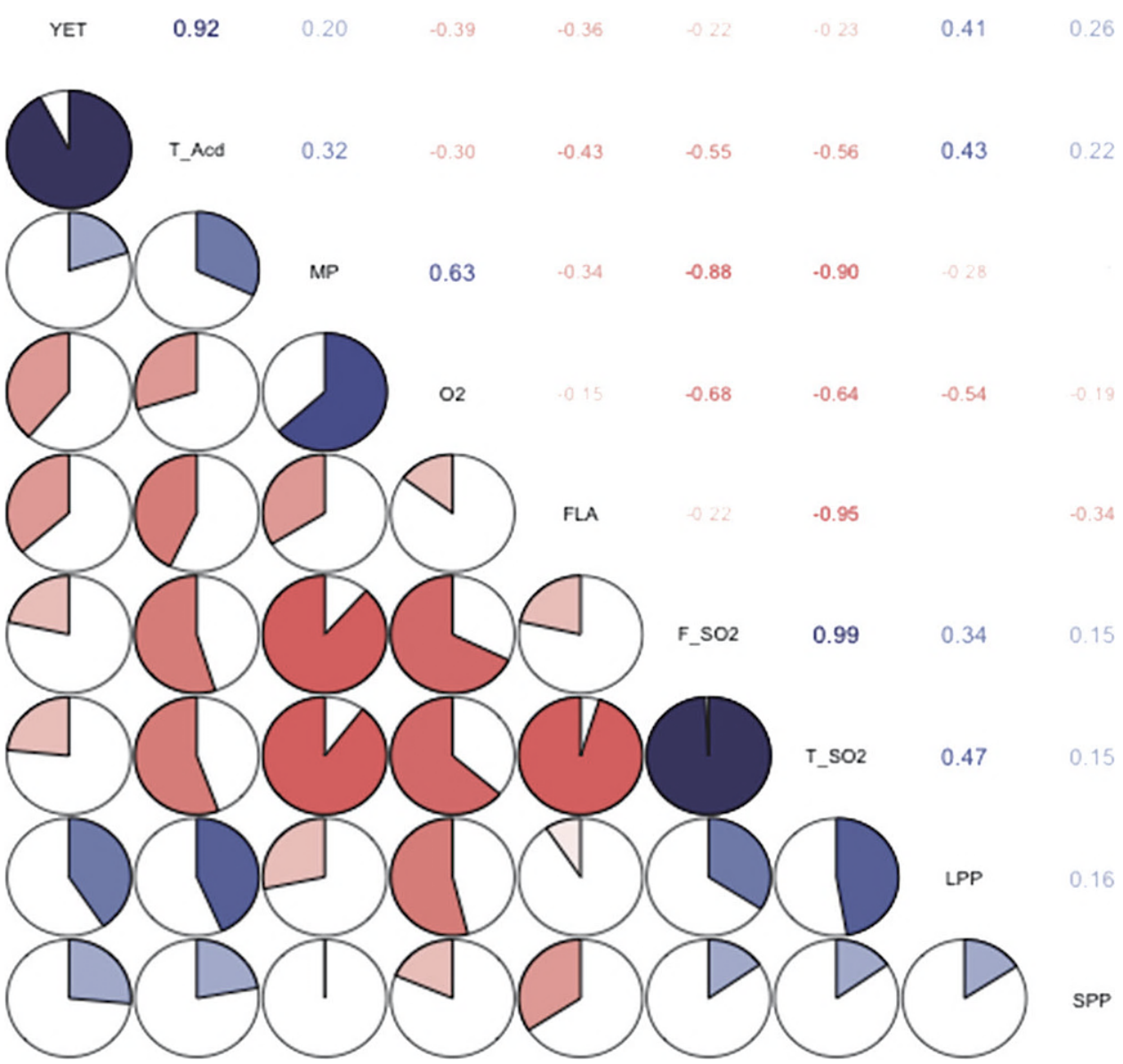

Figure 5.5 Correlations between oxygen consumption rate (O2), total acetaldehyde (T_Acd), yeast (YET), free SO_2 (F_SO2), total SO_2 (T_SO2), vanillin-reactive flavans (FLA), monomeric pigments (MP), small polymeric pigments (SPP), and large polymeric pigments (LPP) in the MOx experiment.

5.4.1.6 Correlation. To investigate which aspects of wine composition were the most predictive of oxygen consumption and acetaldehyde production, correlation analyses were conducted with the aforementioned compositional variables, including yeast (YET), free SO_2 (F_SO_2), total SO_2 (T_SO_2), vanillin-reactive flavans (FLA), monomeric pigments (MP), small polymeric pigments (SPP) and large polymeric pigments (LPP) (Figure 5.5). The positive correlation between total acetaldehyde production and yeast concentration was significant (0.92), indicating the importance of the presence of yeast to the formation of acetaldehyde. The compositional variables most strongly associated with O_2 consumption rate were MP (0.63), free SO_2 (-0.68), and total SO_2 (-0.64). The correlation coefficient for O_2 consumption rate and yeast was only -0.39, likely because the presence of yeast could be correlated with O_2 consumption only after appearance of culturable yeast populations. When such yeast were not yet present, O_2 consumption was highly correlated with MP, free SO_2, and total SO_2, in accordance with previous observations of chemical oxidation reactions (Danilewicz 2011, 2012, Ma and Waterhouse 2018). However, no obvious correlation was observed between O_2 consumption and FLA, SPP, and LPP, suggesting the weak effects of MOx on the development of polymeric phenols.

5.4.2 Oxygen Saturation Study

5.4.2.1 Compositional Variables. After saturating the wines with air and sealing their containers with no headspace, dissolved oxygen levels were monitored until virtually all of the oxygen was consumed. Acetaldehyde, SO_2, and a host of other compositional variables were measured before and after oxygen consumption to determine how these variables changed in relation to oxidation. Calculations for these compositional variables were the same as described above in the MOx study. Dissolved oxygen concentrations appeared to decay exponentially, with a consumption rate that was dependent on the concentration of oxygen, thus exponential regression equations were computed to fit the traces of declining oxygen levels. The rate constant k was taken from the value of the exponent in each regression equation. The half-life of oxygen was calculated, to represent oxygen consumption rates, according to the equation [$t_{1/2} = \ln(2) / k$] for first-order reactions.

Table 5.2. Bacteria identified by colony appearance and cell morphology, including suspected *Oenococcus oeni* populations and contaminant species, in the oxygen saturation experiment.

Wine	Colony appearance on 50% MRS media	Cell morphology	Species Identification
CS3	Medium size, round, white	Medium cocci; pairs, clumps, and some tetrads	*Micrococcus luteus*
CS4	Very small, round, white	Small cocci; pairs and short chains	*Oenococcus oeni* (suspected)
AB	Very small, round, white	Small cocci; pairs and short chains	*Oenococcus oeni* (suspected)
TN	Medium size, round, white	Medium cocci; pairs and small clumps	*Staphylococcus pasteuri*
RR	Very small, round, white	Small cocci; pairs and short chains	*Oenococcus oeni* (suspected)
RR	Medium size, round, white	Medium cocci; mostly pairs, some clumps	*Staphylococcus hominis*

All yeast populations were positively identified as *S. cerevisiae* by amplification and sequencing. At the start of the experiment, yeast was detected in only one of the wines, the Cabernet sauvignon-Merlot blend, and only one colony was observed in the most concentrated lane of the plate (corresponding to 100 CFU/mL). By the end of the experiment, yeast populations were present in 9 of the 10 unfiltered wines, with concentrations ranging from 150 to 5350 CFU/mL based on the average of the plate replicates. Small yeast populations emerged in four of the filtered wines as well, with a maximum concentration of 350 CFU/mL. Bacterial populations were found in one wine at the start of the experiment (the Rubired) and in five wines by the end of the experiment (CS3, CS4, AB, TN, and RR), both in filtered and unfiltered treatments. Cell densities were one to two orders of magnitude larger in the unfiltered treatments in all but one instance. A summary of colony and cell morphology as well as species identification is presented in Table 5.2. In two of the wines (CS3 and TN), plus one of the unfiltered Rubired wines, bacterial species were identified as contaminants from the genera *Staphylococus* or *Micrococcus*, which could have entered the wines at any point during the handling process before or during the experiment. In the other three wines (CS4, AB, and RR), the bacteria exhibited growth and morphological characteristics strongly indicative of *Oenococcus oeni*, including slow-growing colonies that were not detectable until several days after plate inoculation and very small (<1 mm) coccus-shaped cells arranged in pairs and short chains. Although sequencing was not

able to confirm these bacteria as *O. oeni*, these populations were considered to be *O. oeni* for the purposes of the following analysis.

5.4.2.2 Correlation. Initial values for compositional variables are shown in Table 5.1. Correlation analysis was conducted using initial values or changes in value for variables including O_2 half-life, acetaldehyde, yeast, *O. oeni*, phenolic variables such as vanillin-reactive flavans (FLA), total polyphenol index (TPI), MP, SPP, LPP, residual sugar (RS), iron and copper, and free and total SO_2 (Figure 5.6). O_2 half-life was significantly correlated with total SO_2 (0.82), yeast concentration (-0.56) and acetaldehyde production (-0.67). Acetaldehyde concentration was also correlated with yeast (0.84) and total SO_2 (-0.82), unsurprising given the data discussed above. Additionally, there was a significant correlation between yeast and total SO_2 (-0.73), and between yeast and residual sugar (0.47). These results suggest that yeast played an essential role in O_2 consumption and acetaldehyde production, and that total SO_2 and residual sugar may affect the growth of this yeast. Concentrations of phenolic compounds, iron, and copper, and *O. oeni* cell densities were not correlated with the half-life of oxygen or changes to acetaldehyde concentrations.

5.4.2.3 Yeast Effects. As oxygen half-life, acetaldehyde production, and total SO_2 were all significantly correlated with yeast, a comparison of each of these variables between filtered and unfiltered treatments was done to further elucidate the effects of yeast. Oxygen half-lives were much shorter in the unfiltered wines than in their filtered counterparts ($p < 0.05$, Figure 5.7A), indicating faster oxygen consumption rates in the unfiltered wines. Interestingly, a similar conclusion may be reached by classifying wines based on their final *S. cerevisiae* cell densities rather than by filtration. Wines with more than 400 yeast CFU/mL also had shorter oxygen half-lives than wines with less than 400 yeast CFU/mL ($p < 0.05$, Figure 5.7B). Additionally, filtered wines consumed significantly more SO_2 than unfiltered wines ($p < 0.05$, Figure 5.7C). These differences could also be related to yeast content: the decrease in total SO_2 in wines with less than 400 CFU/mL was significantly greater than in the wines with higher yeast levels ($p < 0.05$, Figure 5.7D). The rate of SO_2 consumption paralleled the rate of oxygen consumption in the filtered wines, but not the unfiltered wines.

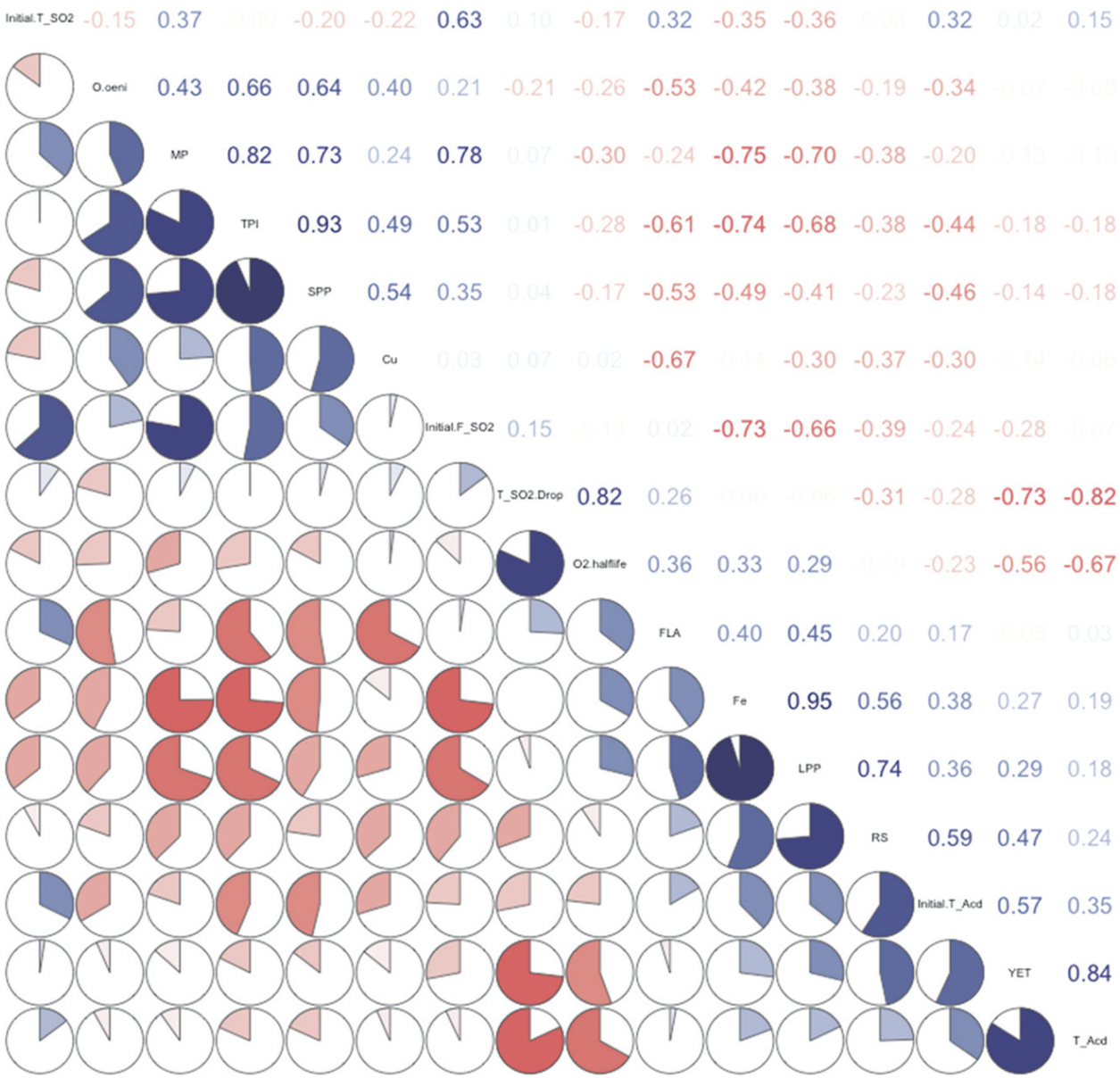

Figure 5.6 Correlations between oxygen half-life (O2.halflife), total acetaldehyde production (T_Acd), yeast (YET), *Oenococcus oeni* (O.oeni), free SO_2 (Initial.F_SO2), total SO_2 (Initial.T_SO2), vanillin-reactive flavans (FLA), total polyphenol index (TPI), monomeric pigments (MP), small polymeric pigments (SPP), large polymeric pigments (LPP), residual sugar (RS), iron (Fe), and copper (Cu) in the oxygen saturation experiment.

Initial values were used for most variables, but changes were used for T_SO2.Drop, YET, T_Acd, and O.oeni.

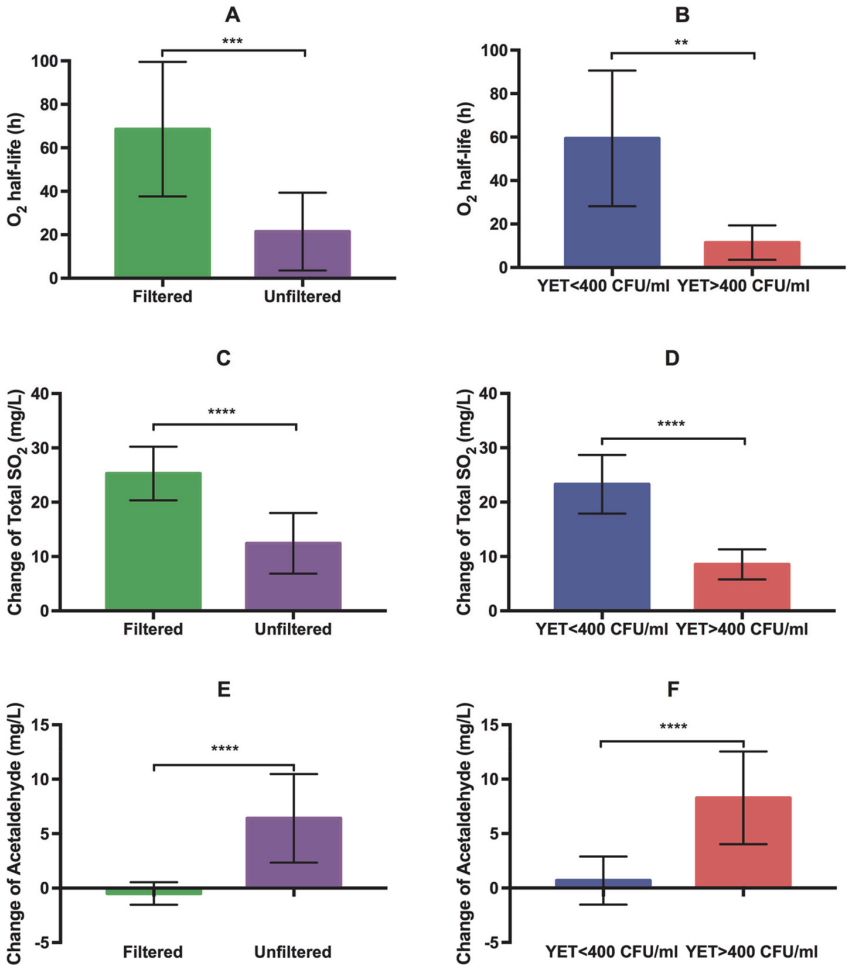

Figure 5.7 Significant differences in oxygen half-life (A, B), total SO_2 (C, D), and acetaldehyde (E, F) between filtered and unfiltered treatments, and between wines with greater or less than 400 CFU/mL yeast in the oxygen saturation experiment ($p<0.05$).

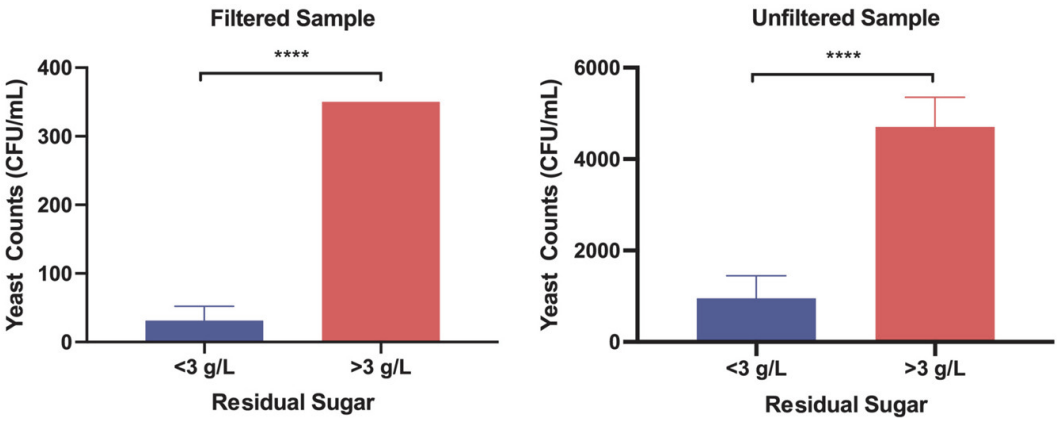

Figure 5.8 Significant differences in *Saccharomyces cerevisiae* cell counts by plating between wines with greater or less than 3 g/L initial residual sugar in the filtered and unfiltered treatments in the oxygen saturation experiment ($p<0.05$).

Regarding acetaldehyde production, unfiltered wines had significantly higher concentrations of acetaldehyde than filtered wines ($p < 0.05$, Figure 5.7E), which was consistent with findings that generation of acetaldehyde was higher in wines with high yeast levels than in wines with lower yeast cell densities ($p < 0.05$, Figure 5.7F). It was possible that after fermentation when sugars disappear, yeast can alter their gene expression to utilize ethanol as an alternate carbon source, oxidizing it to acetaldehyde (Tessier et al. 1998), or more likely, that with a small amount of residual sugar (3 g/L), the presence of oxygen facilitates the consumption of this sugar via partial fermentation (leaving acetaldehyde, not ethanol) stimulated by the regeneration of NAD^+ from NADH through the electron transport chain (Al-Dhabi et al. 2017, Hopp et al. 2019, Mei and Brenner 2014), rather than through the reduction of acetaldehyde to ethanol. However, this speculative explanation needs to be addressed in investigations targeting cellular metabolism, as our experiments were not designed to study this issue. Additionally, it should be noted that post-fermentation oxygenation in the presence of yeast appears to yield wines with exceptionally low residual sugar levels.

5.4.2.4 Residual Sugar. As residual sugar may affect the growth of yeast, changes of yeast cell counts in filtered and unfiltered wines with different initial residual sugar levels were analyzed (Figure 5.8). It was revealed that wines with higher residual sugar levels (>3 g/L) had higher yeast cell densities both in filtered and unfiltered wines, indicating that residual sugar can still significantly affect the growth of yeast after alcoholic fermentation.

The results of the oxygen saturation experiment followed the same trends that were observed in the MOx study with regards to oxygen consumption and acetaldehyde production. Unfiltered wines, in particular those with substantial residual sugar (>3 g/L), consumed oxygen more quickly and produced more acetaldehyde than filtered wines, and the size of the yeast population was correlated with both of these variables. In fact, yeast cell density was one of only two compositional variables significantly correlated with oxygen consumption and acetaldehyde production.

5.4.3 Residual Sugar Experiment. The use of a synthetic medium allowed for stricter control of microbial and chemical parameters, to focus solely on the effects of sugar and oxygen on the post-fermentation production of acetaldehyde by yeast. Yeast cell densities decreased from initial post-fermentation levels

(1.33 x 10^8 CFU/mL) after 10 days for all experimental treatments. Glucose addition and oxygenation both had significant effects on cell counts ($p < 0.05$); a significant interaction effect between oxygen and glucose was also identified ($p < 0.05$). The nGlu_nOx treatment resulted in the lowest cell count, while the other treatments worked to effectively maintain yeast populations on the order of 10^6 CFU/mL (Figure 5.9A). The addition of glucose essentially constitutes a refermentation of the wine, allowing the yeast to continue with metabolism, while the provision of oxygen has long been known to support cell viability (Rosenfeld and Beauvoit 2003). The data suggests only either glucose addition or oxygenation is necessary for the upkeep of cell density as no synergism between the two factors was observed for the Glu_Ox treatment. In fact, the highest cell density was maintained by the Glu_nOx treatment (3.95 x 10^6 CFU/mL), though the reason for this is uncertain; it may simply be that this treatment most closely matches the conditions during fermentation prior. It is worth noting the glucose added (3 g/L) was virtually completely consumed in 10 days regardless of whether the wine was oxygenated, reaching undetectable levels for the Glu_Ox treatment and 0.12 g/L for the Glu_nOx treatment.

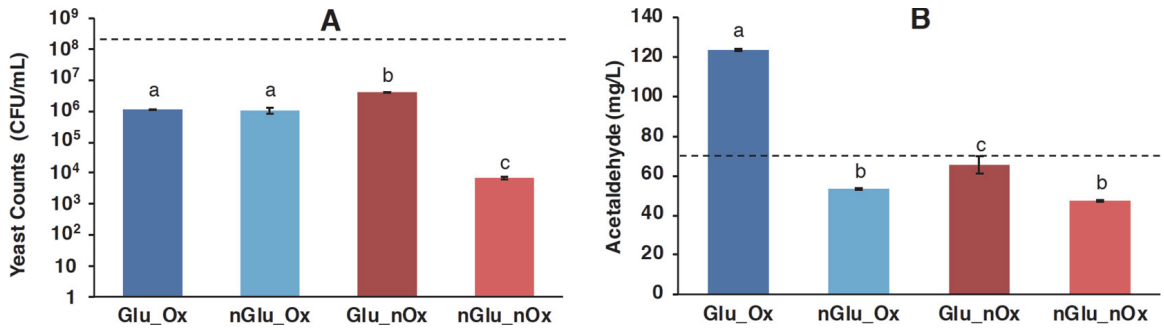

Figure 5.9 Final *Saccarhomyces cerevisiae* cell counts by plating for the synthetic wines in the residual sugar experiment (A); initial cell density (1.33 x 10^8 CFU/mL) is indicated by the dashed line. Total acetaldehyde levels (B); initial concentration (70.4 mg/L) is indicated by the dashed line. Different lowercase letters indicate significant differences ($p<0.05$).

The acetaldehyde concentration at the end of fermentation of this synthetic wine (70.4 mg/L) was much higher than those observed during the above experiments, and in red wines elsewhere, likely due to the lack of phenolic compounds to sequester acetaldehyde (Peterson and Waterhouse 2016, Sheridan and Elias 2016). Glucose, oxygen, and their interaction were all found to significantly affect acetaldehyde levels ($p < 0.05$). Concentrations decreased most significantly in the absence of glucose, while only a slight decrease was observed for the Glu_nOx treatment (Figure 5.9B), likely indicating simply the continuation of

usual metabolic processes. However, the concentration of acetaldehyde nearly doubled in the Glu_Ox treatment, indicating the importance of both glucose and oxygen as factors in yeast acetaldehyde production. This is in agreement with the findings presented above regarding the effects of residual sugar in the oxygen saturation experiment. These results suggest oxygen precludes the need to convert acetaldehyde into ethanol, normally required by yeast to regenerate NAD^+ from NADH during fermentation (Pronk et al. 1996). In the presence of oxygen, redox balance of the cell can be maintained instead by NADH oxidation by the electron transport chain (Bakker et al. 2001). However, rather than a complete switch to respiratory metabolism, it is possible the fermentative pathway remains active in yeast with the exception of the final step of ethanol production in the presence of oxygen, allowing acetaldehyde to accumulate. Future experiments should investigate the metabolic pathway directly.

In conclusion, yeast populations arose when a low level of residual sugar was present, despite the nutrient-poor post-fermentation environment. Wines with yeast consumed oxygen quickly and produced substantial quantities of acetaldehyde, and the growth of these yeast coincided with the depletion of SO_2 to minimal levels. Therefore, it is important for winemakers to consider the microbial status of their wines prior to the start of MOx, regardless of whether the treatment occurs before or after malolactic fermentation. In fact, we would argue that inoculations of yeast might be called for to properly manage MOx treatments if acetaldehyde production is desired. In the future, it would be worthwhile to investigate these microbial factors at the production scale to see if they can be used to predict the behavior of MOx treatments in a commercial setting, and whether yeast inoculations and management of residual sugar levels should be used to better control the process.

Concluding Remarks

Several reactions of the wine oxidation pathway are catalyzed by iron. The redox cycling of iron couples the primary reactions of the cascade: the reduction of oxygen by iron(II) and the oxidation of wine phenols by iron(III). Iron also catalyzes the Fenton reaction and subsequent oxidation of ethanol into acetaldehyde; whether it redox cycles appears to depend on prevailing dissolved oxygen concentrations. The importance of complexation to iron's role in wine oxidation may be considered the overarching "theme" for most of the work presented in the preceding chapters.

The differential selectivity for iron(II) and iron(III) of ferrozine and ethylenediaminetetraacetic acid (EDTA) respectively was utilized as a means of stabilizing iron(II):iron(III) ratios for spectrophotometric analysis. As discussed in Chapter 2, it would appear that any increase to the reduction potential of iron caused by complexation with ferrozine was negated by a decrease in potential due to EDTA (section 2.4.2). Such modifications to the reduction potential of iron would constitute a thermodynamic effect on its reactivity, though kinetics must also be considered. By physically occupy the coordination sites of iron, in some cases these chelators may lower the effective concentration of iron available to react by blocking interactions with other compounds.

This effect was apparent in the reactions of iron(III) with 4-methylcatechol in model wine, described in Chapter 3. While phenols are commonly thought to oxidize more quickly with higher pH, this was not found to be the case when the oxidant is iron(III) complexed by tartrate (section 3.4.2). With increases in pH, a greater proportion of tartaric acid deprotonates, consequently resulting in more abundant, more thermodynamically and kinetically stable iron(III)-tartrate complexes.

The effects of iron complexation could also be observed further along the oxidation cascade, as investigated in Chapter 4, during the Fenton oxidation of ethanol into acetaldehyde. Given this process entails the oxidation of iron(II) to iron(III), the opposite effect of pH on rate was observed, with acetaldehyde being produced more quickly at a higher pH level (section 4.4.2). In this case, not only is iron(III) stabilized, but increased complexation of iron(II) facilitates its oxidation by creating an electrically neutral complex from which an electron can be more easily removed. Moreover, tartaric, malic, and citric acid appeared to vary

with regards to their effects on the reactivity of iron, with citrate complexation resulting in the most rapid acetaldehyde production (section 4.4.3).

The findings presented in Chapter 5 are interesting given the clear indication that input of oxygen does not guarantee output of acetaldehyde. Despite indisputable observations of acetaldehyde in aged wines, and decades of research having elucidated the reaction mechanisms producing it (section 1.2), micro-oxygenation treatments in the absence of residual sugar and yeast failed to result in any acetaldehyde accumulation. As other have noted (section 1.1.3), the word “accumulation” is key: acetaldehyde is not necessarily an end-product of oxidation, also participating in further reactions with various wine constituents (section 1.3.1). It is likely that early on in a wine’s development these reactions outpace the production of acetaldehyde, such that it hovers at low steady-state concentrations, only to accumulate with time and oxygen exposure when its pool of reactants is exhausted. A method to selectively quantify acetaldehyde-reactive compounds would be of interest, as this could be used to predict wine’s “tipping point” as it ages.

However, in keeping with this dissertation’s theme, another possible explanation for the poor predictability of acetaldehyde accumulation with oxygen exposure may lie with iron and the effects of complexation on its ability to function as a catalyst. Evaluated in Chapter 4 were the main iron-chelating carboxylic acids found in wine, which have oxygen atoms as ligands to preferentially bind iron(III) and thereby decrease the reduction potential of iron. On the other hand, nitrogen and sulfur ligands, being softer bases, stabilize iron(II) and increase the reduction potential of iron; this is the basis for the use of EDTA and ferrozine together to halt redox cycling. As noted in the conclusion of Chapter 4 (section 4.4.4), many other wine constituents are capable of forming complexes with iron, some of which will invariably possess nitrogen or sulfur as ligands. While at this point a largely speculative hypothesis, it can be reasoned that such a halt or slowing of iron redox cycling is possible in wines containing a particular balance of complexing agents, consequently impeding the formation of acetaldehyde.

References

Amerine MA. 1964. Acids, grapes, wine and people. Am J Enol Vitic 15:106-115.

Anastacio AS, Harris B, Yoo HI, Fabris JD, and Stucki JW. 2008. Limitations of the ferrozine method for quantitative assay of mineral systems for ferrous and total iron. Geochim Cosmochim Acta 72:5001-5008.

Andersen ML and Skibsted LH. Electron spin resonance spin trapping identification of radicals formed during aerobic forced aging of beer. J Agric Food Chem 46:1272-1275

Anli RE and Cavuldak OA. 2013. A review of microoxygenation application in wine. J Inst Brew 118:368-385.

Ajlec R and Stupar J. 1989. Determination of iron species in wine by ion-exchange chromatography-flame atomic absorption spectroscopy. Analyst 114:137-142.

Aranda A, Querol A, del Olmo M. 2002. Correlation between acetaldehyde and ethanol resistance and expression of HSP genes in yeast strains isolated during the biological aging of sherry wines. Arch Microbiol 177:304-312.

Arapitsas P, Scholz M, Vrhovsek U, Di Blasi S, Bartolini AB, Masuero D, Perenzoni D, Rigo A, and Mattivi F. 2012. A metabolomic approach to the study of wine micro-oxygenation. PLOS One 7:e37783

Arfelli G, Sartini E, Corazni C, and Fabiani A. 2011. Chips, lees, and micro-oxygenation: Influence on some flavors and sensory profile of a bottled red Sangiovese wine. Eur Food Res Technol 233:1-10.

Atanasova V, Fulcrand H, Cheynier V, and Moutounet M. 2002. Effect of oxygenation on polyphenol changes occurring in the course of winemaking. Anal Chim Acta 458:15-27.

Avdeef A, Sofen SR, Bregante TL, and Raymond KN. 1978. Coordination chemistry of microbial iron transport compounds. 9. Stability constants for catechol models of enterobactin. J Am Chem Soc 100:5362-5370.

Bakker BM, Overkamp KM, van Maris AJA, Kötter P, Luttik MAH, van Dijken JP, and Pronk JT 2001. Stoichiometry and compartmentation of NADH metabolism in *Saccharomyces cerevisiae*. FEMS Microbiol Rev 25:15-37.

Bakker J, Bridle P, Honda T, Kuwano H, Saito N, Terahara N, and Timberlake CF. 1997. Identification of an anthocyanin occuring in some red wines. Phytochemistry 44:1375-1382.

Bakker J and Timberlake CF. 1997. Isolation, identification, and characterization of new color-stable anthocyanins occurring in some red wines. J Agric Food Chem 45:35-43.

Barril C, Clark AC, and Scollary GR. 2012. Chemistry of ascorbic acid and sulfur dioxide as an antioxidant system relevant to white wine. Anal Chim Acta 732:186-193.

Bartowsky SJ and Pretorius IS. 2009. Microbial formation and modification of flavor and off-flavor compounds in wine. *In* Biology of Microorganisms on Grapes, in Must and in Wine, pp 209-231. Konig H, Unden G, Frohlick J (eds). Springer, Berlin/Heidelberg.

Beech FW, Burroughs LF, Timberlake CF, and Whiting GC. 1979. Recent progress on chemical aspects and the microbial action of SO_2. Bull OIV 52:1001-1022.

Behar D, Czapski G, Rabani J, Dorfman LM, and Schwarz HA. 1970. Acid dissociation constant and decay kinetics of the perhydroxyl radical. J Phys Chem 74:3209-3213.

Benzie IFF and Strain JJ. 1996. The ferric reducing ability of plasma (FRAP) as a measure of "antioxidant power": The FRAP assay. Anal Biochem 239:70-76.

Berg HW, Filipello F, Hinreiner E, and Webb AD. 1955. Evaluation of thresholds and minimum difference concentrations for various constituents of wines. I. Water solutions of pure substances. Food Technol 9:23-26.

Bielski BHJ and Gebicki JM. 1982. Generation of superoxide radicals by photolysis of oxygenated ethanol solutions. J Am Chem Soc 104:796-798.

Blanchard L, Darriet P, and Dubourdieu D. 2004. Reactivity of 3-mercaptohexanol in red wine: Impact of oxygen, phenolic fractions, and sulfur dioxide. Am J Enol Vitic 55:115-120.

Boulton RB, Singleton VL, Bisson LF, and Kunkee RE. 1996. Principles and Practices of Winemaking. Chapman & Hall, New York, NY.

Bradshaw MP, Prenzler PD, and Scollary GR. 2001. Ascorbic acid-induced browning of (+)-catechin in a model wine system. J Agric Food Chem 49:380-384.

Brajkovich M, Tibbits N, Peron G, Lund CM, Dykes SI, Kilmartin PA, and Nicolau L. 2005. Effect of screwcap and cork closures on SO_2 levels and aromas in a Sauvignon blanc wine. J Agric Food Chem 53:10006-10011.

Bueno M, Carrascón V, and Ferreira V. 2015. Release and formation of oxidation-related aldehydes during wine oxidation. J Agric Food Chem 64:608-617.

Burns TR and Osborne JP. 2013. Impact of malolactic fermentation on the color and color stability of Pinot noir and Merlot wine. Am J Enol Vitic 64:370-377.

Burns TR and Osborne JP. 2015. Loss of Pinot noir wine color and polymeric pigment after malolactic fermentation and potential causes. Am J Enol Vitic 66:130-137.

Burroughs LF and Sparks AH. 1973. Sulphite-binding power of wines and ciders. I. Equilibrium constants for the dissociation of carbonyl bisulphite compounds. J Sci Food Agric 24:187-198.

Buxton GV, Greenstock CL, Helman WP, and Ross AB. 1988. Critical review of rate constants for reactions of hydrated electrons, hydrogen atoms, and hydroxyl radicals in aqueous solution. J Phys Chem Ref Data 17:513-886.

Caillé S, Samson A, Wirth J, Dieval J-B, Vidal S, and Cheynier V. 2010. Sensory characteristics changes of red Grenache wines submitted to different oxygen exposures pre and post bottling. Anal Chim Acta 660:35-42.

Câmara JS, Alves MA, and Marques JC. 2006. Changes in volatile composition of Madeira wines during their oxidative aging. Anal Chim Acta 563:188-197.

Câmara JS, Marques JC, Alves A, and Silva Ferreira AC. 2003. Heterocyclic acetals in Madeira wines. Anal Bioanal Chem 275:1221-1224.

Carlton WK, Gump B, Fugelsang K, and Hasson AS. 2007. Monitoring acetaldehyde concentrations during micro-oxygenation of red wine by headspace solid-phase microextraction with on-fiber derivatization. J Agric Food Chem 55:5620-5625.

Carrascón V, Fernandez-Zurbano P, Bueno M, and Ferreira V. 2015. Oxygen consumption by red wines. Part II: Differential effects on color and chemical composition caused by oxygen taken in different sulfur dioxide-related oxidation contexts. J Agric Food Chem 63:10938-10947.

Carrascón V, Vallverdú-Queralt A, Meudec E. Sommerer N, Fernandez-Zurbano P, and Ferreira V. 2018. The kinetics of oxygen and SO_2 consumption by red wines. What do they tell about oxidation mechanisms and about changes in wine composition? Food Chem 241:206-214.

Castellari M, Arfelli G, Riponi C, and Amati A. 1998. Evolution of phenolic compounds in red winemaking as affected by must oxygenation. Am J Enol Vitic 49:91-94.

Castellari M, Matricardi L, Arfelli G, Galassi S, and Amati A. 2000. Level of single bioactive phenolics in red wine as a function of the oxygen supplied during storage. Food Chem 69:61-67.

Castellari M, Simonato B, Tornielli GB, Spinelli P, and Ferrarini R. 2004. Effects of different enological treatments on dissolved oxygen in wines. Ital J Food Sci 16:387-396.

Cano-López M, López-Roca JM, Pardo-Minguez F, and Gómez-Plaza E. 2010. Oak barrel maturation vs. micro-oxygenation: Effect on the formation of anthocyanin-derived pigments and wine color. Food Chem 119:191-195.

Cano-López M, Pardo-Minguez F, Schmauch G, Saucier C, Teissedre PL, López-Roca JM, and Gómez-Plaza E. 2008. Effect of micro-oxygenation on color and anthocyanin-related compounds of wines with different phenolic contents. J Agric Food Chem 56:5932-5941.

Cejudo-Bastante MJ, Pérez-Coello MS, and Hermosin-Gutiérrez I. 2011a. Effect of wine micro-oxygenation treatment and storage period on colour-related phenolics, volatile composition and sensory characteristics. LWT 44:866-874.

Cejudo-Bastante MJ, Hermosin-Gutiérrez I, and Pérez-Coello MS. 2011b. Micro-oxygenation and oak chip treatments of red wines: Effects on colour-related phenolics, volatile composition and sensory characteristics. Part II: Merlot wines. Food Chem 124:738-748.

Chang C-Y, Hsieh Y-H, Cheng K-Y, Hsieh L-L, Cheng T-C, and Yao K-S. 2008. Effect of pH on Fenton process using estimation of hydroxyl radical with salicylic acid as trapping reagent. Water Sci Technol 58:837-879.

Cheraiti N, Geuzenec S, and Salmon J-M. 2010. Very early acetaldehyde production by industrial *Saccharomyces cerevisiae* strains: a new intrinsic character. Appl Microbiol Biotechnol 86:693-700.

Cheynier V, Basire N, and Rigaud J. 1989. Mechanism of trans-caffeoyltartaric acid and catechin oxidation in model solutions containing grape polyphenoloxidase. J Agric Food Chem 37:1069-1071.

Clark AC, Dias DA, Smith TA, Ghiggino KP, and Scollary GR. 2011. Iron(III) tartrate as a potential precursor of light-induced oxidative degradation of white wine: Studies in a model wine system. J Agric Food Chem 59:3575-3581.

Clark AC, Prenzler PD, and Scollary GR. 2007. Impact of the condition of storage of tartaric acid solutions on the production and stability of glyoxylic acid. Food Chem 102:905-916.

Coehlo JM, Howe PA, and Sacks GL. 2015. A headspace gas detection tube method to measure SO_2 in wine without disrupting SO_2 equilibria. Am J Enol Vitic 66:257-265.

Coleman RE, Boulton RB, and Stuchebrukhov AA. 2020. Kinetics of autoxidation of tartaric acid in presence of iron. J Chem Phys 153:064503.

Collins EB and Speckman RA. 1974. Influence of acetaldehyde on growth and acetoin production by *Leuconostoc citrovorum*. J Dairy Sci 57:1428-1431.

Cruz L, Brás NF, Teixeira N, Fernandes A, Mateus N, Ramos MJ, Rodríguez-Borges J, and de Freitas V. 2009. Synthesis and structural characterization of two diastereoisomers of vinylcatechin dimers. J Agric Food Chem 57:10341-10348.

Danilewicz JC. 2003. Review of reaction mechanisms of oxygen and proposed intermediate reduction products in wine: Central role of iron and copper. Am J Enol Vitic 54:73-85.

Danilewicz JC. 2007. Interaction of sulfur dioxide, polyphenols, and oxygen in a wine-model system: Central role of iron and copper. Am J Enol Vitic 58:53-60.

Danilewicz JC. 2011. Mechanism of autoxidation of polyphenols and participation of sulfite in wine: Key role of iron. Am J Enol Vitic 62:319-328

Danilewicz JC. 2012. Review of oxidative processes in wine and value of reduction potentials in enology. Am J Enol Vitic 63:1-10.

Danilewicz JC. 2013. Reactions involving iron in mediating catechol oxidation in model wine. Am J Enol Vitic 64:316-324.

Danilewicz JC. 2016a. Chemistry of manganese and interaction with iron and copper in wine. Am J Enol Vitic 67:377-384.

Danilewicz JC. 2016b. Fe(II):Fe(III) ratio and redox status of white wines. Am J Enol Vitic 67:146-152.

Danilewicz JC. 2016c. Reaction of oxygen and sulfite in wine. Am J Enol Vitic 67:13-17.

Danilewicz JC. 2018. Fe(III):Fe(II) ratio and redox status of red wines: Relation to so-called “reduction potential”. Am J Enol Vitic 69:141-147.

Danilewicz JC, Seccombe JT, and Whelan J. 2008. Mechanism of interaction of polyphenols, oxygen, and sulfur dioxide in model wine and wine. Am J Enol Vitic 59:128-136.

Danilewicz JC and Wallbridge PJ. 2010. Further studies on the mechanism of interaction of polyphenols, oxygen, and sulfite in wine. Am J Enol Vitic 61:166-175.

da Silva Ferreira AC, Barbe JC, and Bertrand A. 2002. Heterocyclic acetals from glycerol and acetaldehyde in port wines: Evolution with aging. J Agric Food Chem 50:2560-2564.

de Azevedo LC, Reis MM, Motta LF, da Rocha GO, Silva LA, and de Andrede JB. 2007. Evaluation of the formation and stability of hydroxyalkylsulfonic acids in wine. J Agric Food Chem 55:8670-8680.

de Beer D, Joubert E, Marais J, and Manley M. 2008. Effect of oxygenation during maturation on phenolic composition, total antioxidant capacity, colour and sensory quality on Pinotage wine. S Afr J Enol Vitic 29:13-25.

de Freitas V and Mateus N. 2011. Formation of pyranoanthocyanins in red wines: A new and diverse class of anthocyanin derivatives. Anal Bioanal Chem 401:1463-1473.

del Alamo-Sanza M and Nevares I. 2014. Recent Advances in the Evaluation of the Oxygen Transfer Rate in Oak Barrels. J Agric Food Chem 62:8892-8899.

del Alamo-Sanza M and Nevares I. 2018. Oak wine barrel as an active vessel: A critical review of past and current knowledge. Crit Rev Food Sci Nutr 58:2711-2726.

del Carmen Llaudy M, Canals R, González-Manzano S, Canals JM, Santos-Buelga C, and Zamora F. 2006. Influence of micro-oxygenation treatment before oak aging on phenolic compounds composition, astringency, and color of red wine. J Agric Food Chem 54:4246-4252.

Dimkou E, Ugliano M, Dieval JB, Vidal S, Aagard O, Rauhut D, and Jung R. 2011. Impact of headspace oxygen and closure on sulfur dioxide, color, and hydrogen sulfide levels in a Riesling wine. Am J Enol Vitic 62:261-269.

Drinkine J, Lopes P, Kennedy JA, Teissedre PL, and Saucier C. 2007. Ethylidene-bridged flavan-3-ols in red wine and correlation with wine age. J Agric Food Chem 55:6292-6299.

Dueñas M, Fulcrand H, and Cheynier V. 2006. Formation of anthocyanin-flavanol adducts in model wine solutions. Anal Chim Acta 563:15-25.

Durner D, Nickolaus P, and Trieu H. 2015. Micro-oxygenation and its impact on polyphenols and sensory characteristics of Pinot noir. Wine Vitic J 30:26-30

Durner D, Weber F, Neddermeyer J, Koopman J, Winterhalter P, and Fischer U. 2010. Sensory and color changes induced by microoxygenation treatments of Pinot noir before and after malolactic fermentation. Am J Enol Vitic 61:474-485.

du Toit WJ, Marais J, Pretorius IS, and du Toit M. 2006. Oxygen in must and wine: A review. S Afr J Enol Vitic 27:76-94.

Elias RJ, Andersen ML, Skibsted LH, and Waterhouse AL. 2009. Identification of free radical intermediates in oxidized wine using electron paramagnetic resonance spin trapping. J Agric Food Chem 57:4359-4365.

Elias RJ and Waterhouse AL. 2010. Controlling the Fenton reaction in wine. J Agric Food Chem 58:1699-1707.

Escudero A, Asensio E, Cacho J, and Ferreira V. 2000. Isolation and identification of odorants generated in wine during its oxidation: A gas chromatography-olfactometric study. Eur Food Res Technol 211:105-110.

Es-Safi N-E, Fulcrand H, Cheynbier V, and Moutounet M. 1999. Studies on the acetaldehyde-induced condensation of (-)-epicatechin and malvidin 3-O-glucoside in a model solution system. J Agric Food Chem 47:2096-2102.

Esteve-Zarzoso B, Peris-Torán MJ, García-Maiquez E, Uruburu F, and Querol A. 2001. Yeast population dynamics during the fermentation and biological aging of sherry wines. Appl Environ Microbiol 67:2056-2061.

Farinelli G, Minella M, Pazzi M, Giannakis S, Pulgarin C, Vione D, and Tiraferri A. 2020. Natural iron ligands promote a metal-based oxidation mechanism for the Fenton reaction in water environments. J Hazard Mater 393:122413

Fenton HJH. 1894. Oxidation of tartaric acid in presence of iron. J Chem Soc 65:899-910.

Ferreira V, Carrascon V, Bueno M, Ugliano M, and Fernandez-Zurbano P. 2015. Oxygen consumption by red wines. Part I: Consumption rates, relationship with composition, and role of SO_2. J Agric Food Chem 63:10928-10937.

Ferreira SLC, Ferreira HS, de Jesus RM, Santos JVS, Brandao GC, and Souza AS. 2007. Development of method for the speciation of inorganic iron in wine samples. Anal Chem Acta 602:89-93.

Ferreira V, Franco-Luesma E, Vela E, Lopez R, and Hernandez-Orte P. 2018. Elusive chemistry of hydrogen sulfide and mercaptans in wine. J Agric Food Chem 66:2237-2246.

Fornachon JC. 1953. The accumulation of acetaldehyde in suspensions of yeasts. Aust J Biol Sci 6:222-233.

Fornairon-Bonnefond C, Demartez V, Rosenfeld E, and Salmon JM. 2002. Oxygen addition and sterol synthesis in *Saccharomyces cerevisiae* during enological fermentation. J Biosci Bioeng 93:176-182.

Fulcrand H, Cameira dos Santos P-J, Sarni-Manchado P, Cheynier V, and Favre-Bonvin J. 1996. Structure of new anthocyanin-derived wine pigments. J Chem Soc Perkin Trans I 1:735-739.

Fulcrand H, Dueñas M, Salas E, and Cheynier V. 2006. Phenolic reactions during winemaking and aging. Am J Enol Vitic 57:289-297.

Fukuzawa K, Tadokoro T, Kishikawa K, Mukai K, and Gebicki JM. 1988. Site-specific induction of lipid peroxidation by iron in charged micelles. Arch Biochem Biophys 260:146-152.

Gambuti A, Han G, Peterson AL, and Waterhouse AL. 2015. Sulfur dioxide and glutathione alter the outcome of microoxygenation. Am J Enol Vitic 66:411-423.

Geldenhuys L, Oberholster A, and du Toit WJ. 2012. Monitoring the effect of micro-oxygenation before malolactic fermentation on South African Pinotage red wine with different colour and phenolic analysis. S Afr J Enol Vitic 33:150-160.

Gislason NE, Currie BL, and Waterhouse AL. 2011. Novel antioxidant reactions of cinnamates in wine. J Agric Food Chem 59:6221-6226.

Gómez-Plaza E and Cano-López M. 2011. A review on micro-oxygenation of red wines: Claims, benefits and the underlying chemistry. Food Chem 125:1131-1140.

Gonzalez A, Vidal S, and Ugliano M. 2018. Untargeted voltammetric approaches for characterization of oxidation patterns in white wines. Food Chem 269:1-8.

Gorman JE and Clydesdale FM. 1984. Thermodynamic and kinetic stability constants of selected carboxylic acids and iron. J Food Sci 49:500-503.

Green MJ and Hill HAO. 1984. Chemistry of dioxygen. Methods Enzymol 105:3-22.

Green RW and Parkins GM. 1961. Complexes of iron with D-tartaric and meso-tartaric acids. J Phys Chem 65:1658-1659.

Han G, Wang H, Webb MR, and Waterhouse AL. 2015. A rapid, one step preparation for measuring selected free plus SO_2-bound wine carbonyls by HPLC-DAD/MS. Talanta 134:596-602.

Han G, Webb MR, Richter C Parsons J, and Waterhouse AL. 2017. Yeast alter micro-oxygenation of wine: Oxygen consumption and aldehyde production. J Sci Food Agric 97:3847-3854.

Harbertson JF, Picciotto EA, and Adams DO. 2003. Measurement of polymeric pigments in grape berry extracts and wines using a protein precipitation assay combined with bisulfite bleaching. Am J Enol Vitic 54:301-306.

Hayasaka Y, Birse M, Eglinton J, and Herderich M. 2007. The effect of *Saccharomyces cerevisiae* and *Saccharomyces bayanus* yeast and colour properties and pigment profiles of a Cabernet sauvignon red wine. Aust J Grape Wine Res 13:176-185.

He F, Liang NN, Mu L, Pan QH, Wang J, Reeves MJ, and Duan CQ. 2012. Anthocyanins and their variations in red wines II. Anthocyanin derived pigments and their color evolution. Molecules 12:1483-1519.

Héretier J, Bach B, Schönenberger P, Gaillard V, Ducruet J, and Segura J-M. 2016. Quantification of the production of hydrogen peroxide H_2O_2 during accelerated wine oxidation. Food Chem 211:957-962.

Hider RC, Liu ZD, and Khodr HH. 2001. Metal chelation of polyphenols. Methods Enzymol 335:190-203.

Homsher R and Zak B. 1985. Spectrophotometric investigation of sensitive complexing agents for the determination of zinc in serum. Clin Chem 31:1310-1313.

Hopp AK, Grüter P, and Hottinger MO. 2019. Regulation of glucose metabolism by NAD(+) and ADP-ribosylation. Cell 8:890.

Horner L and Geyer E. 1965. Die polarographische bestimmung der redoxpotentiale von brenzcatechin-derivaten. Chem Ber 98:2009-2015.

Hynes MJ and O'Coinceanainn M. 2001. The kinetics and mechanisms of the reaction of iron(III) with gallic acid, gallic acid methyl ester and catechin. J Inorg Biochem 85:131-142.

Ilan YA and Czapski G. 1977. Reaction of superoxide radical with iron complexes with EDTA studied by pulse radiolysis. Biochim Biophys Acta Gen Subj 498:386-394.

Iland P, Bruer N, Edwards G, Caloghiris S, and Wilkes E. 2004. Chemical Analysis of Grapes and Wine: Techniques and Concepts. Patrick Iland Wine Promotions Pty Ltd, Campbelltown, Australia.

Im J, Lee J, and Loffler FE. 2013. Interference of ferric ions with ferrous ion quantification using the ferrozine assay. J Microbiol Methods 95:366-367.

Ingram LO and Buttke TM. 1985. Effects of alcohols on micro-organisms. Adv Microb Physiol 25:253-300.

International Union of Pure and Applied Chemistry – Analytical Chemistry Division. 1978. Nomenclature, symbols, units and their usage in spectrochemical analysis – II. Data interpretation. Spectrochim Acta Part B 33:241-245.

Jackson R. 2016. Shelf life of wine. *In* The Stability and Shelf Life of Food, 2nd edition. pp 311-346. Woodhead Publishing, Cambridge.

Jenkins TW, Howe PA, Sacks GL, and Waterhouse AL. 2020. Determination of molecular and "truly" free sulfur dioxide in wine: A comparison of headspace and conventional methods. Am J Enol Vitic 71:222-230.

Jones RP. 1989. Biological principles for the effects of ethanol. Enzyme Microb Technol 11:130-153.

Joslyn MA and Comar CL. 1941. Role of acetaldehyde in red wines. Ind Eng Chem 33:919-928.

Karadjova I, Izgi B, and Gucer S. 2002. Fractionation and speciation of Cu, Zn and Fe in wine samples by atomic absorption spectrometry. Spectrochim Acta B 57:581-590.

Katalinic V, Milos M, Modun D, Music I, and Boban M. 2004. Antioxidant effectiveness of selected wines in comparison with (+)-catechin. Food Chem 86:593-600.

Kilmartin PA. 2010. Microoxidation in wine production. Adv Food Nutr Res 61:149-186.

Kilmartin PA, Zou HL, and Waterhouse AL. 2001. A cyclic voltammetry method suitable for characterizing antioxidant properties of wine and wine phenolics. J Agric Food Chem 49:1957-1965.

Kilmartin PA, Zou HL, and Waterhouse AL. 2002. Correlation of wine phenolic composition versus cyclic voltammetry response. Am J Enol Vitic 53:294-302.

Kliewer WM, Horwath L, and Omori M. 1967. Concentrations of tartaric acid and malic acids and their salts in *Vitis vinifera* grapes. Am J Enol Vitic 18:42-54.

Kolthoff IM and Medalia AI. 1949a. The reaction between ferrous iron and peroxides. I. Reaction with hydrogen peroxide in the absence of oxygen. J Am Chem Soc 71:3777-3783.

Kolthoff IM and Medalia AI. 1949b. The reaction between ferrous iron and peroxides. II. Reaction with hydrogen peroxide, in the presence of oxygen. J Am Chem Soc 71:3784-3788.

Kreitman GY, Cantu A, Waterhouse AL, and Elias RJ. 2013a. Effect of metal chelators on the oxidative stability of model wine. J Agric Food Chem 61:9480-9487.

Kreitman GY, Laurie VF, and Elias RJ. 2013b. Investigation of ethyl radical quenching by phenolics and thiols in model wine. J Agric Food Chem 61:685-692.

Laurie VF and Clark AC. 2010. Wine oxidation. *In* Oxidation in Foods and Beverages and Antioxidant Applications. Decker EA, Elias RJ, and McClements DJ (eds). Vol 2, pp 445-475. Woodhead Publishing, Cambridge.

Laurie VF and Waterhouse AL. 2006. Oxidation of glycerol in the presence of hydrogen peroxide and iron in model solutions and wine. Potential effects on wine color. J Agric Food Chem 54:4668-4673.

Li E and Mira de Orduña R. 2011. Evaluation of the acetaldehyde production and degradation potential of 26 enological Saccharomyces and non-Saccharomyces yeast strains in a resting cell model system. J Ind Microbiol Biotechnol 38:1391-1398.

Lin YH, Chien WS, Duan KJ, and Change PR. 2011. Effect of aeration timing and interval during very-high-gravity ethanol fermentations. Process Biochem 46:1025-1028.

Liu S-Q and Pilone GL. 2000. An overview of formation and roles of acetaldehyde in winemaking with emphasis on microbiological implications. Int J Food Sci Technol 35:49-61.

Lonvaud-Funel A. 1999. Lactic acid bacteria in the quality improvement and depreciation of wine. Antonie van Leeuwenhoek 76:317-331.

Lopes P, Saucier C, and Glories Y. 2005. Nondestructive colorimetric method to determine the oxygen diffusion rate through closures used in winemaking. J Agric Food Chem 53:6967-6973.

Lopes P, Saucier C, Teissedre P-L, and Glories Y. 2006. Impact of storage position on oxygen ingress through different closures into wine bottles. J Agric Food Chem 54:6741-6746.

Lopes P, Saucier C, Teissedre P-L, and Glories Y. 2007. Main routes of oxygen ingress through different closures into wine bottles. J Agric Food Chem 55:5167-5170.

Lopez-Lopez JA, Albendin G, Arufe MI, and Manuel-Vez MP. 2015. Simplication of iron speciation in wine samples: A spectrophotometric approach. J Agric Food Chem 63:4545-4550.

Ma L, Bueschl C, Schuhmacher R, and Waterhouse AL. 2019. Tracing oxidation reaction pathways in wine using ^{13}C isotopolog patterns and a putative compound database. Anal Chim Acta 1054:74-83.

Ma L and Waterhouse AL. 2018. Flavanols react preferentially with quinones through an electron transfer reaction, stimulating rather than preventing wine browning. Anal Chim Acta 1039:162-171.

Ma L, Watrelot AA, Addison B, and Waterhouse AL. 2018. Condensed tannin reacts with SO_2 durign wine aging, yielding flavan-3-ol sulfonates. J Agric Food Chem 66:9259-9268.

Margalit, Y. 2012. Concepts in Wine Chemistry, 3rd edition. Wine Appreciation Guild, San Francisco, CA.

Martins RC, Oliveira R, Bento F, Geraldo D, Lopes VV, de Pinho PG, Oliveira CM, and Ferreira ACS. 2008. Oxidation management of white wines using cyclic voltammetry and multivariate process monitoring. J Agric Food Chem 56:12092-12098.

Mateus N, Silva AMS, Santos-Buelga C, Rivas-Gonzalo JC, and de Freitas V. 2002. Identification of anthocyanin-flavanol pigments in red wines by NMR and mass spectrometry. J Agric Food Chem 50:2110-2116.

McArdle JV and Hoffman MR. 1983. Kinetics and mechanism of the oxidation of aquated sulfur dioxide by hydrogen peroxide at low pH. J Phys Chem 87:5425-5429.

McCloskey LP and Mahaney P. 1981. An enzymatic assay for acetaldehyde in grape juice and wine. Am J Enol Vitic 32:159-162.

McGee EJT and Diosady LL. 2018. Prevention of iron-polyphenol complex formation by chelation in black tea. LWT 89:756-762.

Mei S-C and Brenner C. 2014. Quantification of protein copy number in yeast: The NAD(+) metabolome. PLoS One 9:e106496

Mentasti E and Pelizzetti E. 1973. Reactions between iron(III) and catechol (o-dihydroxybenzene). 1. Equilibria and kinetics of complex formation in aqueous acid solution J Chem Soc-Dalton Trans:2605-2608.

Michaelis L and Friedheim E. 1931. Potentiometric studies on complex iron systems. J Biol Chem 91:343-353.

Michaelis L and Smythe CV. 1931. The correlation between rate of oxidation and potential in iron systems. J Biol Chem 94:329-340.

Miller DM, Buettner GR, and Aust SD. 1990. Transition metals as catalysts of autoxidation reactions. Free Radical Biol Med 8:95-108.

Mira L, Fernandez MT, Santos M, Rocha R, Florêncio MH, and Jennings KR. 2002. Interactions of flavonoids with iron and copper ions: A mechanism for their antioxidant activity. Free Radical Res 36:1199-1208.

Moran JF, Klucas RV, Grayer RJ, Abian J, and Becana M. 1997. Complexes of iron with phenolic compounds from soybean nodules and other legume tissues: Prooxidant and antioxidant properties. Free Radical Biol Med 22:861-870.

Morata A, Gómez-Cordovéz MC, Colomo B, and Suárez JA. 2003. Pyruvic acid and acetaldehyde production by different strains of *Saccharomyces cerevisiae*: Relationship with vitisin A and B formation in red wines. J Agric Food Chem 51:7402-7409.

Morata A, Loira I, Heras JM, Callejo MJ, Tesfaye W, González C, and Suárez-Lepe JA. 2016. Yeast influence on the formation of stable pigments in red winemaking. Food Chem 197:686-691.

Morozova K, Schmidt O, and Schwack W. 2014. Impact of headspace oxygen and copper and iron addition on oxygen consumption rate, sulphur dioxide loss, colour and sensory properties of Riesling wine. Eur Food Res Technol 238:652-663.

Muñoz D, Peinado RA, Medina M, and Moreno J. 2005. Biological aging of sherry wines using pure cultures of two flor yeast strains under controlled microaeration. J Agric Food Chem 53:5258-5264.

Nguyen D-D, Nicolau L, Dykes SI, and Kilmartin PA. 2010. Influence of microoxygenation on reductive sulfur off-odors and color development in a Cabernet sauvignon wine. Am J Enol Vitic 61:457-464.

Nguyen TH and Waterhouse AL. 2019. A production-accessible method: Spectrophotometric iron speciation in wine using ferrozine and ethylenediaminetetraacetic acid. J Agric Food Chem 67:680-687.

Nguyen TH and Waterhouse AL. 2021. Redox cycling of iron: Effects of chemical composition on reaction rates with phenols and oxygen in model wine. Am J Enol Vitic 72:209-216.

Nikolantonaki M, Coelho C, Noret L, Zerbib M, Vileno B, Champion D, and Gougeon RD. 2019. Measurement of white wines resistance against oxidation by electron paramagnetic resonance spectroscopy. Food Chem 270:156-161.

Nikolantonaki M and Waterhouse AL. 2012. A method to quantify quinone reaction rates with wine relevant nucleophiles: A key to the understanding of oxidative loss of varietal thiols. J Agric Food Chem 60:8484-8491.

Oberholster A, Elmendorf BL, Lerno LA, King ES, Heyman H, Brenneman CE, and Boulton RB. 2015. Barrel maturation, oak alternatives and micro-oxygenation: Influence on red wine aging and quality. Food Chem 173:1250-1258.

Oh HS, Kim J-J, and Kim Y-H. 2016. Stabilization of hydrogen peroxide using tartaric acids in Fenton and Fenton-like oxidation. Korean J Chem Eng 33:885-892.

Ohyoshi E, Hamada Y, Nakata K, and Kohata S. 1999. The interaction between human and bovine serum albumin and zinc studied by a competitive spectrophotometry. J Inorg Biochem 75:213-218.

Oliveira CM, Ferreira ACS, de Freitas V, and Silva AMS. 2011. Oxidation mechanisms occurring in wines. Food Res Int 44:1115-1126.

Oliveira V, Lopes P, Cabral M, and Pereira H. 2013. Kinetics of oxygen ingress into wine bottles closed with natural cork stoppers of different qualities. Am J Enol Vitic 64:395-399.

Oliveira V, Lopes P, Cabral M, and Pereira H. 2015. Influence of cork defects in the oxygen ingress through wine stoppers: Insights with X-ray tomography. J Food Eng 165:66-73.

Osborne JP, Dubé Morneau A, and Mira de Orduña R. 2006. Degradation of free and sulfur-dioxide-bound acetaldehyde by malolactic acid bacteria in white wine. J Appl Microbiol 101:474-479.

Osborne JP, Mira de Orduña R, Pilone GJ, and Liu S-Q. 2000. Acetaldehyde metabolism by wine lactic acid bacteria. FEMS Microbiol Lett 191:51-55.

Ough CS and Amerine MA. 1972. Further studies with submerged flor sherry. Am J Enol Vitic 23:128-131.

Park JSB, Wood PM, Gilbert BC, and Whitwood AC. 1997. A kinetic and ESR investigation of iron(II) oxalate oxidation by hydrogen peroxide and dioxygen as a source of hydroxy radicals. Free Radical Res 27:447-458.

Parpinello GP, Plumejeau F, Maury C, and Versari A. 2012. Effect of micro-oxygenation on sensory characteristics and consumer preference of Cabernet sauvignon wines. J Sci Food Agric 92:1238-1244.

Pasteur ML. 1866. *Etudes sur le vin*. *Imprimerie impériale*, Paris.

Pearson RG. Hard and soft acids and bases. *J Am Chem Soc 85:3533-3539*.

Perestrelo R, Barros AS, Câmara JS, and Rocha SM. 2011. In-depth search focused on furans, lactones, volatile phenols, and acetals as potential age markers of Madeira wines by comprehensive two-

dimensional gas chromatography with time-of-flight mass spectrometry combined with solid phase microextraction. J Agric Food Chem 59:3186-3204.

Perron NR and Brumaghim JL. 2009. A review of the antioxidant mechanisms of polyphenol compounds related to iron binding. Cell Biochem Biophys 53:75-100.

Peterson AL, Gambuti A, and Waterhouse AL. 2015. Rapid analysis of heterocyclic acetals in wine by stable isotope dilution gas chromatography-mass spectrometry. Tetrahedron 71:3032-3038.

Peterson AL and Waterhouse AL. 2016. ^{1}H NMR: A novel approach to determining the thermodynamic properties of acetaldehyde condensation reactions with glycerol, (+)-catechin, and glutathione in model wine. J Agric Food Chem 64:6869-6878.

Petrozziello M, Torchio F, Piano F, Giacosa S, Ugliano M, Bosso A, and Rolle L. 2018. Impact of increasing levels of oxygen consumption on the evolution of color, phenolic, and volatile compounds of Nebbiolo wines. Front Chem 6:137

Picariello L, Gambuti A, Picariello B, and Moio L. 2017. Evolution of pigments, tannins and acetaldehyde during forced oxidation of red wine: Effect of tannins addition. LWT 77:370-375.

Picariello L, Rinaldi A, Martino F, Petracca F, Moio L, and Gambuti A. 2019. Modification of the organic acid profile of grapes due to climate changes alters the stability of red wine phenolics during controlled oxidation. Vitis 58:127-134.

Picariello L, Slaghenaufi D, Ugliano M. 2020. Fermentative and post-fermentative oxygenation of Corvina red wine: Influence on phenolic and volatile composition, colour and wine oxidative response. J Sci Food Agric 100:2522-2533.

Pignatello JJ, Oliveros E, and MacKay A. 2006. Advanced oxidation processes for organic contaminant destruction based on the Fenton reaction and related chemistry. Crit Rev Env Sci Tec 36:1-84.

Pissarra J, Mateus N, Rivas-Gonzalo J, Santos Buelga C, and de Freitas V. 2003. Reaction between malvidin 3-glucoside and (+)-catechin in model solutions containing different aldehydes. J Food Sci 68:476-481.

Powell HKJ and Taylor MC. 1982. Interactions of iron(II) and iron(III) with gallic acid and its homologs - A potentiometric and spectrophotometric study. Aust J Chem 35:739-756.

Pozo-Bayón MA and Moreno-Arribas MV. 2011. Sherry wines. Adv Food Nutr Res 63:17-40.

Pronk JT, Steensma HY, and van Dijken JP. 1996. Pyruvate metabolism in *Saccharomyces cerevisiae*. Yeast 12:1607-1633.

Pulido-Tofino P, Barrero-Moreno JM, and Perez-Conde MC. 2000. A flow-through fluorescent sensor to determine Fe(III) and total inorganic iron. Talanta 51:537-545.

Rentzch M, Schwarz M, and Winterhalter P. 2007. Pyranoanthocyanins – An overview on structures, occurrence, and pathways of formation. Trends Food Sci Technol 18:526-534.

Robinson J (ed) and Harding J (asst ed). 2015. The Oxford Companion to Wine, 4th ed. Smart RE, Lavigne V, and Dubourdieu D (adv eds). Oxford University Press.

Rodrigues A, Ferreira ACS, de Pinho PG, Bento F, and Geraldo D. 2007. Resistance to oxidation of white wines assessed by voltammetric means. J Agric Food Chem 55:10557-10562.

Roginsky V, de Beer D, Harbertson JF, Kilmartin PA, Barsukoval T, and Adams DO. 2006. The antioxidant activity of Californian red wines does not correlate with wine age. J Sci Food Agric 86:834-840.

Romanet R, Bahut F, Nikolantonaki M, and Gougeon RD. 2020. Molecular characterization of white wines antioxidant metabolome by ultra-high performance liquid chromatography high-resolution mass spectrometry. Antioxidants 9:115.

Romano P, Suzzi G, Turbanti L, and Polsinelli M. 1994. Acetaldehyde production in *Saccharomyces cerevisiae* wine yeasts. FEMS Microbiol Lett 118:213-218.

Rosenfeld E and Beauvoit B. 2003. Role of the non-respiratory pathways in the utilization of molecular oxygen by *Saccharomyces cerevisiae*. Yeast 20:1115-1144.

Ribéreau-Gayon J. 1931. *Contribution à l'étude des oxydations et reductions dans les vins. Thèse Doctorat ès Sciences Physiques,* Bordeaux Institute of Enology.

Rossi JA and Singleton VL. 1966. Contributions of grape phenols to oxygen absorption and browning of wines. Am J Enol Vitic 17:231-239.

Sáenz-Navajas MP, Henschen C, Cantu A, Watrelot AA, and Waterhouse AL. 2018. Understanding microoxygenation: effect of viable yeasts and sulfur dioxide levels on the sensory properties of a Merlot red wine. Feed Res Int 108:505-515.

Sánchez-Iglesias M, González-Sanjosé ML, Pérez-Magariño S, Ortega-Heras M, and González-Huerta C. 2009. Effect of micro-oxygenation and wood type on the phenolic composition and color of an aged red wine. J Agric Food Chem 57:11498-11509.

Saucier C, Guerra C, Pianet I, Laguerre M, and Glories Y. 1997. (+)-Catechin-acetaldehyde condensation products in relation to wine-ageing. Phytochemistry 46:229-234.

Schmidtke LM, Clark AC, and Scollary GR. 2011. Micro-oxygenation of red wine: Techniques, applications, and outcomes. Crit Rev Food Sci 51:115-131.

Schwarz M, Quast P, von Baer D, and Winterhalter P. 2003. Vitisin A content in Chilean Wines from *Vitis vinifera* cv. Cabernet sauvignon and contribution to the color of aged red wines. J Agric Food Chem 51:6261-6267.

Sheridan MK and Elias RJ. 2016. Reaction of acetaldehyde with wine flavonoids in the presence of sulfur dioxide. J Agric Food Chem 64:8615-8624.

Singleton VL. 1987. Oxygen with phenols and related reactions in musts, wines, and model systems - Observations and practical implications. Am J Enol Vitic 38:69-77.

Singleton VL and Kramling TE. 1976. Browning of white wines and an accelerated test for browning capacity. Am J Enol Vitic 27:157-160.

Singleton VL, Trousdale E, and Zaya J. 1979. Oxidation of wines. I. Young white wines periodically exposed to air. Am J Enol Vitic 30:49-54.

Skouroumounis GK, Kwiatkowski MJ, Francis IL, Oakey H, Capone DL, Duncan B, Sefton MA, and Waters EH. 2005. The impact of closure type and storage conditions on the composition, colour and flavour properties of a Riesling and a wooded Chardonnay wine during five years' storage. Aust J Grape Wine Res 11:369-377.

Smythe CV. 1931. The mechanism of iron catalysis in certain oxidations. J Biol Chem 90:251-265.

Somers TC and Evans ME. 1977. Spectral evalution of young red wines – Anthocyanin equilibria, total phenolics, free and molecular SO_2, chemical age. J Sci Food Agric 28:279-287.

Spiropoulos A, Tanaka J, Fleiranos I, and Bisson LF. 2000. Characterization of hydrogen sulfide formation in commercial and natural wine isolates of *Saccharomyces*. Am J Enol Vitic 51:233-248.

Stookey LL. 1970. Ferrozine – A new spectrophotometric reagent for iron. Anal Chem 42:779-781.

Sun B, Ricardo-da-Silva JM, and Spranger I. 1998. Critical factors of vanillin assay for catechins and proanthocyanidins. J Agric Food Chem 46:4267-4274.

Swanson WH and Clifton CE. 1948. Growth and assimilation in cultures of *Saccharomyces cerevisiae*. J Bacteriol 56:115-124.

Tachiev G, Roth JA, and Bowers AR. 2000. Kinetics of hydrogen peroxide decomposition with complexed and “free” iron catalysts. Int J Chem Kinet 32:24-35.

Tao J, Dykes SI, and Kilmartin PA. 2007. Effect of SO_2 concentration on polyphenol development during red wine micro-oxygenation. J Agric Food Chem 55:6104-6109.

Tessier WD, Meaden PG, Dickinson FM, and Midgley M. 1998. Identification and disruption of the genes encoding the K^+-activated acetaldehyde dehydrogenase of *Saccharomyces cerevisiae*. FEMS Micobiol Lett 164:29-34.

Thomsen JC and Mottola HA. 1984. Kinetics of the complexation of iron(II) with ferrozine. Anal Chem 56:755-757.

Timberlake CF. 1964. Iron-tartrate complexes. J Chem Soc 1229-1240.

Timberlake CF. 1964b. Iron-malate and iron-citrate complexes. J Chem Soc 5078-5085.

Timberlake CF and Bridle P. 1976. Interactions between anthocyanins, phenolic compounds, and acetaldehyde and their significance in red wines. Am J Enol Vitic 27:97-105.

Ugliano M. 2013. Oxygen contribution to wine aroma evolution during bottle aging. J Agric Food Chem 61:6125-6136.

Ugliano M. 2016. Rapid fingerprinting of white wine oxidizable fraction and classification of white wines using disposable screen printed sensors and derivative voltammetry. Food Chem 212:837-843.

US EPA. 1996. Method 8315A (SW-846): Determination of carbonyl compounds by high performance liquid chromatography (HPLC), Revision 1. Washington, DC.

Vallverdú-Queralt A, Meudec E, Eder M, Lamuela-Raventos RM, Sommerer N, and Cheynier V. 2017. The hidden face of wine polyphenol polymerization highlighted by high-resolution mass spectrometry. ChemistryOpen 6:336-339.

van Dijken JP and Scheffers WA. 1986. Redox balances in the metabolism of sugars by yeasts. FEMS Microbiol Rev 32:199-224.

Verschoor MJ and Molot LA. A comparison of three colorimetric methods for ferrous and total reactive iron measurements in freshwaters. Limnol Oceanogr Methods 11:113-125.

Vidal JC, Caille S, Samson A, and Salmon JM. 2017. Comparison of the effect of 8 closures in controlled industrial conditions on the shelf life of a red wine. *In* 40th World Congress of Vine and Wine. Aurand J-M (ed). BIO Web Conf 9:02024

Viollier E, Inglett PW, Hunter K, Roychoudhury AN, and van Cappellen P. 2000. The ferrozine method revisited: Fe(II)/Fe(III) determination in natural waters. Appl Geochem 15:785-790.

Vivela A. 2019. Use of nonconventional yeasts for modulating wine acidity. Fermentation 5:27.

Voelker BM and Sulzberger B. 1996. Effects of fulvic acid on Fe(II) oxidation by hydrogen peroxide. Environ Sci Technol 30:1106-1114.

Wang J and Mannino S. 1989. Application of adsorptive stripping voltammetry to the speciation and determination of iron(III) and total iron in wines. Analyst 114:643-645.

Wang S. 2008. A comparative study of Fenton and Fenton-like reaction kinetics in decolourisation of wastewater. Dyes Pigm 76: 714-720.

Waterhouse AL and Elias RJ. 2010. Chemical and physical deterioration of wine. *In* Chemical Deterioration and Physical Instability of Food and Beverages. Skibsted LH, Risbo J, and Andersen ML (eds). pp 466-482. Woodhead Publishing, Cambridge.

Waterhouse AL and Laurie VF. 2006. Oxidation of wine phenolics: A critical evaluation and hypotheses. Am J Enol Vitic 57:306-313.

Waterhouse AL and Nikolantonaki M. 2015. Quinone reactions in wine oxidation. *In* Advances in Wine Research. Ebeler SB, Sacks G, Vidal S, and Winterhalter P (eds). Vol 1203, pp 291-301. ACS Symposium Series.

Waterhouse AL, Sacks GL, and Jeffery DW. 2016. Understanding Wine Chemistry. John Wiley & Sons, Chichester, West Sussex.

Welch KD, Davis TZ, and Aust SD. 2002. Iron autoxidation and free radical generation: Effects of buffers, ligands, and chelators. Arch Biochem Biophys 397:360-369.

Wells CF and Salam MA. 1968. The effect of pH on the kinetics of the reaction of iron(II) with hydrogen peroxide in perchlorate media. J Chem Soc A 24-29.

Weusthuis RA, Visser W, Pronk JT, Scheffers WA, and van Dijken JP. 1994. Effects of oxygen limitation on sugar metabolism of yeasts: A continuous-culture study of the Kluyver effect. Microbiology 140:703-715.

Wildenradt HL and Singleton VL. 1974. The production of aldehydes as a result of oxidation of polyphenolic compounds and its relation to wine aging. Am J Enol Vitic 25:119-126.

Xu H, Li M, Wang H, Miao J, and Zou L. 2012. Fenton reagent oxidation and decolorizing reaction kinetics of Reactive Red SBE. Energy Procedia 16:58-64.

Yokoi H, Mitani T, Mori Y, and Kawata S. 1994. Complex formation between iron(III) and tartaric and citric acids in a wide pH range 1 to 13 as studied by magnetic susceptibility measurements. Chem Lett 23:281-284.

Zoecklein BW, Fugelsang KC, Gump BH, and Nury FS. 1995. Wine Analysis and Production. Chapman & Hall, New York, NY.